REPORT DOCUMENTATION PAGE

AFRL-SR-AR-TR-04-

0434

1. REPORT DATE (DD-MM-YYYY)	2. REPORT TYPE	3. DATES COVERED (From - To)
31-12-2003	FINAL	01-05-2000 TO 30-09-2003

4. TITLE AND SUBTITLE
ELECTRON HEATING IN ATMOSPHERIC PRESSURE AIR

5a. CONTRACT NUMBER

5b. GRANT NUMBER
F49620-00-10079

5c. PROGRAM ELEMENT NUMBER

6. AUTHOR(S)
Karl H. Schoenbach

5d. PROJECT NUMBER

5e. TASK NUMBER

5f. WORK UNIT NUMBER

7. PERFORMING ORGANIZATION NAME(S) AND ADDRESS(ES)
Old Dominion University Research Foundation
P.O. Box 6369
Norfolk, VA 23508

8. PERFORMING ORGANIZATION REPORT NUMBER

9. SPONSORING/MONITORING AGENCY NAME(S) AND ADDRESS(ES)
Dr. Robert J. Barker
AFOSR/NE
4015 Wilson Boulevard, Room 713
Arlington, VA 22203-1954

10. SPONSOR/MONITOR'S ACRONYM(S)
AFOSR/NE

11. SPONSOR/MONITOR'S REPORT NUMBER(S)

12. DISTRIBUTION/AVAILABILITY STATEMENT
UNLIMITED

DISTRIBUTION STATEMENT A
Approved for Public Release
Distribution Unlimited

20040901 093

13. SUPPLEMENTARY NOTES

14. ABSTRACT

The use of microhollow cathode discharges (MHCD) as plasma cathodes has allowed us to generate stable, direct current atmospheric pressure glow discharges in air with dimensions up to centimeters, electron densities of 10^{13} cm^{-3}, and temperatures of not more than 2000 K. By sustaining the discharge through consecutive electrical pulses, with duration of less than the time constant for flow-to-arc transition, the required electrical power density could be drastically reduced, compared to the dc option. The temporal development of electron density and gas temperature in response to 10 ns pulses in single and dual pulse operation has been measured. The electron density increased during an applied pulse with a reduced electric field of 220 Td to values greater than 10^{15} cm^{-3}, before decreasing to 10^{13} cm^{-3} due to recombination over a time of several microseconds. Power densities required to sustain atmospheric air plasmas in a repetitive pulsed mode were found to be less than 50 W/cm^3 for electron densities exceeding 10^{12} cm^{-3} during the discharge cycle.

15. SUBJECT TERMS
weakly ionized gases, atmospheric pressure air, pulsed electron heating, power consumption, gas temperature, electron density

16. SECURITY CLASSIFICATION OF:			17. LIMITATION OF ABSTRACT	18. NUMBER OF PAGES	19a. NAME OF RESPONSIBLE PERSON
a. REPORT	b. ABSTRACT	c. THIS PAGE			Karl H. Schoenbach
unclassified	unclassified	unclassified	none		19b. TELEPHONE NUMBER (Include area code) 757-683-2421

Final Report

on the Project

Electron Heating in Atmospheric Pressure Air

Grant No: F49620-00-1-0079

May 1, 2000 to September 30, 2003

submitted to

Dr. Robert J. Barker
Air Force Office of Scientific Research

801 N. Randolph St., Rm 732
Arlington, VA 22203-1977
Phone: (703) 696-8574
FAX: (703) 696-8481
e-mail: robert.barker@afosr.af.mil

by

Karl H. Schoenbach

Center for Bioelectrics
830 Southampton Ave., Suite 5100
Old Dominion University
Norfolk VA 23510
Phone: (757) 683-2421
FAX: (757) 314 2397
e-mail: schoenbach@ece.odu.edu

Table of Contents

Abstract

The use of microhollow cathode discharges (MHCD) as plasma cathodes has allowed us to generate stable, direct current atmospheric pressure glow discharges in air with dimensions up to centimeters, electron densities of 10^{13} cm^{-3}, and temperatures of not more than 2000 K. By sustaining the discharge through consecutive electrical pulses, rather than a dc voltage, the electrical power density required to sustain such nonthermal plasmas could be drastically reduced. This effect is due to pulsed electron heating, a temporary shift of the electron energy distribution toward higher energies, and consequently, a strongly increased ionization rate. By keeping the pulse duration short enough that glow-to-arc transition can be avoided, and applying the pulses with a repetition rate such that the electron density does not decay below a set value, a high average electron density air plasma can be generated. Experiments with 10 ns long pulses in single and dual pulse operation have shown that the gas temperature increased to 2200 K for only 10 ns after the pulse, and then fell to values at or below 2000 K. The electron density, which was measured using either heterodyne laser interferometry or a conductivity method, increased during an applied pulse with a reduced electric field of 220 Td to values greater than 10^{15} cm^{-3}, before decreasing to 10^{13} cm^{-3} due to recombination over a time of several microseconds. The values of the measured power density agree with that of a simple rate equation model. Minimum electrical power levels of 850 W/cm^{-3} for the sustainment of an ionized air plasma with electron densities greater than 10^{13} cm^{-3}, and 18 W/cm^{-3} for electron densities greater than 10^{12} cm^{-3} were calculated. In a continuation of dc studies of the plasma cathode, it could be shown that, by blowing atmospheric pressure air through the MHCD, it was possible to generate micro plasma jets with gas temperatures as low as room temperature.

Summary

Direct current and pulsed gas discharges in atmospheric air with dimensions into the centimeter range were studied by means of electrical and optical diagnostics. The atmospheric pressure plasma was generated and sustained by using microhollow discharges as plasma cathodes (MHCDs). The atmospheric pressure plasma was generated between the plasma cathode and a metal anode. The length of the glow discharge column was varied up to 2 cm, with the sustaining voltage increasing linearly with length. The MHCD sustained discharges can be operated in parallel and the discharge plasmas were found to merge for discharge distances of 0.4 cm if the gap length exceeds 0.5 cm. Increasing the gap length and placing the MHCD sustained discharges in parallel can generate homogeneous, large volume, atmospheric pressure air plasmas. A patent on this method, which allows the generation of stable high pressure plasmas in any gas, has been issued.

Gas temperatures in the MHCD sustained plasma were measured spatially and temporally resolved using emission spectroscopy. The gas temperature in the MHCD sustained direct current plasmas did not exceed 2000 K for electron densities of 10^{13} cm^{-3}. For pulsed operation with 10 ns pulses, the temperature increased to 2,200 K for 10 ns after the pulse. The electron density, which was measured using heterodyne laser interferometry and a method based on the measurements of the plasma conductivity, increased during an applied pulse with a reduced electric field of 220 Td, to values greater than 10^{15} cm^{-3}. After the pulse application, the electron density decreased, due to recombination, to 10^{13} cm^{-3} over a time of several microseconds. The results show that repetitive pulsing with nanosecond voltage pulses serves as a means to reduce the power consumption for glow discharges in atmospheric pressure air, when compared to direct current operation.

By using a simple rate equation model, with recombination assumed to be the only electron loss mechanism, the electrical power required to sustain plasmas with electron densities exceeding a given value was calculated. The results of this model agree well with measured power values. The minimum electrical power for the sustainment of an atmospheric pressure air plasma with electron densities greater than 10^{13} cm^{-3} is, according to the model, 850 W/cm^3, and 18 W/cm^3 for electron densities greater than 10^{12} cm^{-3}. Dual pulse operation has shown that even without the presence of a direct current driven background plasma, which was previously assumed to be required to keep the plasma temperature above the value where attachment is negligible, strong power savings can be achieved.

Attempts to generate atmospheric pressure plasmas on surfaces (without using a counter electrode to the plasma cathode) were made by flowing air through the microholes that form the plasma cathode. By flowing the gas at high pressure through the microhollow cathode discharge, which is sustained between two molybdenum foils separated by a 250 μm-thick alumina spacer, a well-defined plasma jet is generated with typical dimensions of millimeters in the axial direction. The power consumption ranges from 1 W to 10 W. The gas temperature was measured by means of micro-thermocouples. Increasing the gas flow rate from 0 to 200 ml/min at a constant discharge current resulted in a decrease of

gas temperature to values close to room temperature. By placing the microjets in parallel, large area plasmas can be generated. This cold plasma jet offers the opportunities for applications such as surface treatment of sensitive materials. A patent application on this new method of generating cold atmospheric pressure plasmas has been submitted.

A spin-off project of atmospheric pressure air plasma research was a study of the effect of dc and pulsed plasma on the chemistry of polluted air. The direct current glow discharge has been used to study the remediation of methane and benzene, two of the most stable volatile organic compounds (VOCs). The removal rate for 300-ppm methane in atmospheric pressure air, flowed through the 0.5 mm thick plasma layer, with a residence time of the gas in the plasma of less than 1 ms was measured at 80%. For benzene, the remediation rate is as high as 90%, comparable to results obtained with low-pressure glow discharges. However, the energy efficiency for benzene remediation is 0.9 g/kWh, higher than that obtained for benzene remediation in low-pressure glow discharges in noble gases.

List of Publications and Patents

Journal Publications

Chunqi Jiang, Abdel-Aleam H. Mohamed, Robert H. Stark, James H. Yuan, and Karl H. Schoenbach, "Removal of Volatile Organic Compounds in Atmospheric Pressure Air by Means of Direct Current Glow Discharges," submitted to IEEE Trans. Plasma Science.

K.H. Schoenbach, M. Moselhy, W. Shi, and R. Bentley, "Microhollow Cathode Discharges," Invited Paper, J. Vac. Sci. Technol. A 21, 1260 (2003).

Abdel-Aleam H. Mohamed, Rolf Block, and Karl H. Schoenbach "Direct Current Glow Discharges in Atmospheric Air," IEEE Trans. Plasma Science 30, 182 (2002).

Robert H. Stark and Karl H. Schoenbach, "Electron Heating in Atmospheric Pressure Glow Discharges," J. Appl. Phys. 89, 3568 (2001).

Conference Papers and Book Chapters

Frank Leipold, Abdel-Aleam H. Mohamed, and Karl H. Schoenbach, "High Electron Density, Atmospheric Pressure Air Glow Discharges," Conf. Record, 25th Modulator Symposium, Hollywood, CA, 2002, p. 130.

Robert H. Stark, Hisham Merhi, and Karl H. Schoenbach, "Pulsed Electron Heating of Atmospheric Pressure Air Glow Discharges," Digest of Technical Papers, PPPS2001, Pulsed Power Plasma Science 2001, Las Vegas, NV, p. 281.

Ulrike Hahn, Matthias Herrmann, Frank Leipold, and Karl H. Schoenbach , "Nanosecond, Kilovolt Pulse Generators," Digest of Technical Papers, PPPS2001, Pulsed Power Plasma Science 2001, Las Vegas, NV, p. 1575.

Chunqi Jiang, Robert H. Stark, and Karl H. Schoenbach, "Benzene Destruction in Direct Current and Pulse-Superimposed Atmospheric Pressure Air Glow Discharges," Digest of Technical Papers, PPPS2001, Pulsed Power Plasma Science 2001, Las Vegas, NV, p. 1110.

Book Chapter: Robert H. Stark, Hisham Merhi, Chunqi Jiang, and Karl H. Schoenbach, "Excimer Emission From Pulsed High Pressure Xenon Glow Discharge," Gaseous Dielectrics IX, Loucas G. Christophorou and James K. Olthoff, eds, Kluwer Academic/ Plenum Publishers, New York, 2001, p. 257.

Book Chapter: Chunqi Jiang, Robert H. Stark, and Karl H. Schoenbach, "Benzene Destruction in Direct Current Atmospheric Pressure Air Glow Discharges," Gaseous

Dielectrics IX, Loucas G. Christophorou and James K. Olthoff, eds, Kluwer Academic/ Plenum Publishers, New York, 2001, p. 263.

Manoj Nagulapally, Graham V. Candler, Christophe O. Laux, Lan Yu, Denis Packan, Charles H. Kruger, Robert H. Stark, Karl H. Schoenbach, "Experiments and Simulations of DC and Pulsed Discharges in Air Plasmas," 31st AIAA Plasmadynamics and Lasers Conf., Denver, CO, July 2000, paper AIAA 2000-2417.

Abstracts

Abdel-Aleam H. Mohamed, Frank Leipold, Juergen Kolb, Sususmu Kono, and Karl H. Schoenbach, "Atmospheric Pressure Glow Discharge Micro-Plasma Jet," Conference Record, 2003 IEEE Intern. Conf. Plasma Science, Jeju, Korea, June 2 –5,, 2003, Paper 1PA13, p. 148.

Frank Leipold and Karl H. Schoenbach, "Electron Density and Electron Temperature in Pulsed Atmospheric Pressure Air Plasmas," Conference Record, 2002 IEEE Intern. Conf. Plasma Science, Banff, Alberta, Canada, May 26-30, 2002, Paper 2P03, p. 143.

Frank Leipold, Abdel-Aleam Hufney Mohamed, and Karl H. Schoenbach, "Measurements of Electron Temperature and Gas Temperature in a Pulsed Atmospheric Pressure Air Discharge," GEC, Penn State University, October 2001, Bulletin of the American Physical Soc., Vol. 46, No. 6, Abstract DTP 45, page. 22.

Chunqi Jiang, Robert H. Stark, and Karl H. Schoenbach, "Benzene Dissociation in DC Atmospheric Pressure Air Glow Discharges," GEC, Penn State University, October 2001, Bulletin of the American Physical Soc., Vol. 46, No. 6, Abstract JWP 4, page. 34.

Frank Leipold, Robert Stark, and Karl H. Schoenbach, "Electron Density and Temperature Measurements in Pulsed Atmospheric Pressure Air Plasmas," APP Spring Meeting, Bad Honnef 2001, "Diagnostics of Non-Equilibrium High Pressure Plasmas" Physikzentrum Bad Honnef, Feb. 18-21, 2001, in www.ilp.physik.uni-essen.de/doebele/Spring2001

Robert H. Stark, Hisham Merhi, and Karl H. Schoenbach, "Pulsed Electron Heating in Atmospheric Pressure Glow Discharges," APP Spring Meeting, Bad Honnef 2001, "Diagnostics of Non-Equilibrium High Pressure Plasmas" Physikzentrum Bad Honnef, Feb. 18-21, 2001, in www.ilp.physik.uni-essen.de/doebele/Spring2001

Robert H. Stark, Frank Leipold, Chunqi Jiang, Hisham Merhi, and Karl H. Schoenbach, "Electron Heating in Pulsed Atmospheric Pressure Glow Discharges," Bull APS (GEC), Vol. 45, No. 6, October 2000, CT2 6, p. 17.

Frank Leipold, Robert H. Stark, and Karl H. Schoenbach, "Measurement of Electron Densities in a Pulsed Atmospheric Pressure Air Discharge," Bull APS (GEC), Vol. 45, No. 6, October 2000, ETP 53, p. 30.

Robert H. Stark and Karl H. Schoenbach, "Electron Heating in Atmospheric Pressure Air Discharges," Conf. Record, IEEE Intern. Conf. Plasma Science, New Orleans, 2000, paper 1A05, p. 83.

Rolf Block, Abdel-Aleam H. Mohamed, and Karl H. Schoenbach, "Plasma Cathode Sustained Filamentary Glow Discharges in Atmospheric Air," Conf. Record, IEEE Intern. Conf. Plasma Science, New Orleans, 2000, paper 1P23, p. 110.

Robert H. Stark, Ahmed El-Habachi, and Karl H. Schoenbach, "Parallel Operation of Microhollow Cathode Discharges," Conf. Record, IEEE Intern. Conf. Plasma Science, New Orleans, 2000, paper 1P24, p. 111.

Patent

Direct Current High-Pressure Glow Discharges
Patent No: 6,433,480
Patent Date: August 13, 2002
Inventors: Robert P. Stark and Karl H. Schoenbach

Provisional Patent Application

Micro Plasma Jet
Filed: June 1, 2004
Inventors: Karl H. Schoenbach, Juergen Kolb, and Abdel-Aleam Mohamed

Personnel

PI:	Karl H. Schoenbach
Co-PI:	Ravindra P. Joshi
Co-PI (until July 2000):	Robert Stark
Postdoctoral Research Associate	Frank Leipold
Postdoctoral Research Associate	Juergen Kolb

Graduate (PhD) Student: Chunqui Jiang

Graduated in November 2002, Ph.D. Dissertation: "The Application of Atmospheric Pressure Glow Discharges in Air for VOC Remediation"

Graduate (PhD) Student: Abdel-Aleam Hufney Mohamed

Graduated in April 2004, Ph.D. Dissertation: "Scaling and Characterization of Direct Current Glow Discharge Plasma in Atmospheric Air".

Graduate (MS) Student: Hisham Merhi,

Graduated in August 2001, M.S. Thesis: "Pulsed Electron Heating of Atmospheric Pressure Air Glow Discharges"

Journal Publications

Chunqi Jiang, Abdel-Aleam H. Mohamed, Robert H. Stark, James H. Yuan, and Karl H. Schoenbach, "Removal of Volatile Organic Compounds in Atmospheric Pressure Air by Means of Direct Current Glow Discharges," submitted to IEEE Trans. Plasma Science.

K.H. Schoenbach, M. Moselhy, W. Shi, and R. Bentley, "Microhollow Cathode Discharges," Invited Paper, J. Vac. Sci. Technol. A 21, 1260 (2003).

Abdel-Aleam H. Mohamed, Rolf Block, and Karl H. Schoenbach "Direct Current Glow Discharges in Atmospheric Air," IEEE Trans. Plasma Science 30, 182 (2002).

Robert H. Stark and Karl H. Schoenbach, "Electron Heating in Atmospheric Pressure Glow Discharges," J. Appl. Phys. 89, 3568 (2001).

Removal of Volatile Organic Compounds in Atmospheric Pressure Air by Means of Direct Current Glow Discharges

Chunqi Jiang, Abdel-Aleam H. Mohamed, Robert H. Stark, James H. Yuan*, and Karl H. Schoenbach

Physical Electronics Research Institute, Old Dominion University, Norfolk, VA 23529
*Department of Chemistry and Biochemistry, Old Dominion University, Norfolk, VA 23529

Abstract

A non-thermal plasma with an electron density on the order of 10^{12} cm^{-3} and a gas temperature of 2000 K was generated in atmospheric pressure air, using a microhollow cathode discharge as plasma cathode. The plasma was sustained in a micro reactor with dimensions on the order of 1 mm^3 by applying a voltage of 470 V to the electrodes, separated by a gap of 1.5 mm, at currents ranging from 8 mA to 18 mA. The microhollow cathode discharge required a sustaining voltage of 400 V. The direct current glow discharge has been used to study the remediation of methane and benzene, two of the most stable volatile organic compounds (VOCs). The removal rate for 300 ppm methane in atmospheric pressure air flowed through the 0.5 mm thick plasma layer, with a residence time of the gas in the plasma of less than 1 ms was measured at 80%. For benzene, the remediation rate is as high as 90%, comparable to results obtained with low pressure glow discharges. However, the energy efficiency for benzene remediation is 0.9 g/kWh, higher than that obtained for benzene remediation in low pressure glow discharge in noble gases. In addition to experimental studies, the VOC dissociation mechanism in a VOC/dry air mixture plasma was modeled using a zero-dimensional plasma chemistry code. The modeling results have shown that atomic oxygen impact reactions are the dominant dissociation reactions for VOC destruction in this kind of glow discharges.

Index Terms- Glow discharge, atmospheric pressure air, non-thermal plasma, chemical decontamination, volatile organic compounds

Introduction

Volatile organic compounds (VOCs) such as toluene, xylene, trichloro-ethylene (TCE), trichloroethane (TCA), benzene, and acetone are widely used as solvents and for substrate cleaning [1]. Although most of the VOCs are chemically inactive at atmospheric pressure and room temperature, they pose considerable hazards to our health and the environment. For example, inhalation of toluene with concentrations of 600 ppm for more than eight hours causes headache and dizziness [2]. Benzene is carcinogenic with long term exposure [2]. Some of the VOCs, for instance, methane, are known to accumulate in the upper atmosphere and are one of the reasons for global warming [3].

Conventional methods to eliminate VOC pollutants in air streams include thermal oxidation, catalytic oxidation, adsorption, biofiltration, UV-oxidation, and thermal plasma oxidation [1,4]. In general, conventional VOC remediation methods are mainly used for VOCs with high concentrations (>1000 ppm). They are not practical for diluted VOC mixtures. Thermal oxidation and thermal plasma oxidation require heating of the ambient gases and raise the capital cost for cooling systems. In comparison, catalytic oxidation, adsorption, biofiltration and UV-oxidation are more energy efficient. However, the catalysts, adsorbents, or biofilters require regeneration and disposal. Additionally, both biofiltration and UV-oxidation require long residence times.

As alternative approaches, non-thermal plasma techniques [5-11] have received considerable attention because of their high efficiency [1,4]. Non-thermal plasma techniques, which can effectively treat VOCs with concentrations in the range from 1 to 10,000 ppm [4], utilize either electron beam generated plasmas or gas discharges (barrier, corona or glow). In the non-thermal plasma, the average electron temperature is much higher than the gas temperature. The high-energy electrons in the electron energy distribution of such plasmas cause efficient VOC dissociation.

Electron beam reactors for VOC remediation [4] can be operated in dc, ac and pulsed modes at any pressure. Since the generation of energetic electrons requires a vacuum system and high voltage, the capital cost for these reactors is high. Dielectric-barrier discharges and corona discharges are two types of most promising non-thermal plasma technologies for VOC removal [5]. Barrier discharges can be operated over a wide pressure range including atmospheric pressure, and a high destruction rate can be achieved with a relatively low input of electric power. For example, 90% or 99% removal efficiency was obtained for CFC-113, acetone, trichloroethylene and isopropyl alcohol by using the surface induced plasma chemical processing when the residence time was about 1 second and the input electric power for a 16 cm^3 reactor was about 10W [6]. Barrier discharges are normally driven by 50 Hz to 10 kHz ac power supplies with operating voltages of 5 kV to 20 kV [4]. Dielectrics used in barrier discharges for plasma stabilization are often heated to high temperature due to

Chunqi Jiang, Abdel-Aleam H. Mohamed, Robert H. Stark, James H. Yuan, and Karl H. Schoenbach, "Removal of Volatile Organic Compounds in Atmospheric Pressure Air by Means of Direct Current Glow Discharges," submitted to IEEE Trans. Plasma Science.

dielectric losses, and consequently, a cooling system is needed. Corona discharges can be operated in dc or pulsed mode at any pressures. DC corona discharges with point-to-plane electrodes [7-8], however, are not stable, and need to operate at a high gas flow rate (about 100 m/s) for cooling. Otherwise, glow-to-arc transitions will terminate the nonthermal plasma state. With pulsed corona discharges, using a nanosecond-pulsed corona reactor [9], a removal efficiency of 95% was achieved for methylene chloride. In general, pulsed corona discharges require high pulsed voltages, ranging from 30 kV to 200 kV [4].

Low and medium pressure glow discharges, operating at relatively low voltages (200 V to 2 kV), are the basis of yet another nonthermal plasma technique for VOC remediation. Dissociation of benzene and methylene chloride by dc and pulsed low pressure glow discharges has been studied [10-11] in VOC/rare gas mixtures, and a 99.8% removal rate has been achieved. It was found that the destruction efficiency increased with increasing pressure [10-11]. Higher pressure operation, however, requires an increased sustaining electric field. This causes conventional glow discharges to become unstable and to undergo glow-to-arc transitions. The plasma in the arc mode is thermal and consequently has an electron energy distribution with a strongly reduced concentration of high-energy electrons.

Direct Current Atmospheric Pressure Glow Discharge

Operation of air plasma reactors at atmospheric pressure allows us to simplify the reactor design considerably, since vacuum systems are not required. In addition, the high gas density allows the processing of large quantities of contaminated air per unit of time, important for practical applications. In order to avoid glow-to-arc transitions, various techniques have been developed [12-19]. The use of microhollow cathode discharges [20] as the external electron source (plasma cathode) to sustain a larger volume air plasma at atmospheric pressure is one of the techniques. For a self-sustained discharge, the largest electric field occurs in the cathode fall region, and therefore, the glow-to-arc transition is most likely to be initiated in this region. The microhollow cathode discharge provides a plasma which reduces the cathode fall: it serves as a plasma cathode [17-19].

Microhollow cathode discharges (MHCDs) [20] are high-pressure, direct current gas discharges with electrodes having 100-200 μm diameter openings. Since the sustaining voltage of a discharge is a function of pD (the product of pressure and the cathode hole diameter) [21], the discharge can be operated at higher pressure by decreasing the hole diameter and maintaining a constant voltage. Experiments [17-20] have shown that MHCDs can be operated in atmospheric pressure in a direct current mode in noble gases or in air. When operated in the hollow cathode discharge mode, electrons can be drawn through the microhollow anode opening and will support a stable plasma between the microhollow anode and a positively biased third electrode.

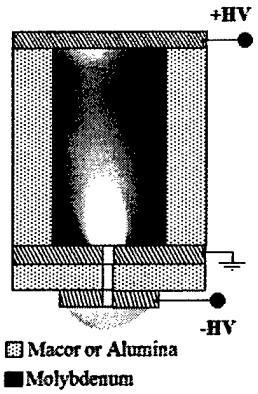

Figure 1 Schematic cross-section of a MHCD-sustained, laterally confined atmospheric pressure glow discharge

The gas temperature of the MHCD sustained (MCS) atmospheric pressure air plasma was obtained by means of emission spectroscopy. Comparisons of the modeled and measured spectra of the 2nd positive system of nitrogen showed that the gas temperature of this plasma reached values of 2000 K [22]. The electron density was measured by using infrared heterodyne interferometry [23]. For a dc MCS atmospheric pressure glow discharge, at a current of 10 mA, the electron density is 10^{13} cm^{-3} in the center, decreasing to half of this value at a radial distance of 0.21 mm. Compared with the dc high pressure glow discharges obtained by Akishev et. al. [24-26], the electron density of the MCS atmospheric pressure glow discharge is about two orders of magnitude higher.

In order to apply the MCS atmospheric pressure glow discharges to VOC remediation, all the processing gas needs to pass though the plasma. This was achieved by confining the discharge plasma in a channel with Macor or alumina walls (Fig. 1), through which the gas flowed. The gas temperature of the confined atmospheric pressure air plasma was measured

by using the same diagnostic method as for the free-standing air plasma [22]. For the dielectric-confined atmospheric pressure air plasma, the gas temperature was measured as 2000 K to 2200 K (with an error margin of ± 50 K) in the current range of 8 mA to 18 mA at a constant MCS glow discharge voltage of 570 V (Fig. 2), linearly fitted using an algorithm for least squares. This temperature is slightly higher than that measured in free-standing atmospheric pressure glow discharges [23], and the laterally-confined glow discharges operate at a higher voltage. This increase in sustaining voltage is assumed to be due to the increased diffusion loss of charged particles to the dielectric walls [27].

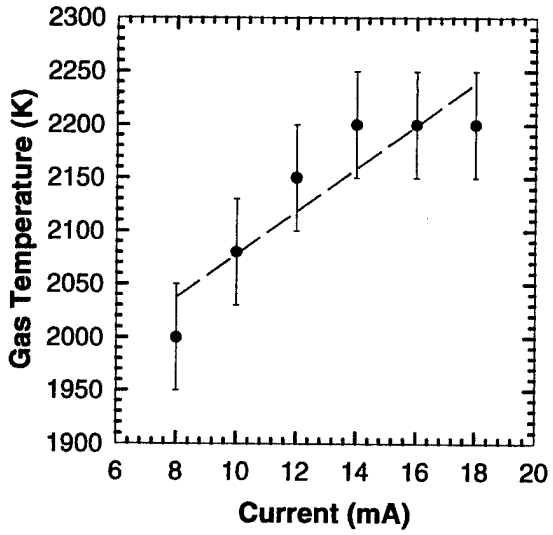

Figure 2 Gas temperature versus glow discharge current at a constant voltage of 570 V in humid air at one atmosphere. The discharge is confined by two 1.5 mm wide and 1.5 mm deep alumina plates, 0.5 mm apart.

Experimental Setup and Procedures

The apparatus used for VOC remediation consists of a plasma discharge cell (Fig. 3(a)) and a gas analytic system. The schematic diagram of the remediation system is shown in Fig. 3(b). The discharge chamber is made of three 2.75-inch diameter Conflat stainless steel flanges. A 1 mm wide and 1.5 mm deep slit is cut into a 5/8-inch diameter Macor rod, embedded in one of the flanges, in order to generate a narrow channel for the gas flowing through the plasma (Fig. 3(a)). The electrodes for the microhollow cathode discharge (MHCD) and the anode are made of molybdenum. The anode of the MHCD, which is separated from the anode of the glow discharge by a gap of 1.5 mm, is at ground potential. The plasma in the reactor is generated by first igniting the MHCD (sustaining voltage: ~400 V) and then igniting the glow discharge. The sustaining voltage for the MCS atmospheric pressure air glow discharge is 470 V, corresponding to an average electric field of 2.85 kV/cm.

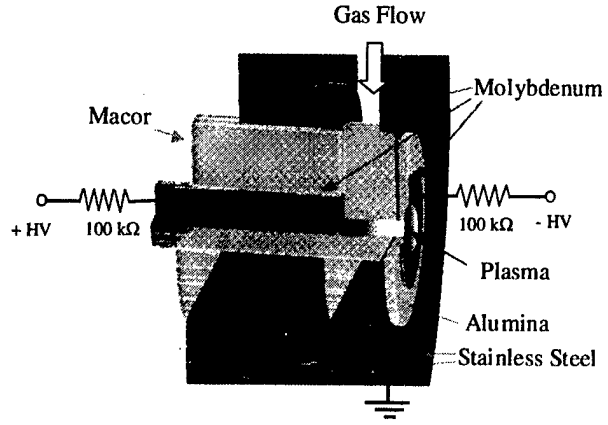

Fig 3(a) cross section of the discharge chamber (including cross section of the glow discharge),

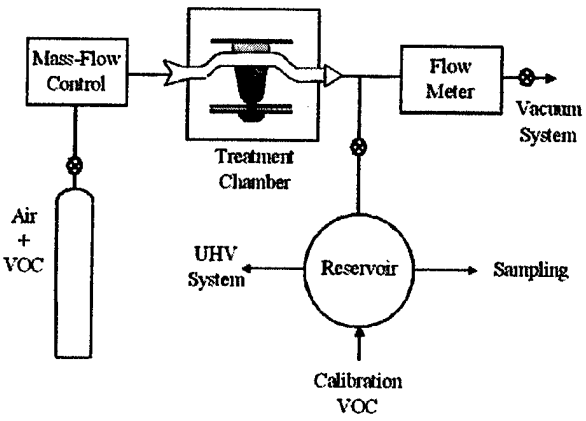

Fig 3(b) schematic diagram of the experimental setup

A premixed mixture of air and diluted VOCs was flowed through the treatment chamber. VOC/air mixtures were provided by Matheson Company. Benzene in dry air (benzene: 296 ppm, dry air: 99.97%) and methane in dry air (methane: 300 ppm, dry air: 99.97%) were used for the experimental study. Hexane in dry air (hexane: 306 ppm, dry air: 99.97%) is used as a calibration VOC. Before introduction of VOC/air mixtures, the whole flow system including the sampling reservoir is evacuated to pressures of less than 1 millitorr. In the experiments, the gas was flowed through the reactor at a rate of 100 sccm at atmospheric pressure (760 torr).

Processed gas samples were collected in the sampling reservoir by opening a Diaphragm valve, connecting the reservoir from the reactor output, without influencing the flow rate and the pressure of the discharge cell (flow rate fluctuation <2 sccm, pressure variance ≤10 torr). At room temperature, the sampling reservoir was filled with processed gas at a pressure of 200 torr and the filling process is slow enough to have the resevoir pressure holds constant at 200 torr for an indefinite period of time after the reservoir is isolated from the reactor. Then the calibration VOC was added to the reservoir to a total pressure of 800 torr. The same sampling procedure was repeated with the unprocessed gas mixture. A 200 μL gas sample was drawn by the syringe from the reservoir and analyzed by the GC/FID. The normalized VOC concentration (the fractional VOC) is the ratio of the area under the treated VOC peak to the area under the hexane peak for the processed case (Fig. 4 (a)), to the ratio of the areas for the unprocessed case (Fig. 4 (b)).

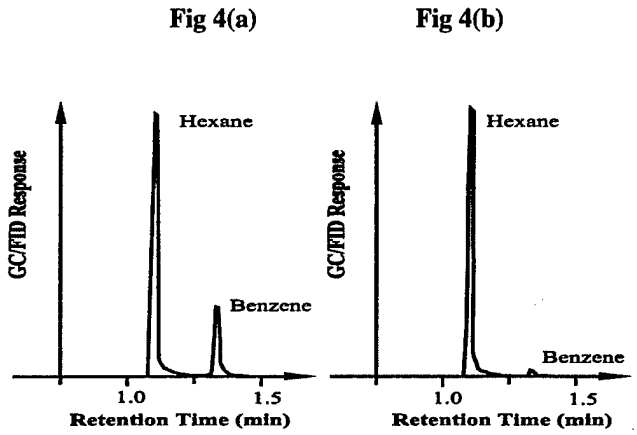

Figure 4 Chromatograms for benzene and hexane (which served as calibration VOC), measured by means of GC/FID: (a) chromatogram without plasma processing, and (b) results after plasma treatment. The benzene peak has been reduced to less than 10% of its initial value.

One of the most important parameters that determine the applicability of non-thermal plasma techniques for pollution control is the efficiency of the process [27]. The energy efficiency, or chemical processing efficiency [27], refers to the amount of the pollutants removed or decomposed for a given amount of energy deposited into the plasma. Since the energy density is related to the input plasma power and the residence time (the time for the gas molecules to pass the plasma column), the VOC concentration was measured with the discharge current at a constant discharge voltage, and with the flow rate as variable parameters.

We have focused in our studies on methane and benzene (300 ppm methane or benzene/dry air mixtures), respectively. Methane and benzene are two most stable and common VOCs with symmetrical chemical structures. In addition, both gases are relatively well-explored regarding their gaseous electronics characteristics, such as cross sections and rate coefficients. This allows us to simulate the chemical kinetics, as discussed in the modeling section.

Experimental Results

The efficiency of the removal of VOCs in a carrier gas, in our case, air, is measured in terms of fractional VOCs dependent on the input energy density. The term, fractional VOC, refers to the ratio of the VOC concentration after treatment to the initial VOC concentration. The fractional VOC versus the MCS glow discharge current is plotted in Fig. 5. The measured standard error for the fractional VOC is 0.02~0.03. The MCS glow discharge voltage was kept constant at 470 V and the flow rate was set to 100 sccm. The MCS glow discharge behaves like a normal glow discharge, with voltage independent of current [17,18]. For both methane and benzene, the fractional VOC decreases with increasing current in the range from 12 mA to 15 mA. For currents in excess of 15 mA, the fractional VOCs approach a constant value.

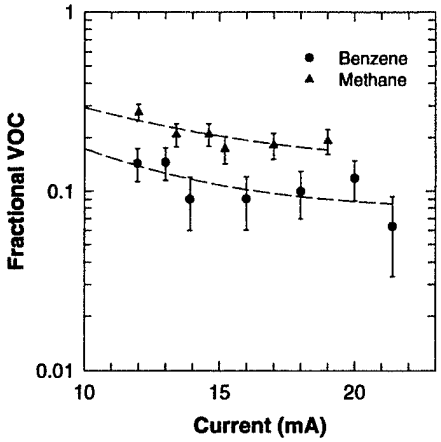

Figure 5 Normalized VOC (benzene and methane) concentrations versus current. The voltage was kept constant at 470 V at a flow rate of 100 sccm.

The input energy density is the input electrical power deposited in a unit volume times the average time, τ, of replacement for the gas in the volume (Vol):

$$\varepsilon = \frac{VI}{Vol} \cdot \tau = \frac{VI}{F}, \qquad (1)$$

where *V*, *I*, and *F* are the MCS glow discharge voltage, the MCS glow discharge current, and the gas flow rate, respectively. The input energy density can be altered by varying the glow discharge current at constant glow discharge voltage and flow rate. For a voltage of 470 V and a flow rate of 100 sccm, the fractional VOC is plotted versus input energy density in Fig. 6.

The decrease in fractional benzene and methane, respectively, can be expressed analytically by the following equation:

$$N_{VOC} = N_{res} + N_{VOC0} \exp(-\alpha \cdot \varepsilon) \qquad (2)$$

where N_{VOC0} and N_{VOC} are the concentration of the VOCs (benzene or methane) before and after the plasma processing, respectively, N_{res} is the residual VOC concentration (the lowest obtainable VOC concentration by the MCS glow discharge under the current condition), and α is a constant to measure the destruction efficiency for a specific VOC. The inverse of α is the energy density needed to reduce the VOC concentration to 1/e of its initial concentration, for the case that the residual VOC concentration is negligible. Equ. 2 was used to fit the data in Fig. 6 and N_{res} and α were determined using an algorithm for least squares. For benzene, the residual concentration, N_{res}, is $0.08\,N_{VOC0}$ and the measure of destruction efficiency, α, is 0.80 L/kJ. The concentration of methane decreases with a α number of 0.60 L/kJ, lower than that for benzene, and saturates at a value of $0.14\,N_{VOC0}$, higher than that for benzene. Thus, it takes more energy to reduce methane than to reduce benzene to the same concentration.

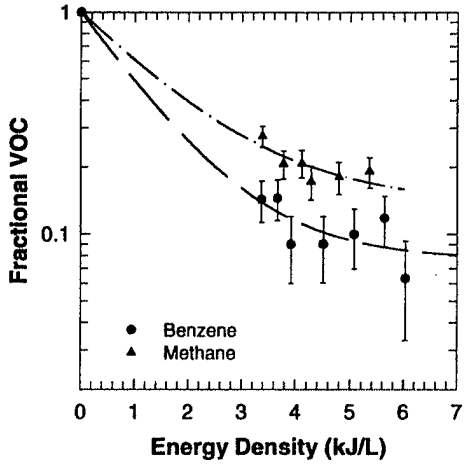

Figure 6 Fractional VOC (benzene and methane) concentrations versus energy density at a flow rate of 100 sccm and a constant MCS glow discharge voltage of 470 V.

The energy efficiency is defined as the mass of VOC molecules that are dissociated per energy input (reduced VOC mass density/ electrical energy density). In the experiment, the MHCDs functioned as the electron source to sustain the large volume glow and did not directly contribute to the reduction of VOCs. Thus, the power consumption of the MHCDs, ranging from 2.9 to 5.8 W, was not included in the efficiency evaluation. The reduced VOC mass density, the mass of the reduced VOC per unit volume, is given as

$$\text{Mass of reduced VOC} = R \times N_g \times (1 - N_{VOC}/N_{VOC0}) \times M_{VOC}/N_{avg}, \quad (3)$$

where R is the VOC concentration in air (300 ppm in our experiment), N_g is the gas number density, M_{VOC} is the molecular weight of a VOC molecule, N_{avg} is Avogadro's number, and N_{VOC}/N_{VOC0} is the fractional VOC. The molecular weight of benzene is 78 and that of methane is 16. The calculated energy efficiency for benzene destruction decreases from 0.87 g/kWh to 0.53 g/kWh for the energy density ranging from 3.37 kJ/L to 6.03 kJ/L [Fig. 7]. For methane, it decreases from 0.10 g/kWh to 0.15 g/kWh for the energy density increasing from 3.38 kJ/L to 5.36 kJ/L.

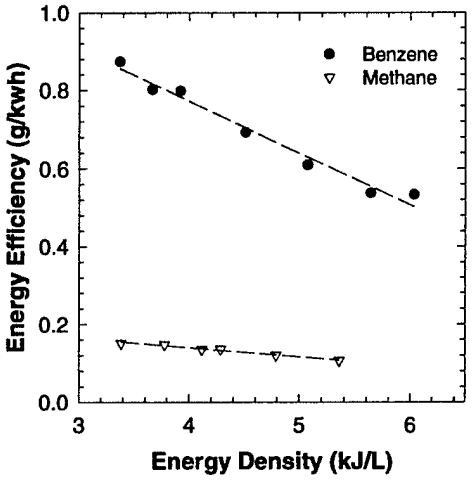

Figure 7 Energy efficiency versus electrical energy density in a direct current atmospheric pressure glow discharge in air

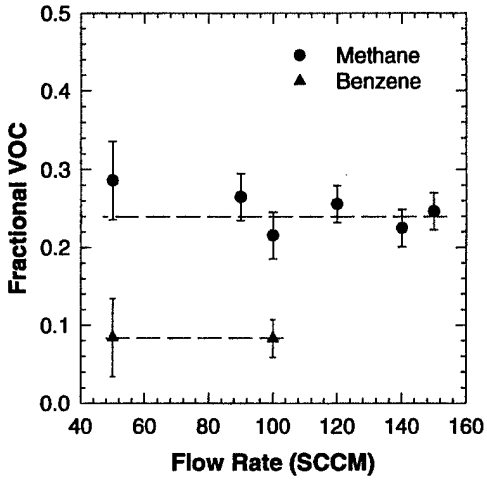

Figure 8 Methane and benzene dynamics: (a) fractional VOC versus flow rate, and (b) fractional VOC versus residence time at a discharge voltage of 470 V. The discharge current was 17 mA for methane/dry air, and 14 mA for benzene/dry air.

The VOC removal rate also depends on the residence time for the gas in the plasma column (equ.1). The residence time can be varied by changing the gas flow rate. At atmospheric pressure, the residence time for the VOC/dry air mixture flow to pass the plasma is:

$$T_{res} = \frac{d}{v_{flow}} = \frac{d \cdot A}{(F/60) \cdot (T_g/300)} \quad (4)$$

where T_{res} is the residence time in s, d is the diameter of the plasma column in cm, v_{flow} is the flow velocity in cm/s, A is the area of the flow cross section in cm^2, and F is the flow rate of the gas mixture in sccm. For the plasma column, an average gas temperature, T_g, of 1000 K with a diameter, d, of 0.5 mm were assumed. The area of the flow cross section is 1.5 mm^2. Consequently, the residence time is

$$T_{res} = 13.5/F \text{ ms} \quad (5),$$

with the flow rate varying from 150 sccm to 50 sccm, it increases from 90 μs to 270 μs.

The effect of residence time on the development of methane and benzene concentration in atmospheric pressure glow discharges was studied by varying the flow rates of the gas while keeping the discharge voltage and current constant (Fig. 8). For the methane/dry air plasma, the discharge voltage was 470 V, the current was 17 mA, and the flow rate was varied from 150 sccm to 50 sccm. For the benzene/dry air plasma, the discharge voltage was 470 V, the discharge current was 14 mA, and the flow rates varied from 100 sccm and 50 sccm. The standard error for the fractional VOCs was measured to be 0.03 to 0.05. Due to the sampling procedure, the error was larger for lower flow rate. In the error range, the fractional VOCs were found to be independent from the flow rate in the range from 50 sccm to 150 sccm. These indicate that neither fractional methane nor fractional benzene decreases when the residence time is increased in the range of flow rates used in

our experiments. The nearly constant value of the fractional VOCs indicates that there is a limitation of hydrocarbon extinction [44] within the applied flow rate range for this method. For lower current value (less than 10 mA) or higher flow rate (higher than 160 sccm), the MCS glow discharge becomes unstable, and therefore, no further measurement was conducted.

Modeling of the VOC Kinetics

The VOC kinetics in VOC/dry air plasmas was simulated by using KINEMA [28], a zero-dimension plasma chemistry simulation code. KINEMA includes a plasma chemistry kinetics simulator and an electron energy distribution function solver (ELENDIF [29]). ELENDIF allows us to calculate the temporal development of the electron energy distribution function by solving the Boltzmann equation. As a result, KINEMA is able to model the plasma chemistry reactions in a non-equilibrium plasma. The plasma chemistry in a non-thermal, atmospheric pressure air plasma was studied using an electric field dependent dry air plasma model [30]. In the model, the gas temperature was assumed constant at 2000 K. Up to 34 species including electrons, ions, radicals and neutrals were considered in the model. Their initial concentrations were given as 79% O_2, 21% N_2, and zero for all other species. For an applied electric field of 70 Td to 110 Td, corresponding to a voltage of 380 V to 604 V across a 1.5 mm gap in the atmospheric 2000 K air plasma, the electron density at steady state was found to vary in the range of 2.0×10^{11} cm^{-3} to 8.0×10^{12} cm^{-3} and the electron temperature varied between 1.1 eV to 1.9 eV. Atomic oxygen was found to have the highest concentration of all byproducts, on the order of 10^{16} cm^{-3} at steady state. The temporal development of the various byproducts in the atmospheric pressure air plasma is shown in Fig. 9 for a reduced electric field, E/N, of 140 Td applied for the first three microseconds and of 95 Td for up to 10 microseconds, as a sustaining electric field. Considering the uncertainty of the gas temperature, the gas temperature was varied from 1850K to 2200 K, it was found that the produced particle number densities have changes within one order of magnitude compared with their values at 2000 K. Increasing or decreasing the gas temperature further, the model becomes unstable under the given external e-field.

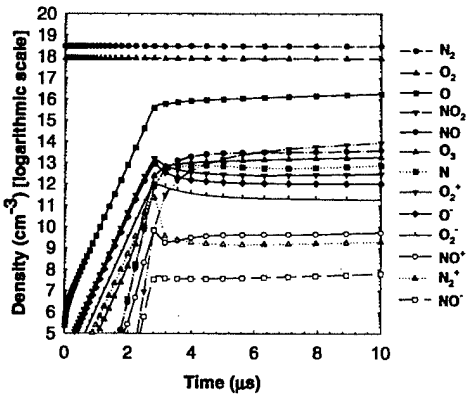

Figure 9 Temporal development of the byproducts in an atmospheric pressure air plasma

In order to obtain information on the temporal development of the VOC concentrations, two-temperature VOC/dry air plasma models were developed based on the simulation results from the dry air plasma model. The gas temperature was assumed to be constant at 2000 K. The electron temperature was calculated by means of ELENDIF, and was used to calculate the rate coefficients for the relevant reactions in the plasma. The reactions (and the rate coefficients) that were considered in the two-temperature plasma models were listed in table 1 and table 2 for methane/dry air and benzene/dry air mixtures, respectively. Only those reactions directly causing the VOC molecule destruction or ionization were considered, including electron impact dissociation, electron impact ionization, dissociative recombination, dissociative attachment, and chemical reactions with radicals and neutrals [10-11, 31-34]. The cross sections for methane and benzene, needed for the rate coefficient calculation, were obtained from references [35-36] and [37-41].

Table 1 The reactions and the rate coefficients of a two-temperature methane/dry air model

Reactions	Rate coefficients, $k = a_1(T_g/300)^{a_2}\exp(-a_3/T_g)$ (T_g: Kelvin)			Ref.
	a_1 (cm^3s^{-1})	a_2	a_3	
$CH_4 + O \rightarrow CH_3 + OH$	5.63e-10	0	6230	[34]

$CH_3 + OH \rightarrow CH_4 + O$	3.27e-14	2.2	2240	[34]
$CH_4 + H \rightarrow H_2 + CH_3$	9.71e-12	1.97	6679.6	[34]
$CH_3 + O + M \rightarrow CH_3O + M$ **	7.40e-14	-2.12	314.0	[34]
$CH_3 + H + M \rightarrow CH_4 + M$ **	3.2e-10	0	137.9	[34]

Reactions	Rate coefficients, $k = a_1 T_e^{a_2} \exp(-a_3/T_e)$ (T_e: eV)			Ref.
	a_1 (cm^3s^{-1})	a_2	a_3	
$CH_4 + e \rightarrow CH_3 + H + e$	9.67e-9	0.707	8.94	Cross section [35-36]*
$CH_4 + e \rightarrow CH_4^+ + 2e$	3.78e-9	0.820	12.83	Cross section [35]*
$CH_4 + e \rightarrow CH_3^+ + H + 2e$	5.43e-9	0.461	14.87	Cross section [35]*

Table 2 The reactions and the rate coefficients used in a two-temperature benzene/dry air model

Reactions	Rate coefficients, $k = a_1 (T_g/300)^{a_2} \exp(-a_3/T_g)$ (T_g: Kelvin)			Ref.
	a_1 (cm^3s^{-1})	a_2	a_3	
$C_6H_6 + O \rightarrow OH + C_6H_5$	1.53e-13	3.8	473	[34]
$C_6H_6 + O_2 \rightarrow HO_2 + C_6H_5$	1.05e-10	0	30198	[34]
$C_6H_6 + H \rightarrow H_2 + C_6H_5$	6.61e-10	0	3620	[34]

Reactions	Rate coefficients, $k = a_1 T_e^{a_2} \exp(-a_3/T_e)$ (T_e: eV)			Ref.
	a_1 (cm^3s^{-1})	a_2	a_3	
$C_6H_6^+ + e \rightarrow C_6H_5 + H^*$	1.0e-6			[33]
$C_6H_6 + e \rightarrow C_6H_5^- + H$	3.74e-12	-0.09	4.19	<5.7e-14, ~1.e-14 Cross section [37-41]*
$C_6H_6 + e \rightarrow C_6H_5 + H + e$	2.59e-9	0.108	5.63	Cross section [37-41]*
$C_6H_6 + e \rightarrow C_6H_6^+ + 2e$	6.98e-9	1.244	8.60	Cross section [34]*

* T_e is the electron temperature, T_g the gas temperature.

The constant a_1, a_2, and a_3 were derived from equation: $a_1 T_e^{a_2} \exp(-a_3/T_e) = \sqrt{\frac{2}{m}} \int_0^\infty f(E)\sigma(E)E \cdot dE$

with E being the energy, and m the electron mass. $k = \sqrt{\frac{2}{m}} \int_0^\infty f(E)\sigma(E)E \cdot dE$ is the rate coefficient;

$f(E)$ is the (normalized) Maxwellian distribution function, $\sigma(E)$ are the cross sections for methane and benzene dissociation and ionization, respectively.

** Reactions are three-body collisions; M stands for O_2 or N_2. In our model the reactions are treated as binary collisions by using equivalent two-body reaction rate constants for a constant density of the third body (atmospheric pressure; gas temperature 300 K to 2000 K).

Free-radical mechanisms based on initial activation of VOC molecules in reaction with oxygen atoms have been studied [5, 32, 42-43] for non-thermal plasma discharges. For CH_4, the primary activation reaction to cause the hydrocarbon molecule destruction can be

$$CH_4 + O \rightarrow CH_3 + OH, \quad (6)$$

with a rate coefficient of 2.50×10^{-11} cm^3s^{-1} at the gas temperature of 2000 K. CH_4 molecules can also be "activated" by energetic electron impact dissociation and ionization,

$$CH_4 + e \rightarrow CH_3 + H + e, \quad (7)$$

$$CH_4 + e \rightarrow CH_4^+ + 2e, \quad (8)$$

$$CH_4 + e \rightarrow CH_3^+ + H + 2e, \quad (9)$$

The reaction rate coefficients for electron impact dissociation (equ. (7)) ranges from 3.06×10^{-12} cm^3s^{-1} to 1.38×10^{-10} cm^3s^{-1} at the electron temperature of 1.1 eV to 1.9 eV. Electron impact ionization (equ. (8)) and dissociative ionization (equ. (9)) have the rate coefficients less than that of the electron impact dissociation for more than one order of magnitude due to their higher activation energy. From the dry air plasma simulation results, the O atom density is on the order of 10^{16} cm^{-3}, while the electron density is in the order of 10^{12} cm^{-3}.

The fractional VOC at time t is

$$\frac{N_{VOC}(t)}{N_{VOC0}} = \exp\left(-k_f N_{rad} t\right), \quad (10)$$

where N_{rad} represents either the atomic oxygen number density or the electron density, and k_f is the forward rate coefficient for chemical reaction or electron impact reaction. The decay rate is the product of k_f and N_{rad}. According to the modelling results, therefore, the decay rate due to atomic oxygen reaction is three orders of magnitude larger than that caused by electron impact. This conclusion still holds for an uncertain gas temperature higher than or less than 2000 K for 100 K.

The important reactions associated with benzene dissociation are

$$C_6H_6 + O \rightarrow OH + C_6H_5, \quad (11)$$

$$C_6H_6 + O_2 \rightarrow HO_2 + C_6H_5, \quad (12)$$

and

$$C_6H_6 + e \rightarrow C_6H_5 + H + e. \quad (13)$$

For gas temperatures of 2000 K and an electron temperature of 1.1 eV to 1.9 eV, the rate coefficients for benzene dissociation are 1.63×10^{-10} cm^3s^{-1}, 2.91×10^{-17} cm^3s^{-1}, and ranging from 1.57×10^{-11} cm^3s^{-1} to 1.43×10^{-10} cm^3s^{-1} for chemical reactions with O, O_2, and for electron impact reactions, respectively. The radical reactions with O cause the highest decay rate for benzene dissociation compared to the reactions with O_2 (five orders of magnitude lower) or electron impact (four orders of magnitude lower).

The rate coefficient of the chemical reaction with O for benzene dissociation, 1.63×10^{-10} cm^3s^{-1}, is larger than that for methane dissociation, 2.50×10^{-11} cm^3s^{-1}. Therefore, benzene decays faster than methane under the same plasma conditions, in agreement with experimental observations. The temporal development of the normalized VOC concentrations in VOC/dry air plasmas at atmospheric pressure with the electron temperature as a parameter is shown in Fig. 10. For the electron temperature ranging from 1.1 eV to 1.9 eV, it takes less than 16 μs for the fractional methane to decay to 10% of its initial value, and it takes about 2.5 μs for the fractional benzene to decay to 10% of its initial value. Simulation results also indicate that for a residence time of 0.1 ms, fractional methane can be reduced to less than 1% and fractional benzene can be completely removed (the value of the calculated fractional benzene reaches less than 10^{-10}). This has not been observed in our experiments. Instead of continuously (exponentially) decreasing with current and energy density, respectively, the fractional methane and benzene approach constant values [Figs 5, 6]. This discrepancy between the results of modeling and experiment may due to that the simplified two-temperature and zero-dimension VOC/dry air plasma models have limitation on quantitative prediction of the plasma chemistry for spatially variable VOC/dry air plasmas.

For a MCS discharge at atmospheric air, the diameter of the plasma column at current of 22 mA is about 0.86 mm [17]. The diameter decreases to half of the size when the plasma current decreases to 8.7 mA [17]. In any case, with a confining distance of 1 mm, the plasma does not fill the volume between the dielectric walls completely. The gas temperature profile of the atmospheric air plasma has a spatial distribution with a full width of the half maximum (FWHM) of 0.42 mm [23]. We can assume the FWHM of the gas temperature spatial profile to be less than 0.9 mm with the current (less than 22 mA) applied in the experiments. Therefore, between the plasma outer boundary and the dielectric walls, there is a cold zone,

where the gas temperature is much lower than that of the center of the plasma column. The reaction rate for oxygen recombination increases rapidly with gas temperature decreasing [45]. This results in a large gradient in atomic oxygen concentration and subsequently a fast diffusion of atomic oxygen towards the walls. As a consequence, as long as the residence time for plasma processing is much longer than the diffusion time (for low gas flow rates), decreasing the flow rate (i.e., increasing the residence time) will not increase the VOC destruction efficiency. Also because of the existence of the cold zone (dead zone for destruction reactions), varying the plasma parameters such as the deposited energy density cannot remove the residue VOCs. In other words, there is a limitation for the hydrocarbon extinction using this method under the applied condition. Similar limitations have been observed in other studies on combustion processes and were described as a quench branch for the dual-limit behavior of the chemical concentration as a function of the flow velocity [44]. However, limitations on the destruction efficiency can be relaxed by increasing the ratio between the overall processed volume and the volume confined in cold zones. This can be achieved by operating several discharges in parallel.

Summary

A non-thermal plasma with an electron density on the order of 10^{12} cm^{-3} and a gas temperature of 2000 K was generated in atmospheric pressure air. This plasma was generated in a direct current high-pressure glow discharge by applying several hundreds of volts to two electrodes. A microhollow cathode discharge (MHCD) was used as an external electron source to prevent glow-to-arc transitions, a common problem for conventional glow discharges. The direct current atmospheric pressure air glow has been applied for VOC remediation. Methane and benzene have been chosen as the target VOCs since they are two of the most stable hydrocarbons. An 80% removal rate has been obtained for methane remediation. The energy efficiency, 0.15 g/kWh for an initial concentration of methane 300 ppm, is in the energy efficiency range, 0.01 g/kWh to 4 g/kWh for an initial concentration of methane from 1000 ppm to 5 ppm in a dielectric barrier corona discharge [42]. For benzene, the remediation rate is as high as 90%, comparable with the results obtained by other non-thermal plasma technologies, for instance, low pressure glow discharges. The energy efficiency for benzene remediation in the system is 0.9 g/kWh, also comparable with efficiency obtained for benzene remediation in low pressure glow discharge in noble gases [10-11].

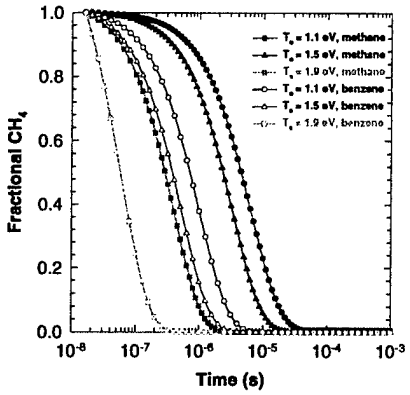

Figure 10 Normalized methane and benzene concentration dynamics in atmospheric VOC/dry air plasmas for various electron temperatures at constant gas temperature of 2000 K

The VOC dissociation mechanism was studied by simulating the kinetics of the species density in a dry air or a VOC/dry air mixture plasma using a zero-dimension plasma chemistry code, KINEMA. Atomic oxygen was found to have the highest concentration among the products in the dry air plasma and the free radical activation based on O atoms were considered as one of the most important dissociation reactions for VOC destruction. The computed decay time of methane and benzene in the high pressure air glow discharge is, even for the lowest assumed electron energy (1.1 eV), still less than the residence time of the gases in our micro reactor (Fig. 10). This fast decay, which is confirmed by our measurements taken while varying flow rates (Fig. 8) indicates that even higher destruction efficiencies can be reached by increasing the flow rate. However, even without further optimization, this dc atmospheric air glow discharge provides an effective technique, easy to implement in a gas stream, and offers an excellent alternative approach for VOC remediation among the non-thermal plasma technologies.

Acknowledgement

This work was supported by a grant from the US Air Force Office of Scientific Research.

References

[1] K. Vercammen, A. Berezin, F. Lox, and J. Chang, "Non-thermal plasma techniques for the reduction of volatile organic compounds in air streams: a critical review," *J. Adv. Oxid. Technol.* vol. 2, no. 2, pp. 312-329, 1997.

[2] L. Forst, L.M. Conroy, "Health effects and exposure assessments of VOCs," in *Odor and VOC Control Handbook*, H. J. Rafson, Ed. McGraw-Hill, 1998, pp. 3.1-3.27.

[3] M.L. Parsons, *Global Warming: The Truth Behind the Myth*, New York: Plenum Press, 1995, pp. 14-15.

[4] K. Urashima and J. Chang, "Removal of volatile organic compunds from air streams and industrial flue gases by non-thermal plasma technology," *IEEE Trans. on Dielectrics and Electrical Insulation*, vol. 7, no. 5, pp. 602-614, 2000.

[5] L.A. Rosocha and R.A. Korzekwa, "Removal of volatile organic compounds (VOCs) by atmospheric-pressure dielectric-barrier and pulsed-corona electrical discharges," *Electrical Discharges for Environmental Purposes – Fundamentals and Applications*, E.M.van Veldhuizen, Ed., Nova Science Publishers, Inc., Huntington, NY, 2000, pp. 245-278.

[6] T. Oda, R. Yamashita, I. Haga, T. Takahashi, and S. Masuda, "Atmospheric pressure discharge plasma decomposition for gaseous air contaminants - trichlorotrifluoroethane and trichloroethylene," *IEEE Tran. Ind. Appl.*, vol. 32, pp. 227-232, 1996.

[7] J. Chang, "Energetic electron induced plasma processes for reduction of acid and greenhouse gases in combustion flue gas," *NATO ASI Series, G 34, Part A: Non-Thermal Plasma Techniques for Pollution Control*, B.M. Penetrante and S.E. Schultheiss, Eds., Springer-Verlag, Berlin, Heidelberg, 1993, pp. 1-31.

[8] J. Chang, T. Myint, A. Chakrabarti and A. Miziolek, "Removal of carbon tetrachloride from air stream by a corona torch plasma reactor," *Jpn. J. Appl. Phys*, vol. 36, pp. 5018-5024, 1997.

[9] T. Yamamoto, P.A. Lawless, and L.E. Sparks, "Triangle-shaped dc corona discharge device for molecular decomposition," *IEEE Trans. Ind. Appl.*, vol. 25, no. 4, pp. 743-749, 1989.

[10] D. L. McCorkle, W. Ding, C. Ma and L. A. Pinnaduwage, "Dissociation of benzene and methylene chloride based on enhanced dissociative electron attachment to highly excited molecules," *J. Phys. D: Appl. Phys.*, vol. 32, pp. 46-54, 1999.

[11] D.L. McCorkle, W. Ding, C. Ma and L. A. Pinnaduwage, "Dissociation of benzene in a pulsed glow discharge," *J. Appl. Phys.*, vol. 86, no. 7, pp. 3550-3557, 1999.

[12] E.E. Kunhardt, "Generation of large-volume, atmospheric-pressure, nonequilibrium plasmas," *IEEE Trans. Plasma Sci.*, vol. 28, no. 1, pp. 189-200, 2000.

[13] E.P. Velikhov, S.A. Golubev, Y.K. Zemtsov, A.F. Pal', I.G. Persiantsrv, V.D. Pis'mennyi, and A.T. Rakhimov, "Non-self-sustained stationary gas discharge induced by electron-beam ionization in N_2-CO_2 mixtures at atmospheric pressures," *Sov. Phys.-JETP*, vol. 38, pp. 267, 1974.

[14] N.W. Harris, F. O'Neill, and W.T. Whitney, "Operation of a 15-atm. electron-beam-controlled CO_2," *Appl. Phys. Lett.*, vol. 25, no. 3, pp. 148-151, 1974.

[15] V.Y. Aleksandrov, D.B. Gurevich, L.V. Kulagina, M.S. Lebedev, and I.V. Podmoshenskii, "Self-sustaining volume discharge at atmospheric pressure," *Sov. Phys. Tech. Phys.*, vol. 20, pp. 62-67, 1975.

[16] A.F. Gibson, T.A. Hall, and C.B. Hatch, "Discharge stabilization in HF lasers using resistive electrodes," *IEEE J. Quantum Electron., QE-13*, vol. 801-803, 1977.

[17] R.H. Stark and K.H. Schoenbach, "Direct current glow discharges in atmospheric air," *Appl. Phys. Lett.*, vol. 74, no. 25, pp. 3770-3772, 1999.

[18] R.H. Stark and K.H. Schoenbach, "Direct current high-pressure glow discharges," *J. Appl. Phys.*, vol. 85, no. 4, pp. 2075-2080, 1999.

[19] R.H. Stark and K.H. Schoenbach, "Electron heating in atmospheric pressure glow discharges," *J. Appl. Phys.*, vol. 89, no. 7, pp. 3568-3572, 2001.

[20] K.H. Schoenbach, A. El-Habachi, W. Shi and M. Ciocca, "High pressure hollow cathode discharges," *Plasma Sources Sci. Technol.*, vol. 6, pp. 468-477, 1997.

[21] A.D. White, "New hollow cathode glow discharge," *J. Appl. Phys.*, vol. 30, no. 5, pp. 711-719, 1959.

[22] R. Block, O. Toedter and K.H. Schoenbach, "Power considerations in the glow discharge at atmospheric pressure," 30th Plasmadynamics and Lasers Conference, AIAA 99-3434, 1999.

[23] F. Leipold, R.H. Stark, A. El-Habachi and K.H. Schoenbach, "Electron density measurements in an atmospheric pressure air plasma by means of infrared heterodyne interferometry," *J. Phys. D: Appl. Phys.*, vol. 33, pp. 2268-2273, 2000.

[24] Y.S. Akishev, A.A. Deryugin, I.V. Kochetov, A.P. Napartovich, and N.L. Trushikin, "DC glow discharge in air flow at atmospheric pressure in connection with waste gases treatment," *J. Phys. D: Appl. Phys.*, vol. 26, pp. 1630-1637, 1993.

[25] Y.S. Akishev, A.A. Deryugin, V.B. Karalnik, I.V. Kochetov, A.P. Napartovich, and N.I. Trushkin, "Numerical-simulation and experimental-study of an atmospheric-pressure direct-current glow-discharge," *Plasma Phys. Rep.*, vol. 20, pp. 511-524, 1994.

[26] Y.S. Akishev, A.A. Deryugin, N.N. Elkin, I.V. Kochetov, A.P. Napartovich, and N.I. Trushkin, "Calculation of air glow-discharge spatial structure," *Plasma Phys. Rep.*, vol. 20, pp. 437-441, 1994.

[27] B.M. Penetrante, J.N. Bardsley and M.C. Hsiao, "Kinetic analysis of non-thermal plasmas used for pollution control," *Jpn. J. Appl. Phys.*, vol. 36, pp. 5007-5017, 1997.

[28] Kinema Research & Software, L.L.C, "Kinema for windows 95, the plasma chemistry code," [Online]. Available: http://www.kinema.com/kinema.

[29] Kinema Research & Software, L.L.C, "Elendif for windows 95, the boltzmann equation solver," [Online]. Available: http://www.kinema.com/kinema.

[30] C. Jiang, *The Application of Atmospheric Pressure Glow Discharges in Air for VOC Remediation*, PhD Dissertation, Old Dominion University, 2002, pp. 71-82.

[31] M.A. Lieberman and A.J. Lichtenberg, *Principles of Plasma Discharges and Materials Processing*, John Wiley & Sons, Inc., 1994, pp. 224-234.

[32] C.M. Nunez, G.H. Ramsey, W.H. Ponder, J.H. Abbott, L.E. Hamel, and P.H. Kariher, "Corona destruction: an innovative control technology for VOCs and air toxics," *Air & Waste*, vol. 43, pp. 242-247, 1993.

[33] H. Abouelaziz, J.C. Gomet, D. Pasquerault, B.R. Rowe, and J.B.A. Mitchell "Measurements of $C_3H_3^+$, $C_5H_3^+$, $C_6H_6^+$, $C_7H_5^+$ and $C_{10}H_8^+$ dissociative recombination rate coefficients," *J. Chem. Phys.*, vol. 99, pp. 237-243, 1993.

[34] NIST, "Chemical Kinetics Database on the Web," *Standard Reference Database 17*, Version 7.0, Release 1.2, [online]. Available: http://kinetics.nist.gov/index.php.

[35] D.K. Davies, L.E. Kline, and W.E. Bies, "Measurements of swarm parameters and derived electron collision cross sections in methane," *J. Appl. Phys.*, vol. 65, no. 9, pp. 3311-3323, 1989.

[36] R.K. Jones, "Absolute total cross section for the scattering of low energy electrons by methane," *J. Chem. Phys.*, vol. 82, no. 12, pp. 5424-5427, 1985.

[37] P. Mozejko, G. Kasperski, C. Szmytkowski, G.P. Karwasz, R.S. Brusa, and A. Zecca, "Absolute total cross section measurements for electron scattering on benzene molecules," *Chem. Phys. Lett.*, vol. 257, pp. 309-313, 1996.

[38] M.H.F. Bettega, C. Winstead, and V. McKoy, "Elastic scattering of low-energy electrons by benzene," *J. Chem. Phys.*, vol. 112, no. 20, pp. 8806-8812, 2000.

[39] NIST, "Table of BEB Cross Sections at Specific Energies," [online]. Available: http://physics.nist.gov/PhysRefData/Ionization/EII_table.html.

[40] R. Azria and G.J. Schulz, "Vibrational and triplet excitation by electron impact in benzene," *J. Chem. Phys.*, vol. 62, no. 2, pp. 573-575, 1975.

[41] E.E. Rennie, C.A.F. Johnson, J.E. Parker, D.M.P. Holland, D.A. Shaw, M.A. Hayes, "A study of the spectroscopic and thermodynamic properties of furan by means of photoabsorption, photoelectron and photoion spectroscopy," *Chem. Phys.*, vol. 236, pp. 365-385, 1998.

[42] L.N. Krasnoperov, L.G. Krishtopa, and J.W. Bozzelli, "Study of volatile organic compounds destruction by dielectric barrier corona discharge," *J. Adv. Oxid. Tech.*, vol. 2, no. 1, pp. 248-256, 1997.

[43] L.G. Krishtopa and L.N. Krasnoperov, "Destruction of isotopically enriched nitric oxide, $^{15}N^{8}O$ in air in corona discharge: direct observation of NO_x reduction to molecular nitrogen," *J. Adv. Oxid. Tech.*, vol. 6, no. 1, pp. 30-34, 2003.

[44] P.D. Ronney, "Understanding combustion processes through microgravity research," in *Twenty-Seventh Symposium (International) on Combustion/The Combustion Institute*, 1998, pp. 2485-2506.

[45] W. Tsang, R.F. Hampson, "Chemical kinetic data base for combustion chemistry, part I. methane and related compounds," *J. Phys. Chem. Ref. Data*, vol. 15, pp. 1087-1279, 1986.

Direct Current Glow Discharges in Atmospheric Air

Abdel-Aleam H. Mohamed, Rolf Block, and Karl H. Schoenbach, *Fellow, IEEE*

***Abstract*—A microhollow cathode discharge was used as plasma cathode to sustain a stable direct current glow discharge in atmospheric pressure air. The length of the glow discharge column was varied from 1 mm to 2 cm, with the sustaining voltage increasing linearly with length. For glow discharges with currents on the order of 10 mA, the electron density in the air plasmas exceeded 10^{11} cm^{-3}, with highest values of almost 10^{13} cm^{-3} close to the plasma cathode. When two 8.5-mA discharges were operated in parallel, at a distance of 0.4 cm, the discharge plasmas were found to merge for electrode gaps exceeding 0.5 cm, an effect that can be used to generate large volume, homogenous air plasmas.**

***Index Terms*—Air, atmospheric pressure, direct current, glow discharge.**

RESEARCH on atmospheric pressure glow discharges in air is motivated by applications such as instantly activated reflectors and absorbers for electromagnetic radiation, detoxification of polluted air, and surface treatment. One of the major obstacles in obtaining stable atmospheric pressure glow discharges in air at high electron densities ($>10^{11}$ cm^{-3}) is the glow-to-arc transition. This instability generally develops in the cathode fall, a high field region, which in self-sustained glow discharges is required for the emission of electrons from the cathode through ion impact. By using a microhollow cathode discharge (MHCD) as electron source, the cathode fall can be reduced or even eliminated. Using this concept, stable air discharges between the plasma cathode and a third positively biased electrode, 2-mm apart, could be generated [1]. The electron density in these discharges may reach values as high as 10^{13} cm^{-3} at a gas temperature of approximately 2000 K [1], [2].

We have explored the scaling of these dc atmospheric pressure air glow discharges to larger dimensions, by extending the gap distance up to 2 cm, and by placing two atmospheric pressure air glows in parallel. The MHCD was sustained between molybdenum electrodes, separated by a 130-μm-thick alumina layer, with a 130-μm hole through the sample. The glow discharge between the MHCD and the third electrode was ignited at small gap lengths, in order to keep the ignition voltage low, and then the gap was extended to the desired distance. The current voltage characteristics of both the plasma cathode (MHCD) and the air glow was measured, and photographs of the discharge in the visible were taken with a charge coupled device (CCD) camera. In Fig. 1, photographs of the 5 mm long air glow at three current levels are shown. The microhollow cathode (plasma cathode) current was held at 6 mA. The voltage across the glow discharge was, in all three cases, 840 V.

Manuscript received July 9, 2001; revised November 13, 2001. This work was supported by a grant from the U.S. Air Force Office of Scientific Research.

The authors are with the Physical Electronics Research Institute, Old Dominion University, Norfolk, VA 23529 USA (schoenbach@ece.odu.edu).

Publisher Item Identifier S 0093-3813(02)03171-5.

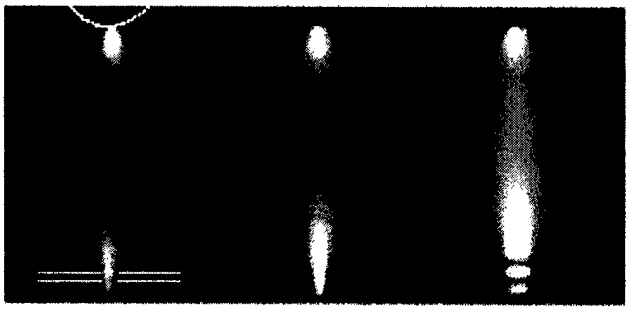

Fig. 1. Photographs of atmospheric pressure air glow discharges at currents of 5.3, 11.1, and 22 mA (from left to right). The electrodes are shown schematically in the photograph on the left.

Fig. 2. Photographs of the air glow discharges with various gap lengths ranging from 0.5 to 2 cm. The current was kept constant at 13 mA. The striations in the photographs are due to the limited resolution of the CCD camera.

Results of such optical measurements and of electrical measurements indicate two stable modes of operation depending on the ratio of glow discharge to MHCD current. For glow discharge currents less than the MHCD current, the center electrode serves as an MHCD anode (Fig. 1, 5.3-mA discharge). For glow discharge currents exceeding the microhollow cathode discharge current, the plasma cathode is not able to provide all the electrons for the glow discharge, and consequently, electron emission from the surface of the center electrode is taking over as electron supply process. The discharge then spreads over the surface of the center electrode, which serves as additional cathode. There is a slight indication of the plasma extending over the center electrode for the 11.1-mA discharge in Fig. 1. The effect is obvious for the 22 mA discharge.

The gap length, which in Fig. 1 is 5 mm, can easily be extended to larger values (Fig. 2). The discharge voltage increases linearly with gap length for constant discharge current. The plasma cross-section increases with increasing distance from the electrodes. For gaps of less than 1 cm, the widest

cross-section is at midpoint, for larger gaps it shifts closer to the anode.

Information on the electric field distribution along the glow discharge axis was obtained by varying the gap distance and recording the voltage at constant current. The electric field E decreases initially with increasing distance from the cathode, but approaches a constant value at a distance of approximately 0.5 cm from the plasma cathode. In the plasma region where E is independent of position, E increases with decreasing discharge current. It was measured as 1.2 kV/cm for a discharge current of 13 mA, and increased to 2 kV/cm for 5-mA currents. Values of the cathode fall voltage were obtained by extrapolating the voltage versus gap distance curve to zero gap distance, and by recording the residual voltage. The cathode fall was found to be dependent on glow discharge current, varying from 40 V at 5 mA, to 22 V at 13 mA.

The electron density n_e was obtained from the plasma conductivity by using the information on the electric field distribution and the average current density, j (discharge current divided by plasma cross section)

$$n_e = j/(ev(E)) \tag{1}$$

where values for the drift velocity $v(E)$ were obtained from [3]. The electron density decreases for discharges with a current of 13 mA from values of 10^{13} cm^{-3} close to the plasma cathode to a constant value of approximately 10^{11} cm^{-3} at a distance from the cathode which corresponds to the largest plasma diameter.

The MHCD sustained air glow discharge has a negative differential resistance. Parallel operation of the high-pressure glow discharges, therefore, requires the use of ballast resistors for individual discharges. Two discharges were operated side by side, each carrying a current of 8.5 mA, with their axes 0.4 cm apart. It was found that for this configuration, the discharge formed individual plasmas up to a gap distance of approximately 0.5 cm. For larger distances, the plasmas merge (Fig. 3, top), and eventually, with increasing gap a homogeneous plasma layer is formed (Fig. 3, bottom). Using arrays of microhollow plasma sustained glow discharges allows us, therefore, to generate large volume, homogeneous atmospheric pressure air plasmas with electron densities exceeding 10^{11} cm^{-3}.

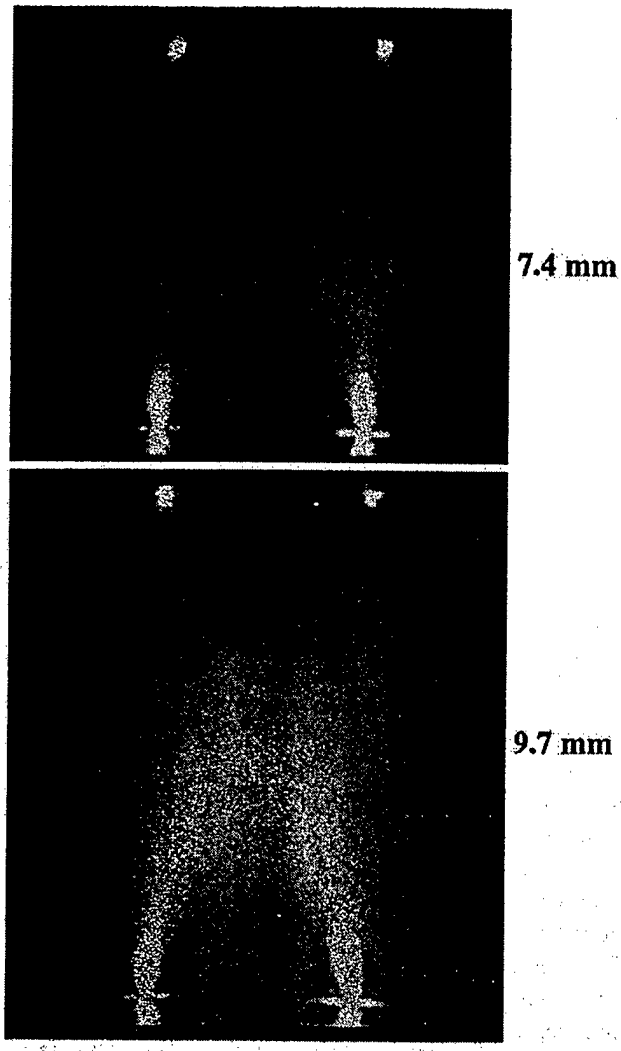

Fig. 3. Parallel operation of two air glow discharges. The individual discharges carry a current of 8.5 mA.

REFERENCES

[1] R. H. Stark and K. H. Schoenbach, "Direct current glow discharges in atmospheric air," *Appl. Phys. Lett.*, vol. 74, pp. 3770–3772, 1999.

[2] F. Leipold, R. H. Stark, A. El-Habachi, and K. H. Schoenbach, "Electron density measurements in an atmospheric pressure air plasma by means of IR heterodyne interferometry," *J. Phys. D, Appl. Phys.*, vol. 33, pp. 2268–2273, 2000.

[3] A. V. Phelps, "Excitation and ionization coefficients," in *Gaseous Dielectrics V*, L. G. Christophourou and D. W. Bouldin, Eds. New York: Pergamon, 1987, pp. 1–9.

Conference Papers and Book Chapters

Frank Leipold, Abdel-Aleam H. Mohamed, and Karl H. Schoenbach, "High Electron Density, Atmospheric Pressure Air Glow Discharges," Conf. Record, 25th Modulator Symposium, Hollywood, CA, 2002, p. 130.

Robert H. Stark, Hisham Merhi, and Karl H. Schoenbach, "Pulsed Electron Heating of Atmóspheric Pressure Air Glow Discharges," Digest of Technical Papers, PPPS2001, Pulsed Power Plasma Science 2001, Las Vegas, NV, p. 281.

Ulrike Hahn, Matthias Herrmann, Frank Leipold, and Karl H. Schoenbach , "Nanosecond, Kilovolt Pulse Generators," Digest of Technical Papers, PPPS2001, Pulsed Power Plasma Science 2001, Las Vegas, NV, p. 1575.

Chunqi Jiang, Robert H. Stark, and Karl H. Schoenbach, "Benzene Destruction in Direct Current and Pulse-Superimposed Atmospheric Pressure Air Glow Discharges," Digest of Technical Papers, PPPS2001, Pulsed Power Plasma Science 2001, Las Vegas, NV, p. 1110.

Book Chapter: Robert H. Stark, Hisham Merhi, Chunqi Jiang, and Karl H. Schoenbach, "Excimer Emission From Pulsed High Pressure Xenon Glow Discharge," Gaseous Dielectrics IX, Loucas G. Christophorou and James K. Olthoff, eds, Kluwer Academic/ Plenum Publishers, New York, 2001, p. 257.

Book Chapter: Chunqi Jiang, Robert H. Stark, and Karl H. Schoenbach, "Benzene Destruction in Direct Current Atmospheric Pressure Air Glow Discharges," Gaseous Dielectrics IX, Loucas G. Christophorou and James K. Olthoff, eds, Kluwer Academic/ Plenum Publishers, New York, 2001, p. 263.

Manoj Nagulapally, Graham V. Candler, Christophe O. Laux, Lan Yu, Denis Packan, Charles H. Kruger, Robert H. Stark, Karl H. Schoenbach, "Experiments and Simulations of DC and Pulsed Discharges in Air Plasmas," 31st AIAA Plasmadynamics and Lasers Conf., Denver, CO, July 2000, paper AIAA 2000-2417.

Conference Record, 25th
Modulator Symposium,
Hollywood, CA 2002

HIGH ELECTRON DENSITY, ATMOSPHERIC PRESSURE AIR GLOW DISCHARGES

Frank Leipold, Abdel-Aleam H. Mohamed, and Karl H. Schoenbach
Physical Electronics Research Institute, Old Dominion University, Norfolk, VA 23529

Abstract

The pulsed electron heating effect has been studied on an atmospheric pressure air glow discharge. Application of a high voltage pulse causes a shift in the electron energy distribution function to higher energies. This causes a temporary increase of the ionization rate and consequently an increase of the electron density. The electron density after a 10 ns pulse application to a direct current glow discharge increased from its dc value of 2 10^{13} cm^{-3} to 2.8 10^{15} cm^{-3}. The average power density, required for sustaining the high pressure plasma with a given minimum electron density, was found to be lowered when the discharge was operated in a repetitive pulsed mode compared to a dc mode. For an atmospheric pressure air plasma, an average power density of 1.5 kW/cm^3 and 50 W/cm^3 is required for an average electron density of 10^{13} cm^{-3} and 10^{12} cm^{-3}, respectively. This value is less by a factor of three than that required to sustain a dc plasma with the same base electron density.

I. INTRODUCTION

Weakly ionized plasmas, generated in high pressure air glow discharges, reflect or absorb electromagnetic radiation in the microwave range and consequently act as temporally controllable barriers for this radiation: as plasma ramparts. Direct current microhollow cathode sustained glow discharges (MCSG) have been shown to provide plasmas with an electron density of 10^{13} cm^{-3}, required for reflection of microwave radiation of up to 30 GHz [1]. The MCSG plasma was found to be scalable in size by extending the electrode gap and by placing the discharges in parallel [2]. However, at equilibrium conditions, the power density required to sustain an atmospheric pressure air plasma of 10^{13} cm^{-3} electron density is approximately 5 kW/cm^3 [3], a value which makes these equilibrium plasmas difficult to scale to large volumes.

Pulsed electron heating has been shown to allow reduction of the electrical power, while keeping the average electron density at the required level for microwave reflection [4]. In order to explore the effect of pulsed electron heating on the temporal development of single discharges and discharge arrays we have measured the electrical and the optical response to pulsed electron heating with a temporal resolution on the order of 10 ns. Laser interferometry, electrical conductivity and optical spectroscopy was used to determine the temporal development of electron density, and gas temperature.

II. EXPERIMENTAL SETUP

The experimental setup is shown in Fig. 1. The atmospheric pressure air discharge(s) were operated in a direct current mode, with a 10 ns to 12 ns voltage pulse superimposed. The gap was set at 0.6 cm, the distance between discharge axes, for a three discharge arrangement, was 0.4 cm (Fig. 2).

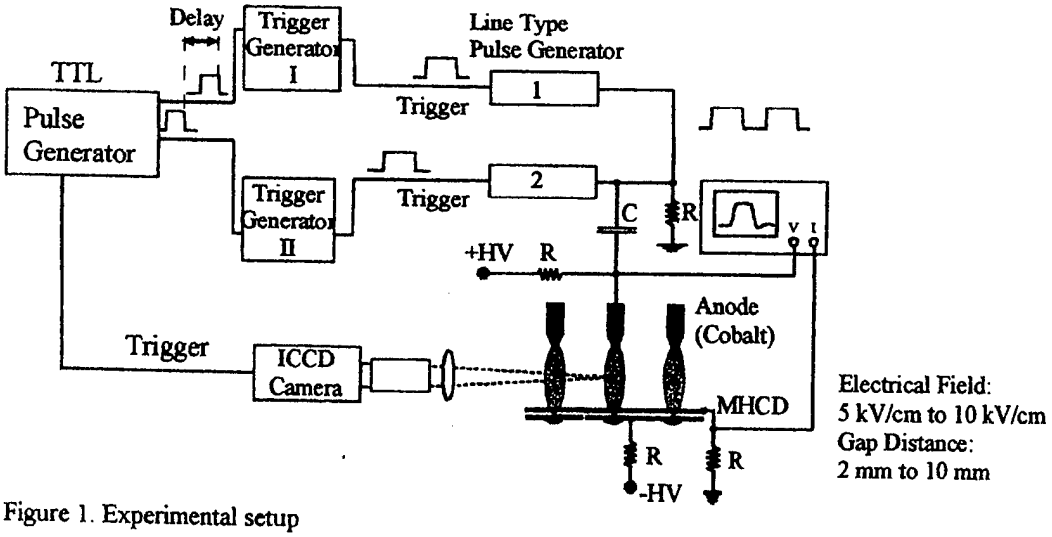

Figure 1. Experimental setup

Microhollow cathode discharges (MHCD) serve as plasma cathodes. In order to increase the size of the plasma, three discharges were operated in parallel [2]. The discharges can be operated either in DC with

superimposed pulses or in pulsed mode only. Two independent triggerable line type pulse generators provided 10 ns pulses. The applied diagnostics are emission spectroscopy for gas temperature measurements, interferometry [1], and conductivity measurements for electron density measurements. High-speed photography was used to obtain the spatial plasma distribution.

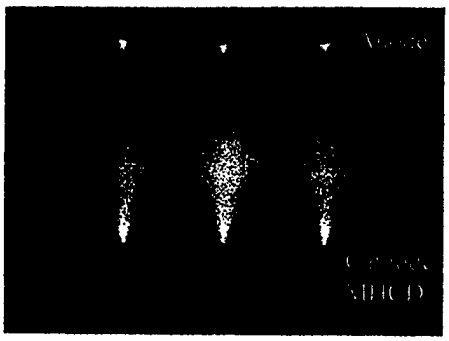

Figure 2. Three MCSGs operated in parallel at atmospheric pressure in air. Electrode gap: 6 mm, distance between two discharges: 4 mm.

III. EXPERIMENTAL RESULTS

A. Gas temperature

The gas temperature is obtained by comparison of a measured and a simulated spectrum of the 2nd positive system of nitrogen. For a DC glow discharge, the gas temperature was found to be 2200 K close to the cathode. The temperature in the plasma column reaches with increasing gap length a constant level of 2000 K (Fig. 3).

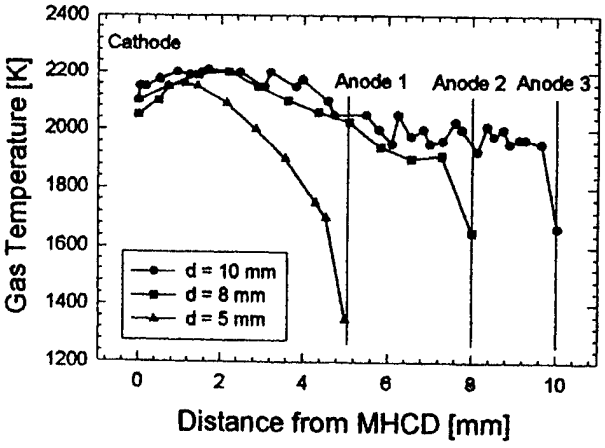

Figure 3. Gas temperature on the axis of a DC MCSG for various electrode distances. The discharge current was 13 mA.

For a DC operated MCSG with a superimposed pulse, an increase of the gas temperature by 300 K was measured 10 ns after pulse application (Fig. 4). Due to the low light intensity 25 ns after pulse application, information on the decay of the temperature could not be obtained with this method.

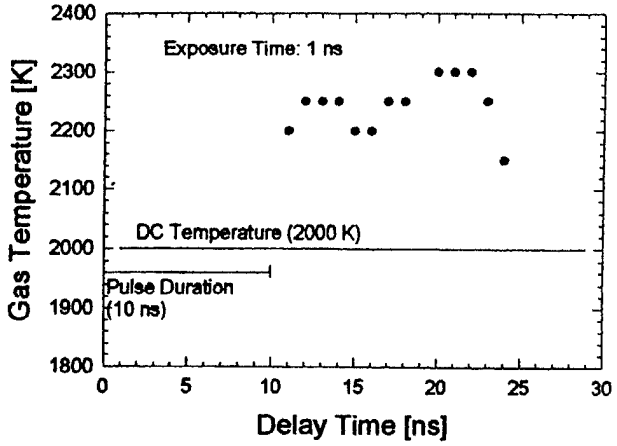

Figure 4. Temporal Development of the gas temperature in the center of a MCSG discharge operated DC with superimposed pulse. Electrode distance: 2 mm, $I_{MCSG\ DC}$ = 10 mA.

B. Electron density

The electron density was measured spatially and temporally resolved by means of infrared heterodyne interferometry. The radial profile was found to be time independent. It can be fit by a gaussian profile with a width of σ = 0.056 mm. Due to the limited temporal resolution, the electron density cannot be measured during the pulse. However, a measurement at 22 ns after pulse application provides an electron density of 2.8 10^{15} cm^{-3} for a discharge with a gap distance of 2 mm and an applied pulsed electrical field of 8 kV/cm. This indicates, that the electron density during the pulse is at least 2.8 10^{15} cm^{-3}. The radial electron density distribution in the center plane of the discharge for different times after pulse application is shown in Fig. 5.

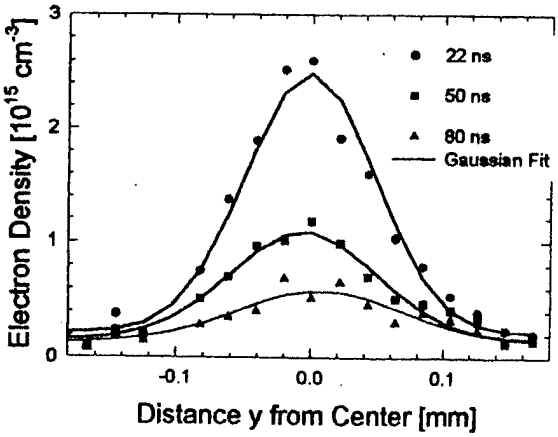

Figure 5. Radially resolved electron density in the center plane of the discharge for different times after pulse application. Electrode Distance: 2 mm, applied electrical field: 8 kV/cm.

The electron density after pulse application can also be obtained from measurements of the electrical field and current density. The relation between current density, electron density and electrical field is given by the equation:

$$J = n_e e v(E/n) \quad (1)$$

The electron density was calculated using average values of electric field (E = V/d) and current density J. The current density is given by the measured current and the spatial distribution profile of the electron density, which is assumed to be represented by the optical emission profile. Photographs of the discharge plasma for different times after pulse application are shown in Fig. 6. The exposure time is 5 ns. The drift velocity v, which depends on the reduced electrical field, varies between 2 10^4 m/s and 10^5 m/s for reduced electrical fields between 10 Td and 200 Td [5].

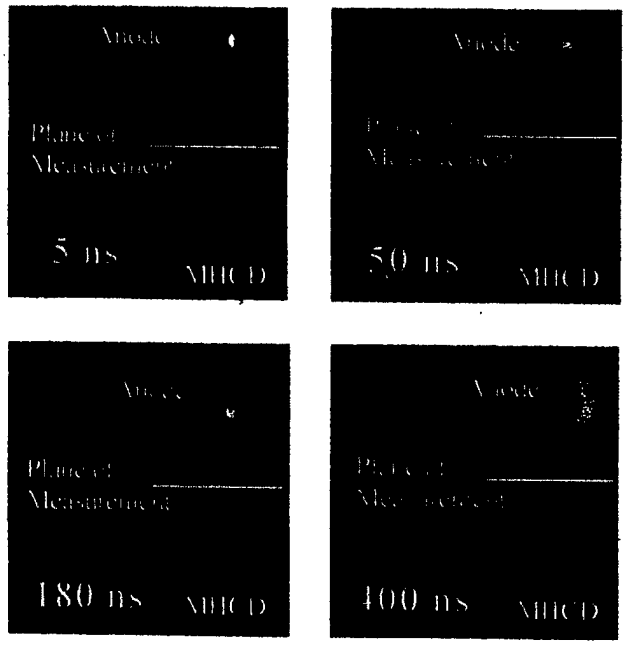

Figure 6. Photographs of the MCSG for different times after pulse application. Electrode gap: 2mm, applied electrical field: 10 kV/cm [6].

For an applied electrical field of 10 kV/cm and an electrode distance of 2 mm, the FWHM of the radial profile was found to be 0.16 mm. The profile is time independent. The electron density after pulse application versus the reduced electrical field is shown in Fig. 7.

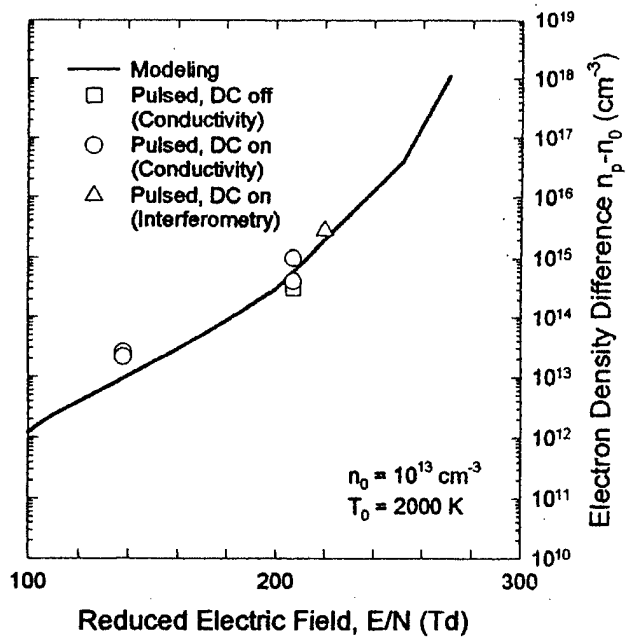

Figure 7. Electron density difference after a 10 ns pulse application versus the applied electrical field. The solid line represents modeling results [4].

For high pulsed electrical field, the dc contribution to the electron density can be neglected. For investigation of the electron heating effect for low applied electrical fields, the current of the discharge has to be turned off before the pulse is applied. A typical temporal development of the current is shown in Fig. 8.

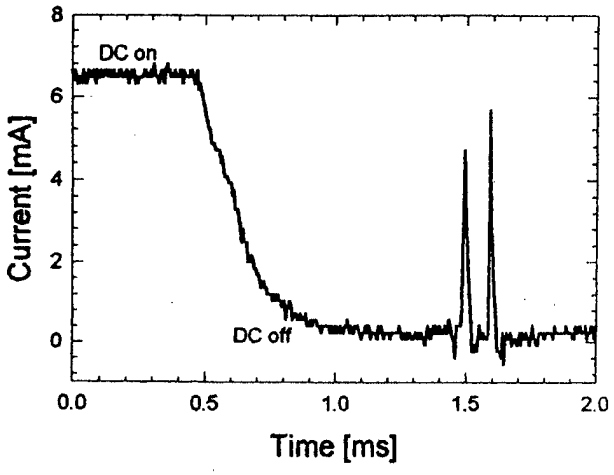

Figure 8. Temporal development of the discharge current. Before the two voltage pulses were applied, the direct current was turned off.

C. Power Density

The power density, P, for repetitive pulsed mode is:

$$P = E\,J\,t_{Pulse} / t_{Rep} \qquad (2)$$

All factors in this equation can be expressed in terms of the electrical field intensity. The expression for the current density is given in equ. 1. The drift velocity in this equation depends on the reduced electrical field [5]. The repetition time, t_{Rep}, is the time, required for the electron density to decay from the peak value to a minimum value. In our case, the major electron loss process is dissociative recombination. Attachment can be neglected in atmospheric pressure air plasmas with a gas temperature exceeding 1500 K [7]. The repetition time t_{Rep} is therefore given by

$$t_{Rep} = (n_p - n_0)/(n_p * n_0\,\beta) \qquad (3)$$

where n_p is the peak electron density after pulse application, n_0 is the minimum electron density, and β is the recombination coefficient. As shown in Fig. 7, the peak electron density is a function of the applied reduced electrical field.

The total power consumption for atmospheric pressure plasmas with minimum electron densities versus the applied electrical field is shown in Fig. 9. The solid lines represents the modeling results and the squares and circles the experimental results. If the applied electrical field is too low, a high repetition rate is required, a mode of operation which approaches direct current operation. Consequently the power increases towards the dc value. With increasing electrical field, most of the energy is used to generate electron densities far exceeding the desired minimum value. This density decreases rapidly due to recombination and as shown in equ. 3, contributes only minimally to the repetition time. Consequently, there is an optimum electrical field for minimum power consumption, as shown in Fig. 9.

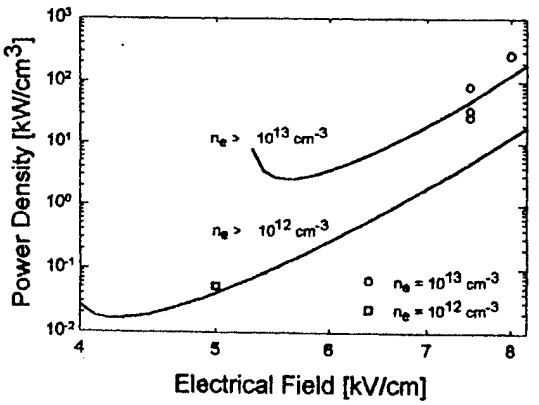

Figure 9. Power density versus the applied electrical field for different electron densities. The solid lines represent the modeling results, circles and squares represent measured values.

For an electron density of 10^{13} cm^{-3}, the minimum power density is 0.85 kW/cm^3. For an electron density of 10^{12} cm^{-3}, the power consumption can be reduced to 18 W/cm^3. The theoretical values are confirmed by the experimental results.

IV. SUMMARY

Atmospheric pressure air plasmas could be generated with characteristic dimensions of centimeters at gas temperatures of 2000 K. A reduction in the power consumption compared to the DC glow discharge could be achieved by operating the discharges in pulsed mode. Minimum power densities required to sustain atmospheric pressure air plasmas with electron densities of 10^{13} cm^{-3} and 10^{12} cm^{-3} are 850 W/cm^3 and 18 W/cm^3, respectively.

V. ACKNOWLEDGEMENT

This work was supported by the US Air Force Office of Scientific Research, and the National Science Foundation (Award # INT-0001438).

VI. REFERENCES

[1] Frank Leipold, Robert H. Stark, Ahmed El-Habachi, and Karl H. Schoenbach, "Electron Density Measurements in an Atmospheric Pressure Air Plasma by Means of IR Heterodyne Interferometry" J. Phys. D: Appl. Phys. 33, 2268 (2000).

[2] Abdel-Aleam H. Mohamed, Rolf Block, and Karl H. Schoenbach "Direct Current Glow Discharges in Atmospheric Air," IEEE Trans. Plasma Science. 30, 182 (2002).

[3] Robert H. Stark and Karl H. Schoenbach, "Direct Current Glow Discharges in Atmospheric Air," Appl. Phys. Lett. 74, 3770 (1999).

[4] Robert H. Stark and Karl H. Schoenbach, "Electron Heating in Pulsed Atmospheric Pressure Glow Discharges," J. Appl. Phys. 89, 3568 (2001).

[5] A. V. Phelps, "Excitation and Ionisation Coefficients", in Gaseous Dielectrics V, L. G. Christophourou, and D. W. Bouldin, eds., Pergamon Press, 1987, p. 1

[6] Hisham Merhi, Masters Thesis, Old Dominion University, Norfolk, VA, August 2001.

[7] Laux, C.O., Yu, L., Packan, D.M., Gessman, R.J., Pierrot, L., Kruger, C.H., and Zare, R.N., 30th AIAA Plasmadynamics and Lasers Conference, Norfolk, VA, June 28-July 1, 1999

Digest of Technical Papers,
PPPS2001, Las Vegas, June
2001

PULSED ELECTRON HEATING OF ATMOSPHERIC PRESSURE AIR GLOW DISCHARGES

Robert H. Stark, Hisham Merhi, and Karl H. Schoenbach
Physical Electronics Research Institute
Old Dominion University, Norfolk, VA 23529

Abstract

By applying electric field pulses with duration small compared to the time constant for glow-to-arc transition it is possible to increase the electron energy in high pressure glow discharges considerably over the steady state value. Repetitive pulsed operation allows us to generate plasmas with high average electron density at lower energy cost than with dc heating only. Measurements of the dynamics of the plasma column after pulse application show that the plasma diameter approaches a steady-state value after initial expansion, which is approximately half the dc plasma diameter. As a first step towards repetitive pulsed electric field operation, required to obtain a semi-dc plasma with high average electron density we have measured the temporal development of the voltage across the plasma for two subsequent pulses. The dual pulse generator, built for this purpose, utilizes two, 10 Ω striplines with high pressure spark gap as switches, which deliver two subsequent pulses directly to the load. The trigger pulses for the two switches can be adjusted in time between 1 μs and 10 ms. Pulse amplitudes of 15 kV have been reached, but amplitudes of up to 50 kV seem to be possible. Experiments with the dual pulse system provide information on the repetition rate required to sustain a certain average electron density. Operation in atmospheric pressure air with applied electric fields of 20 kV/cm and 10 ns duration allowed us to increase the electron density for a time of 2.3 μs to such values that the discharge voltage stayed below 30 V. Continuous operation in this discharge state would consequently require repetition rates of 450 kHz. Higher pulsed electric field operation would allow us to reduce the repetition rate.

I. INTRODUCTION

High pressure glow discharges are used in plasma processing, gas lasers, chemical and bacterial decontamination of gases, and as mirrors and absorbers of microwave radiation. Transient high pressure glow discharges, such as barrier discharges [1] and ac discharges [2] are already well established, but recently high pressure dc discharges in noble gases and in air with dimensions of up to centimeters have been generated by using a microhollow cathode discharge as plasma cathode [3,4,5]. The elimination of the cathode fall, the cradle for glow-to-arc transition has allowed us to generate dc glow discharges with electron densities as high as 10^{13} cm^{-3}, at gas temperature below 2000 K [6].

In these dc discharges the electron energy distribution is determined by the value of the reduced electric field (E/N), where E is the electric field intensity and N is the gas density. For dc atmospheric pressure air discharges with E/N of 32 Td, 1% of the electrons have an energy in excess of 2.1 eV, as computed by means of ELENDIF [7] Applying electric field pulses to these plasmas with amplitudes exceeding the equilibrium reduced fields, but of such duration that glow-to-arc transition is avoided, allows us to shift the electron energy distribution temporarily to much higher energies. Calculations using ELENDIF show a dramatic shift of the electron energy distribution function during a 10 ns, 200 Td high voltage pulse: 1% of the electrons have then an energy exceeding 67 eV at the end of the 10 ns pulse. The increase in the concentration of high-energy electrons causes an increase of the ionization rate coefficient. The consequent rise in charged particle density leads to an increase in electron lifetime. This non-equilibrium electron heating effect can consequently be used to reduce the power consumption of repetitively operated glow discharges from 5 kW/cm^3 for dc to 16 W/cm^3 for 3.5 ns pulses [8].

This power savings effect has been demonstrated with a single 10 ns pulse applied to a dc glow in atmospheric pressure air [9]. Besides reducing the power required for the sustainment of a weakly ionized plasma, pulsed electron heating in high pressure plasmas may also be used to populate excited states of excimer gases, e.g. noble gases, efficiently. The increased density of excited noble gas atoms, the precursors of noble gas dimers, leads to increased intensity of excimer radition as it was shown with pulsed discharges in high pressure xenon [10].

In order to explore the electron heating effect of short, repetitively electric pulses on atmospheric pressure glow discharges we have studied the response of an atmospheric pressure glow discharge to single and double 10 ns voltage pulses.

II. EXPERIMENTAL SETUP

The electrode geometry for the (MCS) glow discharge is shown in Fig. 1. It consists of a microhollow electrode system and a third positively biased electrode (anode) 2 mm apart from the microhollow electrodes. The microhollow electrodes are two molybdenum metal plates (100 μm thickness) with circular opening of 100 μm diameter, separated by a 100 μm thin dielectric layer of alumina. The microhollow cathode discharge (MHCD) between the cathode (-) and the ground electrode serves as

plasma cathode for high pressure glow discharge operation [3].

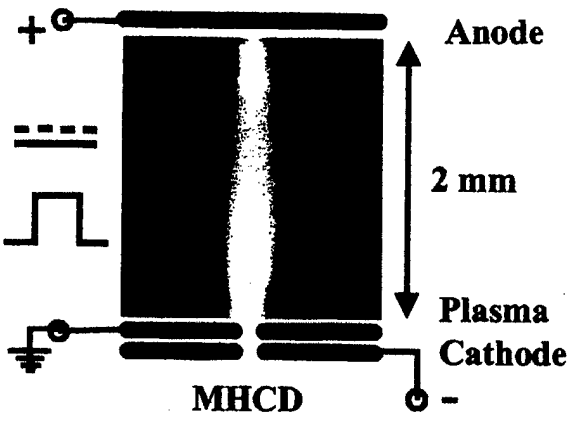

Fig. 1 Experimental setup: microhollow cathode sustained glow discharge in atmospheric pressure air.

In order to study the effect of pulsed electric fields on weakly ionized gases high voltage pulses were superimposed to the dc plasma. For single pulse operation the high voltage pulse was generated by a 10 Ω pulse forming network (PFN) in strip line geometry [9].

A high pressure spark gap was used as switch to transfer the energy stored in the PFN to the load and to allow fast rise time of the high voltage pulse. The rise time of the pulse voltage is 1-2 ns, and the pulse has an approximately rectangular shape. Pulse voltages of up to 4 kV were applied to the dc glow, generating average pulsed electric fields of up to 20 kV/cm in the high pressure plasma.

The schematics of the dual pulse generator is shown in Fig. 2. The pulse generator consists of two pulse forming networks (PFNs) in stripline geometry. Each stripline has 10 Ω impedance and can be charged individually to a maximum voltage of 30 kV. The energy which is stored in the striplines is then discharged into the load using triggerable high pressure spark gaps. This allows to control the temporal separation between the two pulses. Each stripline is matched with 10 Ω in order to avoid reflections

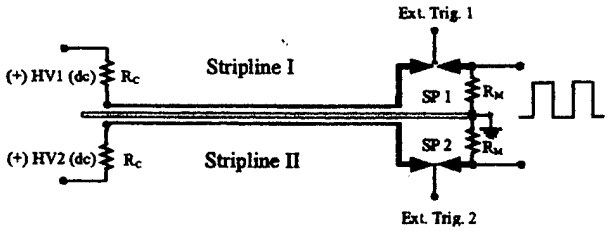

Fig. 2 Dual pulse generator.

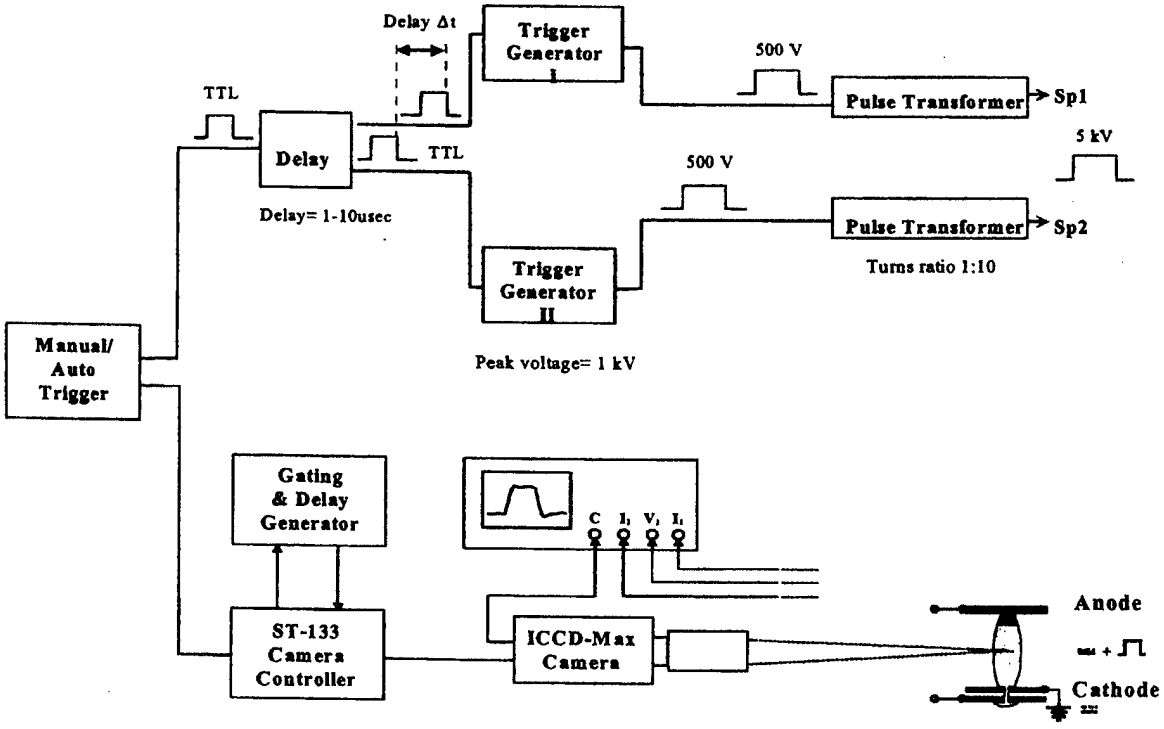

Fig. 3 Digital trigger and delay generator

As a consequence of the impedance matching, the maximum avaiable voltage at the load is only half the charging voltage. The pulse separation can be adjusted between several hundred ns up to several milliseconds. As each stripline can be operated independently from each other, the pulse amplitude can be adjusted independently up to the maximum voltage of approximately 15 kV. This allows not only to study the effect of a sequence of high voltage pulses on such plasmas. It also allows to study the influence of pulses with different amplitudes when the pulses are superimposed to the dc plasma. The pulse duration can be varied by changing the length of the striplines in the PFN.

A digital trigger and delay generator is used to vary the separation between the two high voltage pulses. The schematics is shown in Fig. 3. A 5V-TTL pulse is provided by a main trigger unit and then doubled and time shifted. Integrated MOSFET circuits are used to elevate the TTL level to 500 V. High voltage pulse transformers are utilized to increase the trigger voltage to approximately 5 kV, required to trigger the high pressure spark gaps.

The discharge current and the voltage across the pulsed glow discharge have been monitored by means of fast rise time, high voltage probes and a 500 MHz digitizing oscilloscope (Tektronix TDS 380). In addition, measurements of transient emission of plasma radiation in the visible have been performed. The optical emission from the center of the glow discharge gap was observed side-on by means of a photo multiplier tube (PMT - Hamamatsu 1350) with a sensitivity range between 200 nm and 700 nm. The PMT measurements were complemented by high-speed photography. A high-speed camera (ICCD Max, Stanford Research Institute) was used to study the development of the glow discharge plasma column temporally and spatially resolved. The camera is equipped with an image intensifier (micro-channel plate, MCP) and allows measurements with a temporal resolution up to 2 ns. However, due to the relatively low level of light emitted by the plasma, the exposure time was set to 200 ns. In addition to high speed photography a CCD video monitoring system was used to record the appearance of the glow discharge side-on in the visible and near ultraviolet.

III. RESULTS

A. Single Pulse Operation

Fig. 4 shows the increase in decay time with increasing pulsed electric field amplitudes. The decay time increases nearly linearly with pulsed electric field from 20 ns at 8.75 kV/cm to 3.8 μs at 20 kV/cm. For the intensity measurements the decay time has been defined as the time the intensity decays to approximately 10% of the initial intensity values. For the electrical measurements the decay time has been defined as the time for the voltage to increase from its lowest sustaining voltage level to approximately 70% of the dc value [9]. The dc voltage is in this case approximately 500 V.

The radial distribution of the visible emission of the pulsed plasma, at midgap for various times during and after pulse application (and for dc operation) was recorded with a high speed camera and is shown in Fig. 5. In the steady state the plasma diameter is approximately 200 μm. During the first nanoseconds when the voltage pulse is applied, and shortly after the pulse, the plasma column expands.

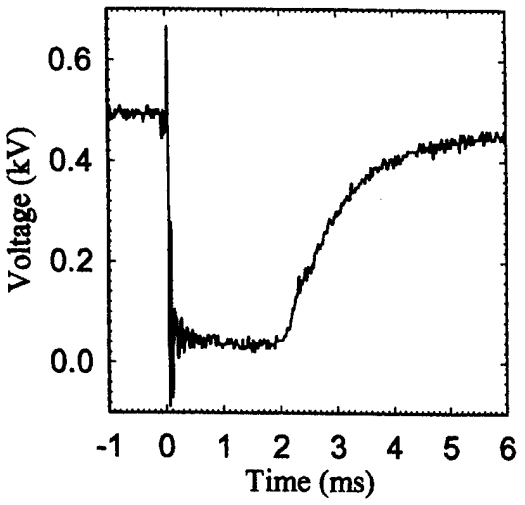

Fig. 4 Temporal development of discharge voltage

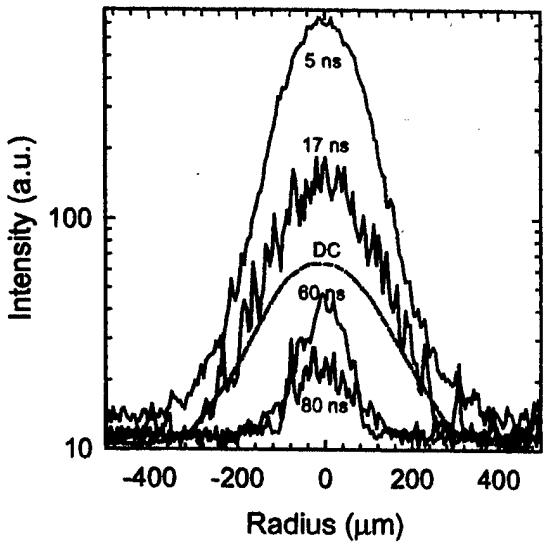

Fig. 5 Intensity distribution (visible) during and after pulse application measured by means of a high speed camera with 5 ns exposure time.

The plasma diameter is then reduced to approximately half of the maximum value for times ≥ 40 ns after the pulse.

B. Dual Pulse operation

In order to study the effect of multiple pulses on high pressure air plasmas, two 10 ns high voltage pulses have been superimposed to the dc atmospheric pressure air plasma. Fig. 6 shows the voltage across the discharge gap in response to two 10 ns high voltage pulses for two different pulse separations: 2.3 μs and 3.3 μs. At the beginning, before the high voltage pulse is applied, the voltage measured corresponds to the voltage required to sustain the dc glow. When the first pulse is applied the voltage drops to approximately 30 V until the plasma recovers and the conductivity decreases on a time scale of microseconds until the second pulse is applied. The second curve shows the voltage signal when the separation between the two pulses is reduced to a value such that the higher conductivity phases merge. For continuous operation in the high conductivity phase the repetition rate would need to be 450 kHz or higher. The repetition rate can be reduced by increasing the pulse electric field.

IV. SUMMARY

Atmospheric pressure plasmas have been generated in air with electron densities of 10^{13} cm^{-3} and above at gas temperatures of about 2000 K. For continuos operation power densities of 5 kW/cm^3 are required to sustain these plasmas.

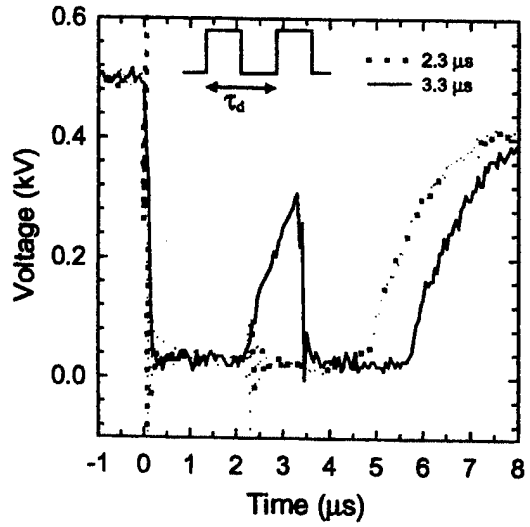

Fig. 6 Voltage across the discharge gap. Response of the plasma to two 10 ns high voltage pulses. (Pulse voltage: 2 kV, gap: 2 mm, pressure: 1 atm, humidity: 70%, microhollow cathode discharge current: 8 mA, glow discharge current: 10 mA)

In previous experiments it could be shown that pulsed electron heating can be used to reduce the power consumption of such plasma by several orders in magnitude. In experiments with dual high voltage pulses it could be shown that continuous operation at elevated electron temperatures requires repetition rates on the order of 500 kHz for 10 ns pulses with a relatively low electric field amplitude of 10 kV/cm. A reduction of the repetition rate can be achieved can be applying pulses with higher electric fields.

ACKNOWLEDGEMENT

This work was funded by the Air Force Office of Scientific Research (AFOSR) in cooperation with the DDR&E Air Plasma Ramparts MURI program and by the National Science Foundation.

V. REFERENCES

[1] B. Eliasson and U. Kogelschatz, IEEE Trans. Plasma Sci. 19, 309 (1991).
[2] S. Kanazawa, M. Kogoma, T. Moriwaki, and S. J. Okazaki, J. Phys. D 21, 836 (1988).
[3] Robert H. Stark and Karl H. Schoenbach, J. Appl. Phys. 85, 2075 (1999).
[4] Robert H. Stark and Karl H. Schoenbach, Appl. Phys. Lett. 74, 3770 (1999).
[5] Abdel-Aleam H. Mohamed, Rolf Block, and Karl H. Schoenbach, "Direct Current Glow Discharges in Atmospheric Air," submitted to IEEE Trans. Plasma Science.
[6] Frank Leipold, Robert H. Stark, Ahmed El-Habachi, and Karl H. Schoenbach, J. Phys. D: Appl. Phys. 33, 2268 (2000).
[7] W.L. Morgan and B.M. Penetrante, Computer Phys. Communications 58, 127 (1990).
[8] Manoj Nagulapally, Graham V. Chandler, Christophe O. Laux, Lan Yu, Denis Packan, Charles H. Kruger, Robert H. Stark, and Karl H. Schoenbach, 31st AIAA Plasmadynamics and Lasers Conference, Denver, CO, July 2000, paper AIAA 2000-2417.
[9] Robert H. Stark and Karl H. Schoenbach, J. Appl. Phys. 89, 3568 (2001).
[10] Robert H. Stark, Hisham Merhi, Chunqi Jiang, and Karl H. Schoenbach, Proc. 9th International Symposium on Gaseous Dielectrics, May 21-25, 2001, Ellicott City, ML, paper 40.

Digest of Technical Papers,
PPPS2001, Las Vegas, June
2001

Nanosecond, Kilovolt Pulse Generators

Ulrike Hahn*, Matthias Herrmann*, Frank Leipold, and Karl H. Schoenbach
Physical Electronic Research Institute, Old Dominion University, Norfolk, VA

Abstract

Nanosecond pulse generators, which provide kilovolt pulses, are required for applications such as pulsed lasers, electro-optical devices, electron heating of plasmas, and bioelectrics. Switches used to generate such short pulses include high-pressure spark gaps, photoconductive switches and semiconductor opening switches. Most of the pulse generators based on these switch technologies are designed for high voltage, high power applications. We have explored two concepts that of a MOSFET triggered, microspark Marx-Bank and a combined microspark-semiconductor switch system as a means to generate simple, inexpensive nanosecond pulse generators. The compact pulse generators allow us to generate electrical pulses of less than 10 ns duration, with amplitudes of several kV. The Mini Marx Bank has been shown to provide 6 kV pulses of 6 ns duration into a 10 MΩ load and 2 kV into a 50 Ω load. The second switch system, which utilizes a microspark switch and a commercially available diode to shorten the pulse, has provided 2.6 kV pulses of 2 ns duration into a 50 Ω load. The low cost of the generator components, and the compact size make these devices easy to built and convenient to use in nanosecond pulsed power experiments.

Introduction

Nanosecond pulse generators, which provide kilovolt pulses, are required for applications such as pulsed lasers, electro-optical devices, electron heating of plasmas, and bioelectrics. Electron heating of atmospheric pressure plasmas, e.g., requires electric field pulses with duration less than the characteristic time constant for glow-to-arc-transition, which is on the order of 10 ns [1,2]. Commercially available semiconductor switches, with long lifetime and easy to trigger, do not have the required fast rise time and don't at time provide voltage amplitudes across low impedance loads of more than 1.5 kV. Spark gaps on the other hand provide fast rise times and can be operated at high voltage, but suffer from limited lifetime.

We have focussed on configurations, which combine semiconductor switches and microdischarges as a means to utilize the advantage of both types of switches. In the following two such systems and experimental results, obtained with them, are described.

I. Micro Marx Bank Pulse Generator

Marx Banks are commonly used to generate short high voltage pulses [3]. We have used the Marx bank concept, with micro spark gaps as switches, and with a MOSFET as controllable, initiating switch. The circuit, shown in figure 1, consists of four stages. The first switch is a high voltage n-channel MOSFET 40N160 type by IXYS [IXYS, Santa Clara, CA, USA]. The maximum drain-source-voltage is limited to 1.6 kV. Its reliable operation and the ability of switching > 1.5 kV voltage made it the number one choice for this task.

Point-point electrodes made of brass are used for the triple microspark gap (Fig. 2). They have a conical shape in order to provide for high fields. The gap distance of this switch is adjusted by using threads. The microspark gaps were operated in atmospheric pressure air, and the gap distance was set to approximately 0.5 millimeters. An optional spark gap across the load shortens the pulse for high impedance loads. Connections to the circuit are made of copper foil, which is soldered onto the printed circuit board.

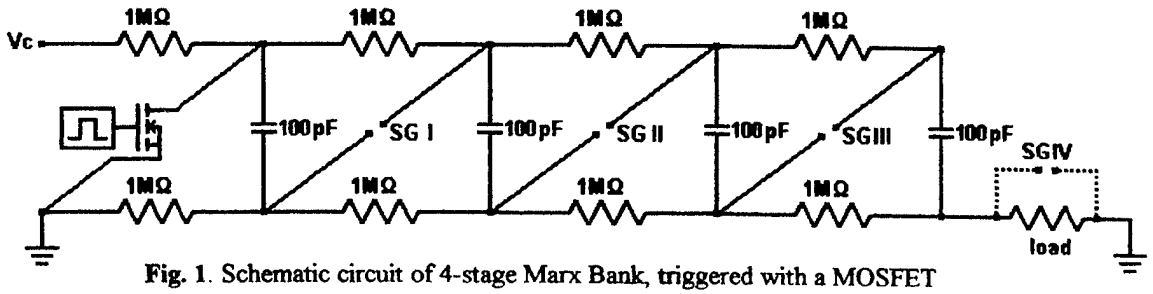

Fig. 1. Schematic circuit of 4-stage Marx Bank, triggered with a MOSFET

0-7803-7120-8/02/$17.00 © 2002 IEEE

Large distributed ground areas on the double-sided PCB ensure a good high-frequency behavior. Due to the need of low-inductive connections all devices of the circuit are surface mounted. The only exception is the MOSFET. The low-inductance ceramic chip capacitors have dimensions of 1.2 mm x 0.6 mm. This compact arrangement reduces the inductance to a minimum. A high voltage power supply was used for charging the capacitors through a charging resistor of 1 MΩ.

For diagnostics a high voltage probe with a rise time of 1.75 ns [Tektronix, Beaverton, Oregon, USA] has been used. The rise time of the 400 MHz oscilloscope is 1.9 ns.

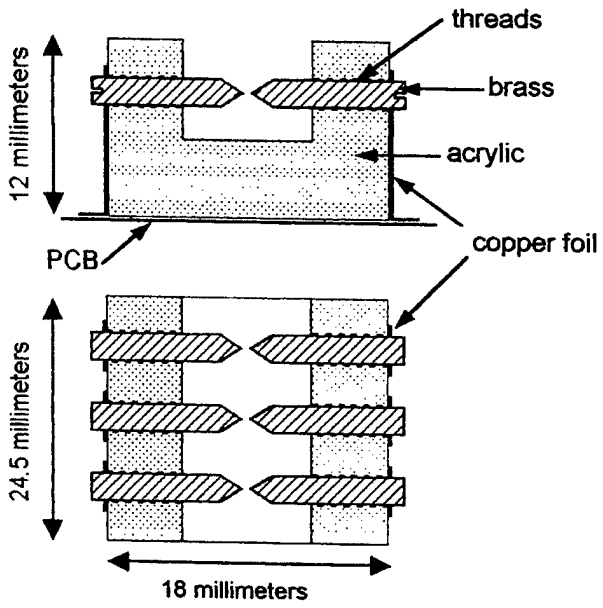

Fig. 2. Side-on and end-on view of electrode arrangement

Experimental results

Voltage pulses with a full width at half maximum (FWHM) of 5-6 ns could be generated with this system. The rise time was 2-3 ns. The amplitude, which can be controlled by the gap length of the microsparks, varied between 1.5 and 2 kV for a load of 50 Ω. In order to shorten the pulse for high impedance loads, by cutting the trailing edge off, a spark gap was placed parallel to the load.

Typical values of the output voltage in this 4-stage system were four times the input voltage for high impedance loads. The output voltage decreases when the load resistance is reduced, and was for 50 Ω only 1.3 times the input voltage. The maximum input voltage of the MOSFET was 1.5 kV.

The FWHM depends on the load. With increasing load resistance, from 50 Ω to 10 MΩ, it increased from 5 to 6 ns. This is still, due to the spark gap across the load, far below the $R_L C$ value of the circuit.

Besides capacitors, striplines and coaxial cables were used as energy storage elements. In the case of coaxial cables and striplines, the generated pulse width is directly proportional to their length. However, it was difficult to reduce the inductance to similarly low values as in the case of capacitors. Consequently the output pulse showed oscillations, even for a matched system.

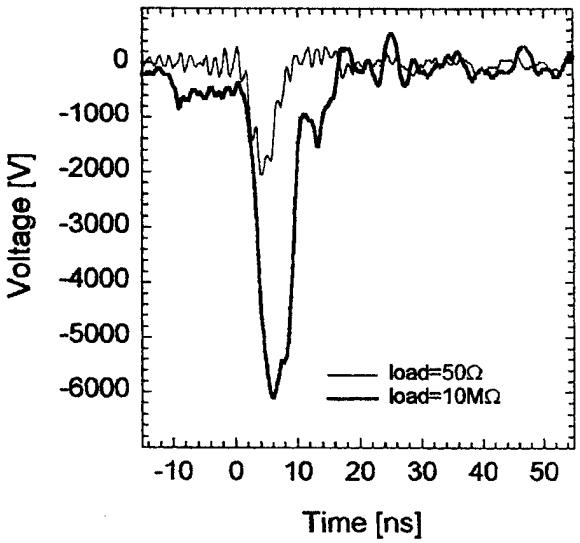

Fig. 3. Output voltage of the Marx bank for various loads

II. Nanosecond Pulse Generator with Cut-Off Diode

In order to generate even shorter pulses the following circuit was used (Fig. 4).

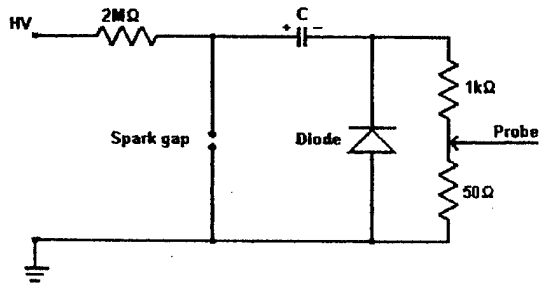

Fig. 4. Circuit with capacitor discharge and cut-off diode

The capacitor C is charged through a charging resistor R and the load resistor. Exceeding the breakdown voltage of the adjustable spark gap pulls the positive electrode of the capacitor to ground potential, causing a negative pulse across the load.

The rise time of the pulse is determined by the capacitance and inductance of the circuit and the plasma formation time of the spark gap. For capacitive discharges the current and consequently the voltage across the load decreases exponentially with a time constant of $R_L C$. In order to cut this tail off, we have added a diode parallel to the load. This does not affect the rise time of the pulse across the load. Initially, the impedance of the diode is much higher than the load resistance. After the forward response time of the diode is exceeded, the impedance drops to very small values, causing a fast decay of the voltage.

The capacitance of ceramic type, low-inductance capacitor was varied from 10 to 15 pF, and the load is a low-inductive 1 kΩ resistor. The spark gap consists of sphere-pin with an adjustable gap distance. The diode is a commercially available MUR 8100E type fast recovery diode (Motorola). All components are mounted on a bread board, known as solderless modular socket (Fig. 5), where component leads and wires are inserted into holes in the insulating plastics and serve as connections to the metal strips underneath [www.llh-publishing.com/pdfsamples/ic/icdemodl.pdf]. The electronic elements are placed on a breadboard in an arrangement, which provides minimum inductance. This minimum inductance configuration is shown in figure 6.

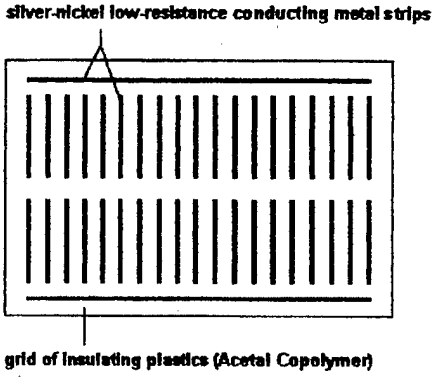

Fig. 5. Bread board (pattern of conducting strips)

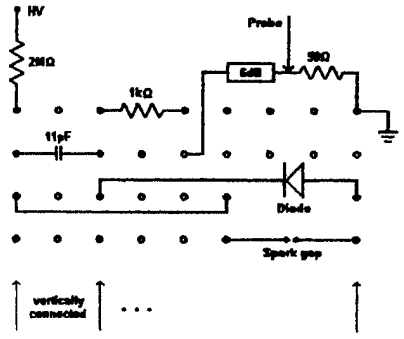

Fig. 6. Minimum inductance configuration on breadboard

The physical arrangement of the circuit elements is very important. Spring loaded contacts have inductive effects and the parallel arranged conducting strips combined with the isolating plastics (Acetal Copolymer) with its dielectric constant (ε_r=3.8) [BASF, Ludwigshafen, Germany] act as capacitance. The effect of these stray capacitances, and inductors is so small that they have no influence on the results in DC or low frequency applications. But at high frequencies they determine to a large extend the output signal.

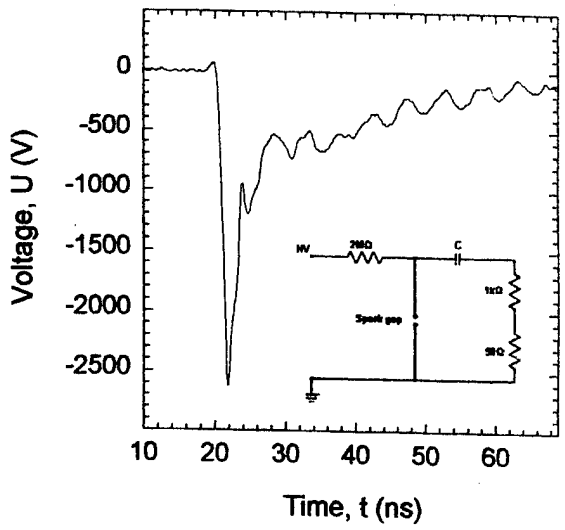

Fig. 7a. Pulse obtained without diode

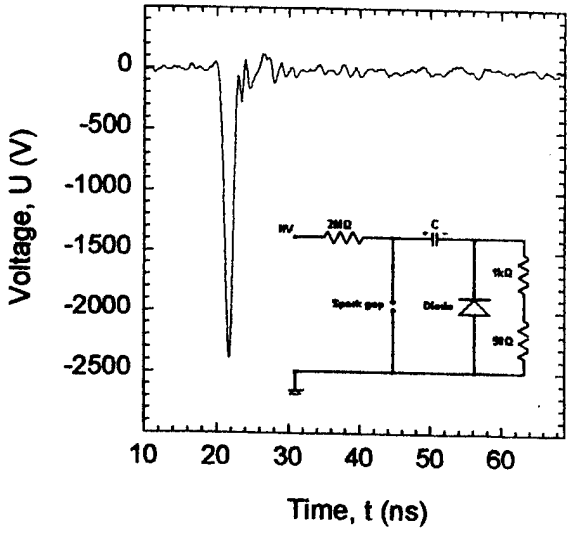

Fig. 7b. Pulse obtained with diode

Experimental Results

The amplitude of the output pulse can be varied by changing the input voltage. The current rise is 3 10^{10} A/s and remains constant when the voltage is varied. This is the reason for the shifting of the peak in the output voltage to larger times at higher voltages (Figure 8).

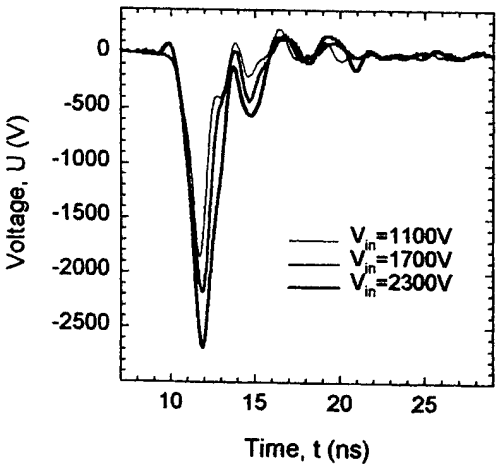

Fig. 8. Pulse amplitude for various input voltages

The pulse amplitude varies linearly with charging voltage. It is almost independent of the load resistance down to R = 50 Ω. This indicates that the source impedance is small compared to 50 Ω. The measured output voltage was found to be larger than the charging voltage. This surprising result, which was reproducible, and was observed using various electrical diagnostic systems, is assumed to be due to interference effects. It was only observed when the circuit elements were placed in a certain arrangement on the breadboard. A more thorough study of this effect is underway.

Summary

Two circuits, based on microsparks and semiconductor elements, have been designed and tested. The Micro Marx bank pulse generator provides up to four times the input voltage. The output voltage in this design is limited by the drain source voltage of the MOSFET to 6 kV into a 10 MΩ load. Improvements are possible by using a new generation of high voltage MOSFETs with a V_{DS} of up to 2.5 kV.

The second system is a capacitive discharge system with a diode, which allows us to shorten the trailing edge of the pulses. The effect is based on the finite response time of diodes in forward direction, and not on the reverse recovery time, as with SOS diodes.

Both systems are easy to build and inexpensive. The small size (2 cm x 3 cm x 5 cm in the case of system 2) and the standardized connections make them attractive for pulsed power applications, e.g. as trigger generator or for basic physics experiments.

Acknowledgement:
This research was supported by AFOSR, "FH Telekom" University of Applied Sciences Leipzig, Germany, and NSF.

References

[1] Robert Stark and K.H. Schoenbach, J. Appl. Phys. 89, 3568 (2001).
[2] Mohamed Moselhy, Wenhui Shi, Robert H. Stark, and Karl H. Schoenbach, „Excimer Emission from Pulsed Microhollow Cathode Discharges," submitted to Appl. Phys. Lett.
[3] W. James Sarjeant, and R. E. Dollinger, High-Power Electronics, Tab Books Inc., Blue Ridge Summit, PA, 1989, Chapter 3.

* on leave from "FH Telekom" University of Applied Sciences Leipzig, Germany.

Digest of Technical Papers,
PPPS2001, Las Vegas, June
2001

BENZENE DESTRUCTION IN DIRECT CURRENT AND PULSE-SUPERIMPOSED ATMOSPHERIC PRESSURE AIR GLOW DISCHARGES

Chunqi Jiang, Robert H. Stark, and Karl H. Schoenbach
Physical Electronics Research Institute, Old Dominion University, Norfolk, VA23529

Abstract

Benzene, a carcinogenic volatile organic compound, is commonly used as a solvent. We have explored the use of a high pressure glow discharge in a near atmospheric and atmospheric pressure benzene/air mixture for benzene remediation. By using a micro-hollow cathode discharge (MHCD) as an electron source to lower or eliminate the cathode fall voltage, a glow discharge could be operated either in a dc mode [1] or in a pulse-superimposed mode [2] at atmospheric pressure air. A higher than 90% destruction rate has been obtained by flowing a benzene/dry air mixture through the dc glow discharge. For a pressure of 720 torr, superimposed electric pulses caused an increase in destruction of benzene, however, for 760 torr, the remediation effect was reversed.

I. INTRODUCTION

Chemical and semiconductor industries are using volatile organic compounds (VOCs) such as toluene, xylene, trichloro-ethylene (TCE), trichloroethane (TCA), benzene, and acetone as solvents and for substrate cleaning [3]. However, the use of VOCs poses considerable health hazards. For example, inhalation of toluene with concentrations of 600 ppm for more than eight hours causes headache and dizziness [4]. Benzene is carcinogenic at long term exposure [4].

Conventional methods to eliminate VOC pollutants in air streams include thermal oxidation, catalytic oxidation, adsorption, biofiltration, membrane separation and UV-oxidation [3]. Alternative approaches based on electron beam treatments and nonthermal plasma technologies are gaining more ground, mainly because of their high removal efficiency and good energy efficiency [5]. One of them is based on the use of glow discharges for VOC remediation. Dissociation of benzene and methylene chloride by dc and pulsed low pressure glow discharges has been studied in VOC/rare gas mixtures [6,7], and 99.8% fractional removal has been achieved.

The operating voltage of glow discharges used for VOC remediation is relatively low, approximately 500 V in the dc mode, and approximately 1.2 kV in the pulsed mode [6,7]. However, the low mass flow rate and the requirement for a vacuum system limit the application of low and medium pressure glow discharges for VOC remediation. When operated at higher pressure, the current density increases. This causes the glow discharges to become unstable and to undergo glow-to-arc transitions. These instabilities originate generally in the cathode fall, the part of the discharge with the highest electric field. Consequently, lowering or eliminating the cathode fall voltage by using a plasma cathode, or external electron source, allows us to extend the operating range of the glow discharge to high pressures.

By using a microhollow cathode discharge (MHCD) as an electron source, a glow discharge in air could be operated in a dc mode [1] or a pulse-superimposed mode [2] at atmospheric pressure air. Electron densities of up to 10^{13} cm^{-3} were measured, at gas temperatures of approximately 2000 K [8]. Superimposing a high electric field pulse with duration of less than the time required for glow-to-arc transitions allows us to temporally heat the electrons without a considerable increase in gas temperature. The shift in the electron energy distribution to higher values favors collisions that require electron energies in excess of the average electron energy in a dc glow. These are, e.g., collisions that cause dissociation of VOCs, and consequently a higher destruction efficiency.

Table 1. Dissociation reactions and corresponding cross-sections and rate coefficients for benzene

Reaction (*XYZ* indicates C_6H_6.)	Cross-section, σ Rate Coefficient, k
Electron impact dissociation: $XYZ + e^-_{fast} \rightarrow X + YZ + e^-_{slow}$	$\sigma \approx 4\times10^{-17}$ cm^2 (electron energy: 0~10eV)[9] $k = \sim10^{-9}$ cm^3/s (electron energy: ~1eV)
Dissociative recombination: $XYZ^+ + e^- \rightarrow X + YZ$	$k = 10^{-6}$ cm^3/s [10]
Dissociative electron attachment: 1) for the ground electronic states, $XYZ + e^-_{slow} \rightarrow X^- + YZ$ 2) for the high Rydberg states, $XYZ^*(HR) + e^-_{slow} \rightarrow X^- + YZ$	1) $\sigma < 10^{-17}$ cm^2 [6] $k < 6.7\times10^{-10}$ cm^3/s (electron energy: ~1eV) 2) $k = 10^{-4}$ cm^3/s [7]
Radical impact dissociation: $XYZ + MN \rightarrow XN + MYZ$ *MN* indicates radicals, e.g. O or O_3.	$k = 10^{-22}$~10^{-14} cm^3/s (for toluene) [5]

We have studied dc and pulse-superimposed atmospheric pressure glow discharges in air with respect to VOC remediation. As a common solvent used in industrial applications, benzene was chosen for this study. The processes that are related to benzene dissociation in atmospheric pressure and dry air include electron impact

dissociation, dissociative recombination, dissociative attachment, and reactions involving radicals. The reactions and corresponding cross-sections and reaction coefficients are listed in table 1.

II. EXPERIMENTAL SETUP AND PROCEDURES

The apparatus used for the study of the effect of high-pressure glow discharges on benzene consist of a plasma discharge cell and a gas analytic system. A schematic diagram of the discharge cell and the gas flow and

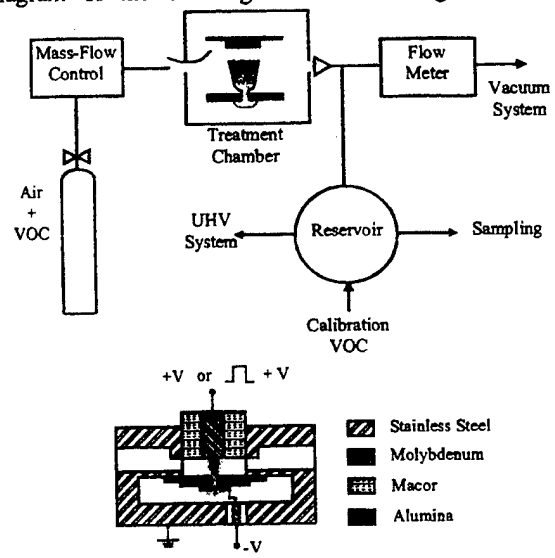

Fig. 1 top: schematic diagram of the experimental setup; bottom: cross section of the discharge chamber.

analytic system is shown in figure 1a. The discharge chamber (cross-section is shown in figure 1b) is made of 2.75-inch diameter stainless steel flanges. A 1 mm wide and 1.5 mm deep slit is cut into a 5/8-inch diameter macor rod in order to generate a narrow channel for the gas flowing through the plasma. The electrodes for the microhollow cathode discharge (MHCD) and the anode are made of molybdenum. The anode of the MHCD, which is separated from the anode of the glow discharge by a distance of 1.5 mm, is on ground potential. The plasma in the reactor is generated by first igniting the MHCD (sustaining voltage: ~400 V) and then igniting the glow discharge (sustaining voltage: 470 V). For the pulse-superimposed case, a transmission line type pulse generator with a spark gap as switch is used to generate 10 ns pulses of kV amplitude [12]. The pulsed voltage is recorded by a high voltage probe in series with a digital oscilloscope. As current viewing resistors, five 22 Ω resistors in parallel are used.

The gas handling system consists of stainless steel or teflon tubing and stainless steel valves. Flow meters and a metering valve are used to control and adjust the flow rate. A Hewlett Packard 6890 gas chromatograph (GC) with a 30 m × 0.32 mm × 0.25 μm capillary column is used for gas analysis. The detector is a flame ionization detector (FID). The GC output signal is recorded by a HP 3396 integrator.

VOC/air mixtures are provided by Matheson Company. Benzene in dry air (benzene: 296 ppm, dry air: 99.97%) is used for the experimental study and hexane in dry air (hexane: 306 ppm, dry air: 99.97%) is used as a calibration VOC. Before introduction of VOC/air mixtures, the flow tube and the sampling reservoir are evacuated to pressures of less than 1 millitorr. In the

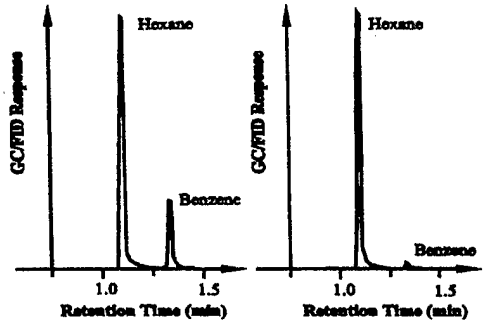

Fig. 2 Chromatograms for benzene and hexane, measured by means of GC/FID. The left chromatogram is obtained for the case without plasma processing, and the right shows the results after plasma treatment

experiments, the gas was flown through the reactor with a rate of 100 sccm at pressures of 720 torr and 760 torr, respectively. The processed gas sample is induced into the sampling reservoir without influencing the flow rate and the pressure of the discharge cell (flow rate fluctuation <2 sccm, pressure variance ≤5 torr). At room temperature, the sampling reservoir is filled with processed gas at a pressure of 200 torr and then the calibration VOC is added to a total pressure of 800 torr. The same sampling procedure is repeated with the unprocessed gas mixture. A 200 μL gas sample is withdrawn with a syringe from the reservoir and analyzed by the GC/FID. The normalized benzene concentration (the remaining benzene fraction) is the ratio of the area of benzene peak to the area of the hexane peak for the processed case (Fig. 2, right), to that for the unprocessed case (Fig. 2, left).

III. RESULTS

The destruction of benzene in both dc and pulse-superimposed dc atmospheric pressure air glow discharges has been studied. For a dc mode, the normalized benzene concentration (fractional benzene) versus input energy density is shown in figure 3. The input energy density is:

$$\varepsilon = VI/F \qquad (1)$$

where V, I, and F are the glow discharge voltage, the glow discharge current, and the gas flow rate, respectively. For a constant flow rate of 100 sccm, the input energy density is varied by varying the glow discharge current from 11.9 mA to 21.4 mA, while keeping the glow discharge voltage constant at 470 V. The relative error was determined for a set of discharges

at one energy density of 5.64 kJ/L as ±17%. With increasing input energy density, the fractional benzene decreases exponentially down to 0.09, and stays almost constant for higher energy densities. The exponential decay can be described by

$$N_e = N_{e0} \exp(-\varepsilon/\beta) \quad (2)$$

where N_{e0} and N_e are the concentration of benzene before and after plasma processing, respectively, and β is the energy density at which the benzene concentration is reduced to 1/e of the initial concentration. The inverse of β is the destruction efficiency. For 760 torr β was found to be 1.76 kJ/L (Fig. 3), whereas previous measurements at 720 torr gave a value of 2.6 kJ/L [13].

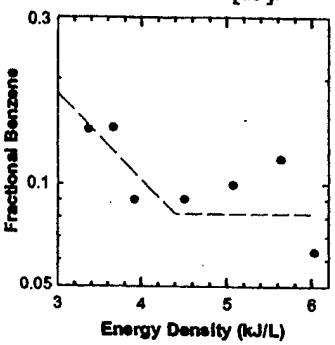

Fig. 3 Normalized benzene concentration versus input energy density in a dc glow discharge in a benzene/dry air mixture at 760 torr with a flow rate of 100 sccm.

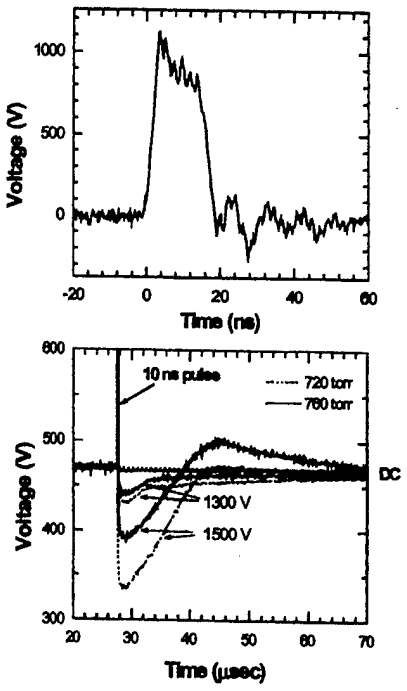

Fig. 4 Top: 10 ns voltage pulse; bottom: discharge voltage vs. time for two pressures, 720 torr and 760 torr and two applied voltages, 1300 V and 1500 V.

The energy efficiency, defined as the mass of VOC molecules which are dissociated per energy input, has also been calculated. The mass of the reduced benzene per unit volume is given as $R \times N_g \times (N_{dc}/N_0) \times m_{ben}$, where R is the VOC concentration in air, N_g is the gas density, N_0 and

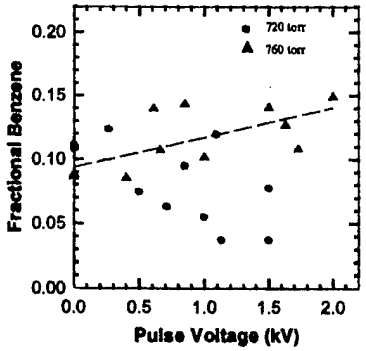

Fig. 5 Normalized Benzene concentration versus superimposed pulse voltage in 100 sccm benzene/dry air flow at 720 torr and 760 torr.

N_{dc} is the benzene concentration before and after glow discharge application, respectively, and m_{ben} is the molecular weight of benzene. The calculated energy efficiency for atmospheric pressure discharge operation, with energy densities ranging from 3.37 kJ/L to 6.03 kJ/L, varies from 0.9 g/kWh to 0.5 g/kWh.

In a second set of experiments, 10 ns pulses (see Fig. 4 (top)) were superimposed to the dc glow discharge. The glow discharges were operated at two pressures, 720 torr and 760 torr, with a flow rate of 100 sccm. The dc voltage was 470 V and the dc current was 14.2 mA. Pulses were superimposed to the glow discharges with amplitudes varying from 300 V to 1500 V with a repetition rate of 100 Hz. The temporal development of the discharge voltage in response to the application of a 1500 V, 10 ns pulse is shown in Fig. 4 (bottom). At a pressure of 760 torr, the discharge voltage drops to 80% of the dc voltage, and it takes 8 μs to recover to the dc value. At 720 torr, the discharge voltage drops to 70% of the dc voltage and the recovery time is 10 μs. For lower pulse voltages (≤1300 V), the differences in the temporal development of the discharge voltages for 760 torr and 720 torr become less and less pronounced.

The destruction results are different for the two pressure conditions. Normalized benzene concentrations versus pulse voltage at 720 torr and 760 torr, respectively, are shown in Fig. 5. Compared with the benzene concentration in a dc glow, the benzene concentration decreases with increasing applied pulse voltage for the 720 torr discharge, while it increases with increasing pulse voltage for the 760 torr discharge. The error was determined as ±10% for a 720 torr discharge at a pulsed voltage of 850 V.

IV. DISCUSSION

Assuming that the destruction of benzene is mainly caused by electron impact dissociation, the change in the benzene concentration is described by the following rate equation:

$$dN_{dc}/dt = - k_e N_{dc} n_e \quad (4)$$

where N_{dc} is the benzene concentration in the dc glow discharge process, n_e is the electron density, and k_e is the rate coefficient of the electron impact dissociation. The energy density dissipated in the discharge plasma over time dt is:

$$d\varepsilon = JEdt, \quad (5)$$

E is the electric field, and J the current density, which is related to E by Ohm's law:

$$J = \sigma E = n_e e^2 E/(m_e \nu_m) \quad (6)$$

with σ being the conductivity, e the electron charge, m the electron mass, and ν_m the electron-neutral collision frequency. Combining equations 4, 5 and 6, we obtain:

$$dN_{dc}/N_{dc} = -[k_e m_e \nu_m/(e^2E^2)]d\varepsilon, \quad (7)$$

with the solution:

$$N_{dc} = N_0 \exp(-\varepsilon/\beta), \quad (8)$$

where β is the coefficient, which was introduced in section 3. β is related to the rate coefficient, k_e, through the following relation

$$\beta = e^2E^2/(k_e m_e \nu_m). \quad (9)$$

The collision frequency, ν_m, is 3×10^{12} s^{-1} for air at room temperature and atmospheric pressure [11]. For the measured gas temperature of 2000 K, ν_m is lowered by a factor of 6.7, i.e., $\nu_m \approx 4.5\times10^{11}$ s^{-1}. Assuming a rate coefficient of 10^{-9} cm^3/s (which is the value for electron impact dissociation [table 1]), with an applied dc electric field of 3×10^3 V/cm, $\beta \approx 5.6$ kJ/L, a value, which is on the same order of magnitude as the experimental value, β = 1.76 kJ/L (observed at 760 torr, see Fig. 3).

For energy densities in excess of 4.5 kJ/L, the normalized benzene concentration remains constant at a value of ~0.08 with increasing energy density. It is not known at this time if this effect is due to recombination of benzene fragments (not considered in the rate equation 4) or due to changes in the discharge plasma parameters at higher energy density.

The reason for the difference in destruction rates for 720 torr and 760 torr in the pulse-superimposed conditions is also not known at this time. The difference in pressure is not substantial. We assume therefore that the differences are not due to three-body collisions. However, the electric characteristics of the discharges at 760 torr and 720 torr are quite different. This difference in power transfer to the plasma might explain the difference in benzene remediation processes.

V. CONCLUSION

A destruction rate in excess of 90% has been obtained by flowing a benzene/dry air mixture through an atmospheric pressure glow discharge. The destruction efficiency in the high pressure dc glow discharge (0.57 L/kJ) is lower by a factor of 12.4 compared to that for a benzene/Ar mixture at 2 torr (7.04 L/kJ) [6], but the energy efficiency of the high pressure discharge (≤0.9 g/kWh) is higher than that of the benzene/Ar mixture (<0.3 g/kWh), or comparable to that of a benzene/Ne mixture (≤0.9 g/kWh) [6]. Superposition of a 10 ns voltage pulse to a dc discharge has shown only small effects which are different for 720 torr and 760 torr. This effect might be due to the low duty cycle (10^{-6}) of the pulsed operation. There is no explanation for the different remediation effects at 720 torr and 760 torr discharges yet.

In order to scale this small glow discharge system to a reactor with high mass flow rates, parallel operation of the glow discharge is possible and easy. If the glow discharges are operated in series, the destruction rate can be increased. For example, for a 90% destruction rate, five discharges in series will raise the destruction rate up to 99.99%.

VI. ACKNOWLEDGMENTS

This work is supported by the Air Force Office of Scientific Research.

VII. REFERENCES

[1] R.H. Stark and K.H. Schoenbach, Appl. Phys. Lett. **74,** 3770 (1999).

[2] R.H. Stark and K.H. Schoenbach, J. Appl. Phys. **89,** 3568 (2001).

[3] K. Vercammen, A. Berezin, F. Lox, and J. Chang, J. Adv. Oxid. Technol. **2,** 312 (1997).

[4] H.J. Rafson, Odor and VOC Control Handbook, McGraw-Hill (1998).

[5] K. Urashima and J. Chang, IEEE Transactions on Dielectrics and Electrical Insulation **7,** 602 (2000).

[6] D.L. McCorkle, W. Ding, C. Ma and L.A. Pinnaduwage, J. Phys. D: Appl. Phys. **32,** 46 (1999).

[7] D.L. McCorkle, W. Ding, C. Ma and L.A. Pinnaduwage, J. Appl. Phys. **86,** 3550 (1999).

[8] F. Leipold, R.H. Stark, A. El-Habachi, and K.H. Schoenbach, J. Phys. D: Appl. Phys. **33,** 2268 (2000).

[9] E.E. Rennie, C.A.F. Johnson, J.E. Parker, D.M.P. Holland, D.A. Shaw, and M.A. Hays, Chem. Phys. **229,** 107 (1998).

[10] H. Abouelaziz, J.C. Gomet, D. Pasquerault, R.B. Rowe, and J.B.A. Mitchell, J. Chem. Phys. **99,** 237 (1993).

[11] Y.P. Raizer, Gas Discharge Physics, 2nd ed. Springer, Berlin, Germany (1991).

[12] J. Deng, R.H. Stark, and K.H. Schoenbach, Conference Record of the 2000 24th International Power Modulator Symposium, p.47.

[13] Chunqi Jiang, Robert H. Stark, and Karl H. Schoenbach, Proc. Ninth International Symposium on Gaseous Dielectrics, May 21-25, 2001, Ellicott City, ML, paper 41.

EXCIMER EMISSION FROM PULSED HIGH PRESSURE XENON GLOW DISCHARGES

Robert H. Stark, Hisham Merhi, Chunqi Jiang, and Karl H. Schoenbach*

1. INTRODUCTION

High pressure glow discharges are used in plasma processing, gas lasers, chemical and bacterial decontamination of gases, and as mirrors and absorbers of microwave radiation. Transient high pressure glow discharges, such as barrier discharges[1] and ac discharges[2] are already well established, but recently high pressure dc discharges in noble gases[3] and in air,[4, 5] with dimensions of up to centimeters have been generated by using novel plasma cathodes. One of them is a microhollow cathode discharge sustained plasma, where the microhollow cathode discharge provides the electrons for the main discharge. The elimination of the cathode fall, the cradle for glow-to-arc transition has allowed us to generate dc glow discharges with electron densities as high as 10^{13} cm^{-3}, at gas temperature below 2000 K.[4, 6]

In these dc discharges the electron energy distribution is determined by the value of the reduced electric field (E/N), where E is the electric field intensity and N is the gas density. For dc atmospheric pressure air discharges with E/N of 32 Td, 1% of the electrons have an energy in excess of 2.1 eV, as computed by means of ELENDIF.[7] Applying electric field pulses to these plasmas with amplitudes exceeding the equilibrium reduced fields, but of such duration that glow-to-arc transition is avoided, allows us to shift the electron energy distribution temporarily to much higher energies. Calculations using ELENDIF show a dramatic shift of the electron energy distribution function (EEDF) during a 10 ns, 200 Td high voltage pulse: 1% of the electrons have then an energy exceeding 67 eV at the end of the 10 ns pulse. The increase in the concentration of high-energy electrons causes an increase of the ionization rate coefficient. The consequent rise in charged particle density has lead to an increase in electron lifetime from 165 ns to 3.6 μs at 17.5 kV/cm and 40 kV/cm, respectively.[8] This non-equilibrium electron heating effect can be used to reduce the power consumption of repetitive operated glow discharges from 5 kW/cm^3 for dc to 16 W/cm^3 for 3.5 ns pulses.

* Robert H. Stark, Hisham Merhi, Chunqi Jiang, and Karl H. Schoenbach, Physical Electronics Research Institute, Department of Electrical and Computer Engineering, Old Dominion University, Norfolk, VA 23529

Gaseous Dielectrics IX, Edited by Christophorou and Olthoff.
Kluwer Academic/Plenum Publishers, New York, 2001

Pulsed electron heating in high pressure plasmas may also be used to populate excited states of excimer gases, e.g. noble gases, efficiently. The increased density of excited noble gas atoms, the precursors of noble gas dimers, promises to lead to high intensity pulsed excimer radiation lamps. In order to explore the electron heating effect of short electric pulses on excimer emission we have studied the VUV spectral response of a high pressure xenon glow discharge to a 10 ns pulse.

2. EXPERIMENTAL SETUP

The electrode geometry for the microhollow cathode sustained (MCS) glow discharge is shown in Fig. 1. It consists of a microhollow electrode system and a third positively biased electrode (anode) 5 mm apart from the microhollow anode which is on ground potential. The microhollow electrodes are two molybdenum metal plates (100 μm thickness) with circular opening of 100 μm diameter, separated by a 100 μm thin dielectric layer of alumina. The microhollow cathode discharge (MHCD) between the cathode (-) and the ground electrode serves as plasma cathode for high pressure glow discharge operation.[3]

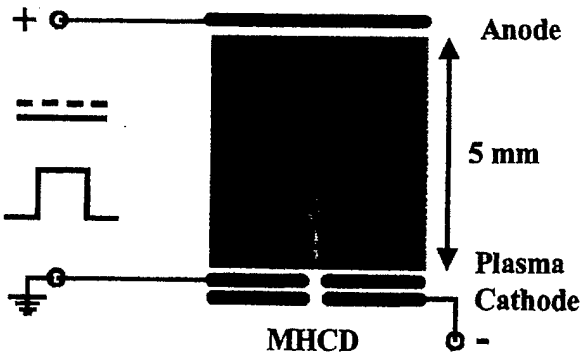

Fig. 1 Photograph of a microhollow cathode discharge sustained glow discharge in xenon at 100 torr and a 2 mA discharge current. In order to study the electron heating effect, a 10 ns high voltage pulse was superimposed to the dc plasma.

The temporal development of discharge current and voltage has been recorded using a 500 MHz oscilloscope. Spectral measurements in the VUV have been performed using a 0.5 m McPherson scanning monochromator, model 219, with a grating blazed at 150 nm. The UHV discharge chamber was mounted directly to the inlet slit of the monochromator. The slit was oriented parallel to the discharge axis and placed at a distance of 6 cm in front of the discharge. Discharge chamber and monochromator were separated by means of a MgF_2 window and evacuated to 10^{-5} torr before beginning of the measurement. The spectrally resolved radiation at the exit slit was recorded with a photomultiplier tube (Hamamatsu 1533) after conversion to visible light, centered around 425 nm, by a sodium salicylate scintillator. In addition to spectral measurements a CCD video monitoring system was used to record the appearance of the glow discharge side-on in the visible and near ultra violet.

The excimer emission of xenon discharge was studied both for dc operation and for pulsed operation. The dc discharge was operated at 1 mA with a sustaining voltage of 70

V, corresponding to an average electric field of 140 V/cm. For pulsed operation a 10 ns high voltage pulse was superimposed to the dc plasma. The high voltage pulse was generated by a 10 Ω pulse forming network (PFN) in strip line geometry.[8] A high pressure spark gap was used as switch to transfer the energy stored in the PFN to the load and to allow fast rise time of the high voltage pulse. The rise time of the pulse voltage is approximately 1-2 ns, and the pulse has an approximately rectangular shape. Pulse voltages of up to 6 kV were applied to the dc glow, generating average pulsed electric fields of up to 12 kV/cm in the high pressure plasma.

3. RESULTS

3.1 Direct Current Operation

The side-on photograph of a xenon MCS discharge at 100 torr and 2 mA discharge current is shown in Fig. 1. The microhollow cathode plasma (bottom), which has a diameter of 100 μm, supplies the electrons for the MCS glow. The glow expands from a diameter determined by the electron source (plasma cathode) to a maximum diameter of 2 mm at the anode.

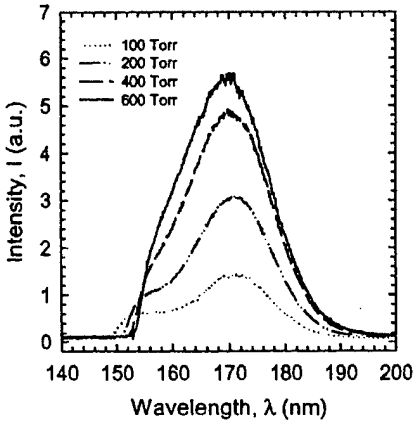

Fig. 2 VUV emission spectrum of a high pressure microhollow cathode sustained glow discharge (MCS) with gas pressure as variable parameter. The current in the MHCD and MCS discharge was kept constant at 1 mA.

The excimer spectrum for xenon was measured by scanning the spectrometer over a of wavelength range from 140 nm to 200 nm in steps of 0.1 nm and recording the resulting PMT voltage across a 1MΩ resistor. The excimer spectrum for a dc glow discharge in xenon at various pressures is shown in Fig. 2. The first excimer continuum extends from the resonance line (147 nm), which in this case is not observed, towards longer wavelength. With increasing pressure the second continuum which peaks at 172 nm becomes more pronounced. The emission increases up to the highest pressure at which we could operate the discharge before instabilities set in (600 torr).

3.2 PULSED OPERATION

In pulsed experiments the temporal development of the VUV emission after the application of the 10 ns high voltage pulse was measured at a wavelength of 172 nm. The response of the plasma at this wavelength to the 10 ns pulse in xenon at 400 torr (I_{MCS} = 1 mA, I_{MHCD} = 5 mA) is shown in Fig. 3. Two peaks have been observed. The first peak is identical to the 10 ns voltage pulse. It is assumed that it is an electrical signal, which is coupled to the diagnostic system. The second peak reaches its maximum intensity at about 250 ns after pulse application and decays exponentially with a time constant of 850 ns to the dc value. The average emission time at half of the peak value is 680 ns.

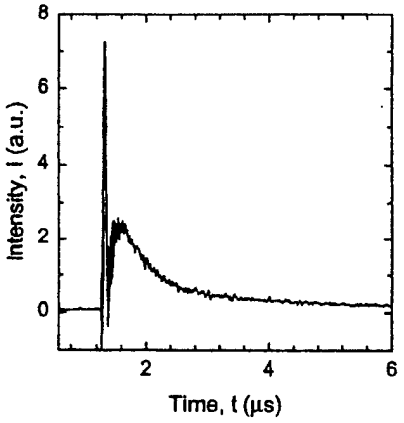

Fig. 3 VUV intensity at 172 nm when a 10 ns, 3.5 kV pulse is applied to the dc discharge (p = 400 torr, I_{MCS} = 1 mA, I_{MHCD} = 5 mA).

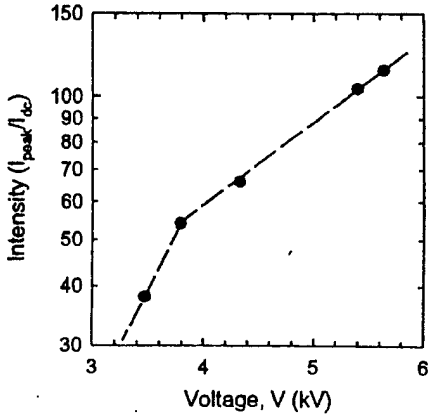

Fig. 4 Ratio of peak intensity for pulsed operation, to the dc intensity value at 172 nm versus pulse voltage for a xenon discharge at 400 torr. The extension of the line connecting the two lower data points passes through the dc data point at V=0 where the intensity, defined as I_{peak}/I_{dc}, equals one.

The amplitude of the emission intensity at 172 nm varies exponentially with the voltage and electric field, E, respectively, of the applied pulse. This is shown in Fig. 4, where the peak intensity at 172 nm is plotted versus the applied pulse voltage.

$$P/P_0 = \exp(E/E_0) \qquad [1]$$

P_0 is the optical power emitted by the dc discharge. The optical power of the pulsed discharge with respect to the dc discharge, P/P_0, increases by more than two orders in magnitude from the dc value to the value at the highest applied voltage of 5.7 kV or 11.4 kV/cm electric field, respectively. For $V > 3.8$ kV, E_0 is approximately 5 kV/cm. For voltages less than 3.8 kV the rise in optical power is even stronger, indicating values of E_0 of 140 V/cm.

4. DISCUSSION

Direct current microhollow cathode sustained high pressure glow discharges, operated in xenon have shown to be sources of excimer radiation in the VUV at center wavelengths of 172 nm. Measurements with pressure as variable parameter have shown that the peak emission intensity increases continuously with pressure in the range of our measurements (Fig. 2). This is different from the results of similar studies in high pressure microhollow cathode discharges, where the VUV emission intensity has a maximum at 400 torr and decreases at higher pressure. In this case it was found that the presence of a maximum is due to the superlinear expansion of the plasma source over the surface of the microhollow cathode.[9] For the filamentary discharge studied in this experiment, the volume of the excimer source, however, seems to gradually decrease. This explains the continuous increase in intensity with pressure.

Much higher excimer intensities, compared to dc operation, were measured when a pulsed electric field was applied to the dc discharge. The total radiative power increased by more than two orders in magnitude with electrical field pulses of 11.4 kV/cm across the 5 mm gap (Fig. 4). The observed response of the excimer emission (Fig. 3) is typical for pulsed operation with pulses in the ns-range. A similar response has been observed when a 20 ns pulse was applied to a barrier discharge.[10, 11]

The possibility to scale these high pressure plasmas to larger dimensions, e.g. by parallel operation of the discharges or by increasing the length of the plasma filament, may allow their use as active media for laser applications. The scalability of such plasmas has already been shown in an earlier experiment.[5]

5. ACKNOWLEDGEMENT

This work was funded by the Air Force Office of Scientific Research (AFOSR) in cooperation with the DDR&E Air Plasma Ramparts MURI program and by the National Science Foundation.

6. REFERENCES

1. B. Eliasson and U. Kogelschatz, IEEE Trans. Plasma Sci. **19**, 309 (1991).
2. S. Kanazawa, M. Kogoma, T. Moriwaki, and S. J. Okazaki, J. Phys. D **21**, 836 (1988).
3. Robert H. Stark and Karl H. Schoenbach, J. Appl. Phys. **85**, 2075 (1999).
4. Robert H. Stark and Karl H. Schoenbach, Appl. Phys. Lett. **74**, 3770 (1999).
5. Rolf Block, Abdel-Aleam H. Mohamed, and Karl H. Schoenbach, Conf. Record, IEEE Intern. Conf. Plasma Science, New Orleans, 2000, paper 1P23, p. 110.

6. Frank Leipold, Robert H. Stark, Ahmed El-Habachi, and Karl H. Schoenbach, J. Phys. D: Appl. Phys. **33**, 2268 (2000).
7. W.L. Morgan and B.M. Penetrante, Computer Phys. Communications **58**, 127 (1990).
8. Robert H. Stark and Karl H. Schoenbach, J. Appl. Phys. **89**, 3568 (2001).
9. Karl H. Schoenbach, Ahmed El-Habachi, Mohamed M. Moselhy, Wenhui Shi, and Robert H. Stark, Physics of Plasmas **7**, 2186 (2000).
10. R.P. Mildren and R.J. Carman, J. Phys. D: Appl. Phys. **34**, L1 (2001).
11. F. Adler and S Mueller, J. Phys. D: Appl. Phys. **33**, 1705 (2000).

BENZENE DESTRUCTION IN DIRECT CURRENT ATMOSPHERIC PRESSURE AIR GLOW DISCHARGES

Chunqi Jiang, Robert H. Stark, and Karl H. Schoenbach*

1. INTRODUCTION

Chemical and semiconductor industries are using volatile organic compounds (VOCs) such as toluene, xylene, trichloro-ethylene (TCE), trichloroethane (TCA), benzene, and acetone as solvents and for substrate cleaning [1]. However, the use of VOCs poses considerable health hazards. For example, inhalation of toluene with concentrations of 600 ppm for more than eight hours causes headache and dizziness [2]. Benzene is carcinogenic at long term exposure [2].

Conventional methods to eliminate VOC pollutants in air streams include thermal oxidation, catalytic oxidation, adsorption, biofiltration, membrane separation and UV-oxidation. Alternative approaches based on electron beam treatments and nonthermal plasma technologies are gaining more ground, mainly because of their high removal efficiency and good energy efficiency [3]. One of them is utilizing glow discharges for VOC remediation. Dissociation of benzene and methylene chloride by dc and pulsed low pressure glow discharges has been studied in VOC/rare gas mixtures [4,5], and 99.8% fractional removal has been achieved. The operating voltage of glow discharges is relatively low, approximately 500 V in the dc mode, and approximately 1.2 kV in the pulsed mode. However, the low mass flow rate and the requirement for a vacuum system limit the application of low and medium pressure glow discharges for VOC remediation. When operated at higher pressure, the current density increases. This causes the glow discharges to become unstable and to undergo glow-to-arc transitions. These instabilities originate generally in the cathode fall, the part of the discharge with the highest electric field. Consequently, lowering or eliminating the cathode fall voltage by using a plasma cathode, or external electron source, allows us to extend the operating range of the glow discharge to high pressures. By using a micro-hollow-cathode-discharge (MHCD) as an electron source [6], a glow discharge in air could be operated in a dc mode at atmospheric pressure air [7]. Electron densities of up to 10^{13} cm^{-3} were measured, at gas temperatures of approximately 2000 K [8].

* **Chunqi Jiang, Robert H. Stark, and Karl H. Schoenbach, Physical Electronics Research Institute, Department of Electrical and Computer Engineering, Old Dominion University, Norfolk, VA 23529.**

Gaseous Dielectrics IX, Edited by Christophorou and Olthoff, Kluwer Academic/Plenum Publishers, New York, 2001

Table 1. Dissociation reactions and corresponding cross-sections and rate coefficients for benzene

Reaction (*XYZ* indicates C_6H_6.)	**Cross-section, σ** **Rate Coefficient, k**
Electron impact dissociation: $XYZ + e^-_{fast} \rightarrow X + YZ + e^-_{slow}$	$\sigma \approx 4\times10^{-17}$ cm^2 (electron energy: 0~10eV)[9] k = ~10^{-9} cm^3/s (electron energy: ~1eV)
Dissociative recombination: $XYZ^+ + e^- \rightarrow X + YZ$	k = 10^{-6} cm^3/s [10]
Dissociative electron attachment: 1) for the ground electronic states, $XYZ + e^-_{slow} \rightarrow X^- + YZ$ 2) for the high Rydberg states, $XYZ^*(HR) + e^-_{slow} \rightarrow X^- + YZ$	1) $\sigma < 10^{-17}$ cm^2 [4] k < 6.7×10^{-10} cm^3/s (electron energy: ~1eV) 2) k = 10^{-4} cm^3/s [5]
Radical impact dissociation: $XYZ + MN \rightarrow XN + MYZ$ *MN* indicates radicals, e.g. O or O_3.	k = 10^{-22}~10^{-14} cm^3/s (for toluene) [3]

We have studied dc atmospheric pressure glow discharges in air with respect to VOC dissociation. As a common solvent used in industrial applications, benzene was chosen for this study. The processes that are related to benzene dissociation in atmospheric pressure and dry air include electron impact dissociation, dissociative recombination, dissociative attachment, and reactions involving radicals. The reactions and corresponding cross-sections and reaction coefficients are listed in table 1.

2. EXPERIMENTAL SETUP AND PROCEDURES

The apparatus used for the study of the effect of high-pressure glow discharges on benzene consist of a plasma discharge cell and a gas analytic system. A schematic diagram of the discharge cell and the gas flow and analytic system is shown in figure 1a. The discharge chamber (cross-section is shown in figure 1b) is made of 2.75-inch diameter stainless steel flanges. A 1 mm wide and 1.5 mm deep slot is cut into a 5/8-inch diameter macor rod in order to generate a narrow channel for the gas flowing through the plasma. The electrodes for the microhollow cathode discharge (MHCD) and the anode are made of molybdenum. The anode of the MHCD, which is separated from the anode of the glow discharge by a distance of 1.5 mm, is on ground potential. The plasma in the reactor is generated by first igniting the MHCD (sustaining voltage: ~400 V) and then igniting the glow discharge (sustaining voltage: 470 V).

The gas handling system consists of stainless steel or Teflon tubing and stainless steel valves. A mass flow controller (Costal Instrument, UFC8160) and a metering valve (Nupro "S" series) are used to control and adjust the flow rate. A Hewlett Packard 6890

gas chromatograph (GC) with a 30 m × 0.32 mm × 0.25 μm capillary column is used for gas analysis. The detector is a flame ionization detector (FID). The GC output signal is recorded by a HP 3396 integrator.

VOC/air mixtures are provided by Matheson Company. Benzene in dry air (benzene: 296 ppm, dry air: 99.97%) is used for the experiment study and hexane in dry air (hexane: 306 ppm, dry air: 99.97%) is used as a calibration VOC. Before introduction of

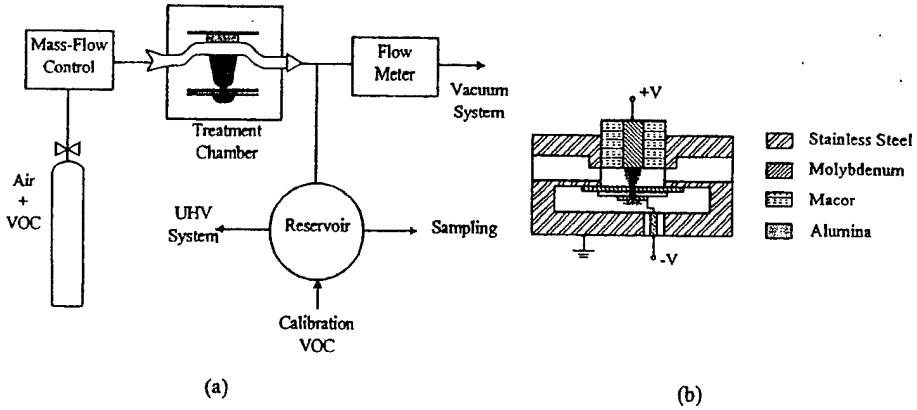

Fig. 1a. Schematic diagram of the experimental setup; **b.** the cross-section of the discharge chamber.

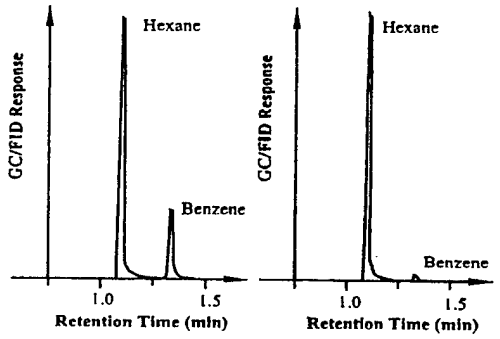

Fig. 2 Chromatograms for benzene and hexane, measured by means of GC/FID. The left chromatogram is obtained for the case without plasma processing, and the right shows the results after plasma treatment.

VOC/air mixtures, the flow tube and the sampling reservoir are evacuated to pressures of less than 1 millitorr. In the experiments, the gas was flown through the reactor with a rate of 100 sccm at 720-730 torr pressure. The processed gas sample is induced into the sampling reservoir without influencing the flow rate and the pressure of the discharge cell (flow rate fluctuation <2 sccm, pressure variance ≤10 torr). At room temperature, the sampling reservoir is filled with processed gas at a pressure of 200 torr and then the calibration VOC is added to a total pressure of 800 torr. The same sampling procedure is repeated with the unprocessed gas mixture. A 200 μL gas sample is withdrawn by a syringe from the reservoir and analyzed by the GC/FID. The normalized benzene concentration (the remaining benzene fraction) is the ratio of the area of benzene peak to

the area of the hexane peak for the processed case (Fig. 2, right), to that for the unprocessed case (Fig. 2, left).

3. RESULTS

The destruction of benzene in dc near atmospheric pressure glow discharges in air has been studied. The normalized benzene concentration (fractional benzene) versus input energy density is shown in figure 3. The input energy density is:

$$\varepsilon = VI/F \quad (1)$$

where V, I, and F are the glow discharge voltage, the glow discharge current, and the gas flow rate, respectively. The data are based on single measurement; this explains the large scatter. For a constant flow rate of 100 sccm, the input energy density is varied by varying the glow discharge current from 10.5 mA to 20.1 mA, while keeping the glow discharge voltage constant at 470 V. With increasing input energy density, the fractional benzene decreases exponentially:

$$N_e = N_{e0} \exp(-\varepsilon/\beta) \quad (2)$$

where N_{e0} and N_e are the concentration of benzene before and after the plasma processing, respectively, and β is the energy density at which the benzene concentration is reduced to 1/e of the initial concentration. The inverse of β is the destruction efficiency. For the given gas and plasma parameters, $\beta \approx 2.6$ kJ/L, which means that it takes 2.6 kJ to reduce the benzene concentration in dry air at near atmospheric pressure in a volume of one liter by a factor of 2.7.

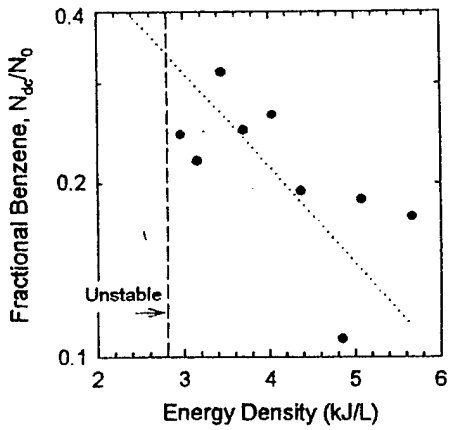

Fig. 3 Normalized benzene concentration versus input energy density in a dc glow discharge. The discharge is operated in a benzene/dry air mixture at 720 torr with a flow rate of 100 sccm, and at a discharge voltage of 470 V. The discharge current is varied from 10.5 mA to 20.1 mA and the corresponding energy density varies from 2.96 kJ/L to 5.66 kJ/L. The lower limit in current is determined by the onset of instabilities; at currents larger than 20 mA, the electrodes are damaged due to excessive Joule heating.

The energy efficiency, defined as the mass of VOC molecules which are dissociated per energy input, has been calculated. The mass of the reduced benzene per unit volume is given as $R \times N_g \times (N_{dc}/N_0) \times m_{ben}$, where R is the VOC concentration in air, N_g is the gas density, and m_{ben} is the molecular weight of benzene. The calculated energy efficiency in the range of the atmospheric pressure discharge operation (for energy densities ranging from 2.96 kJ/L to 5.66 kJ/L) varies from 0.85 g/kWh to 0.5 g/kWh.

4. DISCUSSION

Assuming that the destruction of benzene is mainly caused by electron impact dissociation, the change in the benzene concentration is described by the following rate equation:

$$dN_{dc}/dt = - k_e N_{dc} n_e \quad (4)$$

where N_{dc} is the benzene concentration in the dc glow discharge process, n_e is the electron density, and k_e is the rate coefficient of the electron impact dissociation. The energy density dissipated in the discharge plasma over time dt is:

$$d\varepsilon = JEdt, \quad (5)$$

E is the electric field, and J the current density, which is related to E by Ohm's law:

$$J = \sigma E = n_e e^2 E/(m_e \nu_m) \quad (6)$$

with σ being the conductivity, e the electron charge, m the electron mass, and ν_m the electron-neutral collision frequency. Combining equations 4, 5 and 6, we obtain:

$$dN_{dc}/N_{dc} = -[k_e m_e \nu_m/(e^2 E^2)]d\varepsilon, \quad (7)$$

with the solution:

$$N_{dc} = N_0 \exp(-\varepsilon/\beta), \quad (8)$$

where β is the coefficient, which was introduced in section 3. β is related to the rate coefficient, k_e, through the following relation

$$\beta = e^2 E^2/(k_e m_e \nu_m). \quad (9)$$

The collision frequency, ν_m, is 3×10^{12} s^{-1} for air at room temperature and atmospheric pressure [11]. For the measured gas temperature of 2000 K, ν_m is lowered by a factor of 6.7, i.e., $\nu_m \approx 4.5\times10^{11}$ s^{-1}. Assuming a rate coefficient of 10^{-9} cm^3/s (which is the value for electron impact dissociation [table 1]), with an applied dc electric field of 3×10^3 V/cm, $\beta \approx 5.6$ kJ/L, a value, which is on the same order of magnitude as the experimental value, $\beta \approx 2.6$ kJ/L.

The time required to reduce benzene from an initial value, N_0, to a final value, N_{dc}, can be obtained by solving equ. 4. Integrating this equation, we obtain an expression for the fractional benzene:

$$N_{dc}/N_0 = \exp(-k_e n_e T_s), \quad (10)$$

where T_s is the time required to obtain a reduction in the density of benzene to N_{dc}. The electron density of the dc glow discharge plasma in air at atmospheric pressure has been measured to be about 10^{13} cm^{-3} in the center of the plasma at a current of 10 mA [8], which is the lowest current that supports a stable discharge in our experiment. At a radial distance of 0.21 mm from the center of the plasma column, the electron density decreases to half of this value. Assuming an average electron density of 5×10^{12} cm^{-3}, and using a rate constant of 10^{-9} cm^3/s, the time to reduce the concentration of benzene by a factor of $N_0/N_{dc} = 1/0.3$ (the value for the 10 mA discharge in fig. 3), is consequently 0.24 ms.

The time the flowing gas needs to stream through the plasma column, the residence time of the gas, is given by the plasma dimensions and by the flow velocity. The diameter of the plasma column is assumed to be about 800 µm [7]. The cross section area is 1.5 mm^2. The flow velocity of the gas passing through the discharge cell is consequently 1 m/s at a flow rate of 100 sccm. The residence time is then 0.8 ms, which is more than three times the time required to reduce the concentration to the experimental value for the 10 mA discharge. Considering, however, the relatively crude assumptions in deriving T_s, this discrepancy between the residence time and the benzene destruction time is not surprising.

5. CONCLUSION

A higher than 80% destruction rate has been obtained by flowing a benzene/dry air mixture through a near atmospheric pressure glow discharge. The destruction efficiency in the high pressure dc glow discharge (1/2.6 L/kJ) is lower by a factor of 18.3 compared to that for a benzene/Ar mixture at 2 torr (1/142 L/J) [4], but the energy efficiency of the high pressure discharge (≤0.85 g/kWh) is higher than that of the benzene/Ar mixture (<0.3 g/kWh), or comparable to that of a benzene/Ne mixture (≤0.9 g/kWh) [4].

In order to scale this small glow discharge system to a reactor with high mass flow rates, parallel operation of the glow discharge is possible and easy. Five parallel atmospheric pressure glow discharges have already been run successfully in a stainless steel chamber. The mass flow rate can then be increased five times compared to that of a single discharge. If the glow discharges are operated in series, the destruction rate can be increased. For example, for an 80% destruction rate, five discharges in series will raise the destruction rate up to 99.97%.

6. ACKNOWLEDGMENTS

The authors wish to thank J. H. Yuan for helpful comments and discussions on GC operation and gas analysis and S. Katsuki, and F. Leipold for their valuable experimental help on pulsed current measurement. This work is supported by the Air Force Office of Scientific Research.

7. REFERENCES

[1] K. Vercammen, A. Berezin, F. Lox, and J. Chang, "Non-Thermal Plasma Techniques for the Reduction of Volatile Organic Compounds in Air Streams: A Critical Review," J. Adv. Oxid. Technol. **2**, 312 (1997).

[2] H. J. Rafson, Odor and VOC Control Handbook, McGraw-Hill (1998).

[3] K. Urashima and J. Chang, "Removal of Volatile Organic Compunds from Air Streams and Industrial Flue Gases by Non-Thermal Plasma Technology," IEEE Transactions on Dielectrics and Electrical Insulation **7**, 602 (2000).

[4] D. L. McCorkle, W. Ding, C. Ma and L. A. Pinnaduwage, "Dissociation of Benzene and Methylene Chloride Based on Enhanced Dissociative Electron Attachment to Highly Excited Molecules," J. Phys. D: Appl. Phys. **32**, 46 (1999).

[5] D. L. McCorkle, W. Ding, C. Ma and L. A. Pinnaduwage, "Dissociation of Benzene in a Pulsed Glow Discharge," J. Appl. Phys. **86**, 3550 (1999).

[6] R. H. Stark and K. H. Schoenbach, "Direct Current High-Pressure Glow Discharges," J. Appl. Phys. **85**, 2075 (1999).

[7] R. H. Stark and K. H. Schoenbach, "Direct Current Glow Discharges in Atmospheric Air," Appl. Phys. Lett. **89**, 3568 (2001).

[8] F. Leipold, R. H. Stark, A. El-Habachi, and K. H. Schoenbach, "Electron Density Measurements in an Atmospheric Pressure Air Plasma by Means of Infrared (IR) Heterodyne Interferometry," J. Phys. D: Appl. Phys. **33**, 2268 (2000).

[9] E. E. Rennie, C. A. F. Johnson, J. E. Parker, D. M. P. Holland, D. A. Shaw, and M. A. Hays, "A photoabsorption, photodissociation and photoelectron spectroscopy study of C_6H_6 and C_6D_6," Chem. Phys. **229**, 107 (1998).

[10] H. Abouelaziz, J. C. Gomet, D. Pasquerault, R. B. Rowe, and J. B. A. Mitchell, "Measurements of $C_3H_3^+$, $C_5H_3^+$, $C_6H_6^+$, $C_7H_5^+$, $C_{10}H_8^+$ Dissociative Recombination Rate Coefficients," J. Chem. Phys. **99**, 237 (1993).

[11] Y. P. Raizer, Gas Discharge Physics, 2nd ed. Springer, Berlin, Germany (1991).

A00-33623

AIAA 2000–2417
Experiments and Simulations of DC and Pulsed Discharges in Air Plasmas

M. Nagulapally, G.V. Candler
University of Minnesota
Minneapolis, MN

C.O. Laux, L. Yu, D. Packan, C.H. Kruger
Stanford University
Stanford, CA

R. Stark, K.H. Schoenbach
Old Dominion University
Hampton, VA

31st AIAA Plasmadynamics and Lasers Conference

19–22 June 2000 / Denver, CO

Experiments and Simulations of DC and Pulsed Discharges in Air Plasmas

Manoj Nagulapally*
Graham V. Candler**
Department of Aerospace Engineering and Mechanics
University of Minnesota, Minneapolis MN 55455
Christophe O. Laux†
Lan Yu*
Denis Packan*
Charles H. Kruger‡
Department of Mechanical Engineering
Stanford University, Stanford CA 94305
Robert Stark†
Karl H. Schoenbach**
Department of Electrical and Computer Engineering
Old Dominion University, Hampton VA 23529

Abstract

Experiments were conducted with atmospheric air plasmas at temperatures around 2000 K in order to increase the electron number density to approximately $10^{13}\,cm^{-3}$ by means of an applied DC discharge and an electric pulse in parallel to the DC discharge. The DC discharge produces a stable region of elevated electron number density, in agreement with two-temperature kinetics calculations. In the pulsed experiments at the end of the 10 ns pulse, the ionization level was measured to be about 10^{13} electrons/cm^3. Following the pulse, the electron number density decreased to $10^{12}\,cm^{-3}$ in approximately 12 μs, in good agreement with the chemical kinetics model. This result suggests that elevated electron number densities of the order of $10^{13}\,cm^{-3}$ can be maintained in low temperature air plasmas by means of repetitively pulsed discharges. In this paper, we present results of the DC and pulsed experiments, as well as two-dimensional CFD simulations of the DC experiments. The computational model uses the Stanford two-temperature chemical kinetics model for the plasma, as well as finite-rate models for vibration-electronic energy relaxation and electron translational energy relaxation. The computational results are in good agreement with the measured electron concentration, temperatures, and cathode fall.

* Graduate Research Assistant, Student Member AIAA
** Professor, Senior Member AIAA
† Senior Research Scientist, Member AIAA
‡ Professor and Vice Provost, Dean of Research and Graduate Policy, Member AIAA

Introduction

There has been considerable interest in recent years in finding methods for reducing the power budget required to generate large volumes of atmospheric pressure air plasmas at modest temperatures below 2000 K with electron number densities of the order of $10^{13}\,cm^{-3}$. These reactive air plasmas potentially have numerous applications based on their medical, biological, environmental, electromagnetic, and aerodynamic effects. In order to increase the electron number density without significantly heating the gas, the energy must be added in a targeted fashion. One method is to apply the energy addition to the free electrons by means of an imposed electrical discharge. This approach was successfully demonstrated at Stanford in a series of experiments in atmospheric pressure air at temperatures between 1800 and 3000 K. In these experiments, a DC electric field was applied to flowing air plasmas with initial electron concentration corresponding to the chemical equilibrium value at the corresponding temperature. These experiments showed that it is possible to obtain stable diffuse glow discharges with electron number densities of up to $2 \times 10^{12}\,cm^{-3}$, which is up to six orders of magnitude higher than in the absence of the discharge. This value corresponds to the maximum current that can be drawn from the 250 mA power supply used in the experiments. In principle, the electron number density could be increased to higher values approaching $10^{13}\,cm^{-3}$ with a power supply capable of delivering more current. The diffuse discharges are approximately 3.5 cm in length and 3.2 mm in diameter. No significant degree of gas heating was observed, as the measured gas temperature remained within a few

hundred Kelvin of its value without the discharge applied. The measured power budget was found to be in good agreement with modeling predictions based on a zero-dimensional model of plasma chemistry coupled with an electric discharge model over the entire range of our measurements. For electron number densities of $10^{13}\,cm^{-3}$, the predicted power budget is approximately $20\,kW/cm^3$.

Because the power budget for DC electron heating is too high for the practical use of air plasmas in large-scale applications, methods to reduce the power budget are being explored at Stanford. Based on the predictions of our chemical kinetics and electrical discharge models, it was found that a repetitively pulsed electron heating strategy could provide significant power budget reductions. The basis of the pulsed heating strategy is to leverage the finite recombination time of electrons and to increase the ionization efficiency by using voltage pulses of duration much shorter than the recombination time. Significant increases in ionization efficiency can be obtained by using short electric pulses with peak voltages moderately larger than for the case of DC electron heating. These high voltage pulses significantly enhance the tail of the electron energy distribution function, thereby increasing the rate of ionization relative to vibrational excitation by electron impact, which is the dominant channel for inelastic power losses in the DC discharges investigated.

In this paper, we present a summary of the DC and pulsed experimental results along with numerical simulations of the DC experiments. The calculations are being used to quantify the effect of a DC discharge on the electron concentration in the atmospheric pressure air plasma and to refine our fundamental understanding of ionization kinetics.

Experimental Approach

All experiments described here were conducted with the experimental set-up shown in Figure 1. The device consists of two parts, a gas preheater and a discharge region. The gas preheater comprises a 50 kW radio-frequency inductively-coupled plasma torch operating at a frequency of 4 MHz, a cold gas injection ring, and a water-cooled mixing test-section with an inner diameter of 2 cm and a length of 18 cm. The temperature of the plasma at the exit of the 2 cm diameter torch nozzle is about 5000 K and its velocity is about 100 m/s. The plasma then enters a test-section where it is cooled to the desired temperature by mixing with an adjustable amount of cold air injected into the plasma stream through a radial mixing ring. At the exit of the mixing test-section the air flow is close to local thermodynamic equilibrium (LTE) conditions. Finally, a 1 cm exit diameter converging nozzle is mounted at the exit of the mixing test-section. This nozzle is used to control the velocity, hence the residence time, of the flow within the discharge region. For the pulsed discharge experiments, the centerline temperature, flow velocity, and mass flow rate at the entrance of the discharge region were approximately 2300 K, 440 m/s and 4.9 g/s, respectively.

The discharge region consists of two platinum pin electrodes of 0.5 mm diameter held along the axis of the air stream by two water-cooled $\frac{1}{16}''$ stainless-steel tubes placed crosswise to the plasma flow. The bottom electrode is mounted on the copper nozzle and the upper electrode is affixed to a Lucite ring itself mounted on a vertical translation stage in order to provide adjustable interelectrode distance. Several platinum pins (diameter 0.02″) can be inserted into the discharge region to measure the voltage at various locations along the axis of the discharge in order to determine the electric field. The interelectrode distance was set to 3.5 cm for the DC discharge experiments, and 1.2 cm for the combined pulsed/DC discharges.

The electric pulse was generated with a pulse forming line system developed at Old Dominion University by Stark and Schoenbach. The pulse shape was approximately rectangular, with maximum voltage of 10 kV and duration 10 ns. In the pulsed experiments, a DC discharge of 2 kV and 150 mA was applied in parallel to the pulse in order to pre-ionize the plasma at an electron number density of approximately $6.5 \times 10^{11}\,cm^{-3}$. In all experiments presented here, the bottom electrode was biased to negative potentials and the top electrode was connected to ground.

Experimental Results

DC Discharge Experiments

Figure 2 a photograph of the air plasma plume in the region between the two electrodes without the discharge applied. Figure 3 shows the same region with the DC discharge Applied between the electrodes. In these DC experiments, the interelectrode distance was 3.5 cm, the discharge current 200 mA, and the voltage applied across the electrodes was 5.2 kV. The bright region in Figure 3 corresponds to the discharge-excited plasma. The discharge diameter is approximately 3.5 mm and the electron concentration was determined from electrical conductivity measurements to be approximately $2 \times 10^{12}\,cm^{-3}$. Without the discharge applied, the centerline rotational temperature along the axis of the flow decreases from 2300 K immediately

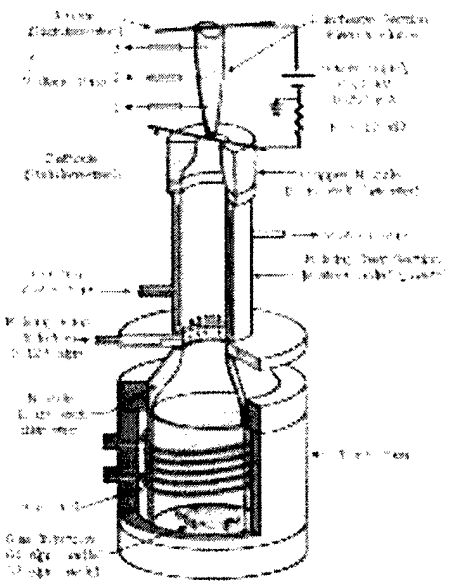

FIGURE 1. Schematic of the Stanford Plasma Torch, showing the location of the discharge section.

above the cathode (bottom electrode) to 2020 K at the anode. With the discharge applied, the measured rotational temperature remains approximately constant at a value of 2300 K along the axis of the discharge region. Thus the applied discharge does not noticeably increase the temperature of the plasma. The cathode fall voltage of the DC discharge was measured from the potential difference between the cathode and a voltage pin placed at a distance of 0.2 mm downstream of the cathode. The measured value of 290 V is in excellent agreement with the cathode fall voltage reported in the literature for glow discharges.[1]

The measured electrical discharge characteristics for this case as well as several additional experimental conditions at plasma temperatures ranging from 1800 to 2900 K are shown in Figure 4. The solid curves in Figure 4 correspond to the predicted discharge characteristics in atmospheric pressure air plasmas at temperatures of 2000 and 3000 K, respectively. A detailed description of the theory underlying these predicted discharge characteristics was presented in Ref. 2. Good agreement is obtained between the measured and predicted discharge characteristics over a range of experiments spanning more than three orders of magnitude in current density. The current density corresponding to an electron number density of $10^{13}\,\mathrm{cm}^{-3}$ is indicated by the dashed line in the figure. The predicted current density j and electric field E required to generate 10^{13} electrons/cm^3 in 2000 K atmospheric pressure air are equal to $17\,\mathrm{A/cm}^2$ and 1.4 kV/cm. The corresponding power budget, jE, is therefore approximately $24\,\mathrm{kW/cm}^3$.

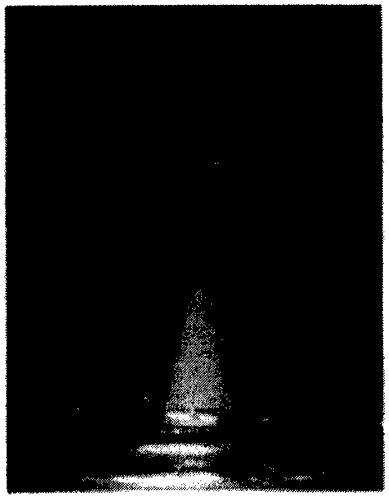

FIGURE 2. Air plasma at 2000 K without discharge.

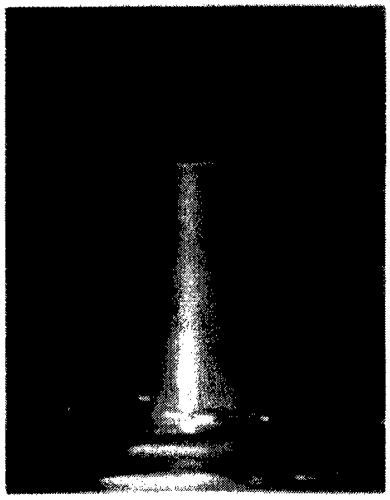

FIGURE 3. Air plasma at 2000 K with DC discharge. The measured electron number density in the bright central region is approximately $2 \times 10^{12}\,\mathrm{cm}^{-3}$.

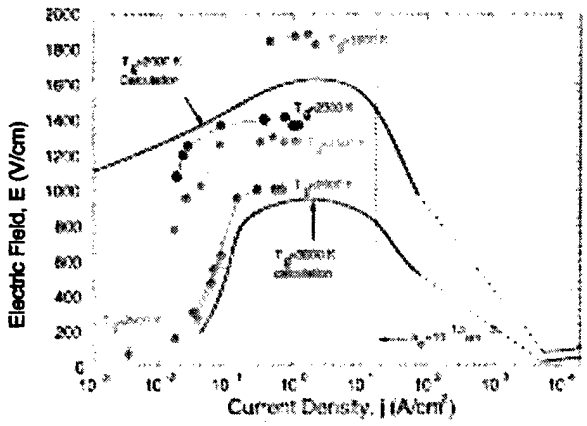

FIGURE 4. Measured and predicted electrical discharge characteristics in atmospheric pressure air plasmas generated by DC electric discharges.

Pulsed Discharge Experiments

As discussed in the previous section, the power budget required to sustain elevated electron number densities with DC electric discharges is too high for practical applications with large volume air plasmas. We have therefore explored new strategies to reduce the power budget required to sustain superionized air plasmas. Our investigations have focused on an approach based on pulsed electron heating. The basis of the pulsed heating strategy is to leverage the finite recombination time of electrons and to increase the ionization efficiency by using short electric pulses with peak voltages moderately larger than for the case of DC electron heating. These high voltage pulses significantly enhance the tail of the electron energy distribution function, thereby increasing the rate of ionization relative to vibrational excitation by electron impact, which is the dominant channel for inelastic power losses in the DC discharges investigated.

This strategy is illustrated in Figure 5. Short voltage pulses are applied intermittently to increase the electron number density. The decay rate between pulses is governed by electron recombination processes. The average electron number density obtained with this system depends on the pulse duration, the interval between two consecutive pulses, and the pulse voltage.

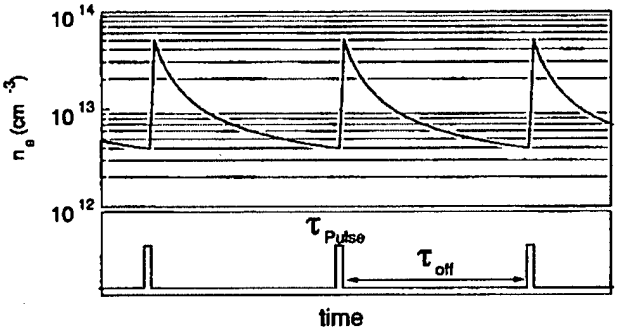

FIGURE 5. Predicted electron number density for a repetitively pulsed discharge.

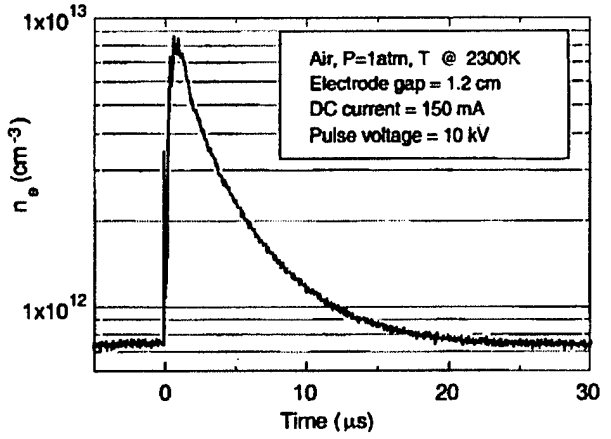

FIGURE 6. Electron number density as a function of time for the pulsed discharge experiment.

In order to test the pulsing scheme, experiments were conducted at Stanford University in collaboration with Old Dominion University. These experiments employed a pulse forming line, designed and built at Old Dominion University, capable of generating a short duration (10 ns) rectangular electric pulse with peak voltages that can be varied in the range 0-16 kV. In order to experimentally simulate a repetitively pulsed discharge, the initial elevated electron number density resulting from the "previous" pulse in a repetitive discharge was created using a DC discharge operated in parallel with the pulse. These experiments enabled us to determine the voltage required to increase the electron number density to approximately $10^{13}\,\mathrm{cm}^{-3}$ with a 10 ns ionizing pulse as well as the recombination time of electrons after the end of the pulse.

In order to determine the effect of the pulse on the plasma, the electrical resistance of the plasma was measured as a function of time from the voltage across the electrodes and the current flowing through the plasma. The electron number density can be obtained from the resistance measurements if the area of the discharge is known. This area was obtained from optical measurements of the light emitted by the plasma during pulse excitation and found to be approximately the same as the DC discharge diameter of 3.2 mm. The electron number density measured in this manner is shown in Figure 6. The electron number density increases from the initial value of $6.5 \times 10^{11}\,\mathrm{cm}^{-3}$ to a peak of $10^{13}\,\mathrm{cm}^{-3}$, then decays to $1 \times 10^{12}\,\mathrm{cm}^{-3}$ in approximately 12 μs. The average measured electron number density over the 12 μs duration is $2.8 \times 10^{12}\,\mathrm{cm}^{-3}$. With careful accounting for the background elevation of the electron temperature and the fact that the gas is flowing during the experiment, the two-temperature kinetic model has been shown to agree very well with the experimental results.

Power Budget

We can now estimate the power reduction afforded by repetitively pulsed electron heating in comparison with DC electron heating. We consider here a repetitively pulsed discharge starting from an initial electron number density of $10^{12}\,\mathrm{cm}^{-3}$. The electron number density is increased to $10^{13}\,\mathrm{cm}^{-3}$ with a 10 ns rectangular voltage pulse. The electron temperature required to produce 10^{13} electrons/cm^3 in 10 ns is calculated to be 32,900 K, corresponding to a field of 4 kV/cm. The

gas temperature is assumed to be 2000 K. In order to simulate the case of a repetitive discharge without background DC electron heating, we consider that the electron temperature is equal to 2000 K throughout the recombination phase. The time predicted for the electrons to recombine to the initial value of $10^{12}\,\mathrm{cm}^{-3}$ is 8.7 μs. The calculated average electron number density over the entire cycle is approximately $2.6 \times 10^{12}\,\mathrm{cm}^{-3}$.

From the results shown in Fig. 4, the current density and electric field required to sustain an electron number density of $2.6 \times 10^{12}\,\mathrm{cm}^{-3}$ using DC electron heating are $4.5\,\mathrm{A/cm^2}$ and 1600 V/cm, respectively. The volumetric power for the DC case is then

$$P_{\mathrm{DC}} \simeq 4.5\,\mathrm{A/cm^2} \times 1600\,\mathrm{V/cm} = 7.2\,\mathrm{kW/cm^3}$$

For the repetitively pulsed system, the average current density during the ionization phase can be calculated from Ohm's law and the predicted electron number density evolution. For the present case, the peak current density at the end of the pulse is approximately $30\,\mathrm{A/cm^2}$ and the average current density during the pulse $10.5\,\mathrm{A/cm^2}$. The average power during the 10 ns pulse is then $10.5\,\mathrm{A/cm^2} \times 4.0\,\mathrm{kV/cm} = 42\,\mathrm{kW/cm^3}$. The total power over one pulse cycle is obtained by multiplying this value by the duty cycle of the pulser, here equal to $(10\,\mathrm{ns})/(8.7\,\mu\mathrm{s}) = 1.15 \times 10^{-3}$. The power requirement for the repetitive pulsed discharge is then

$$P_{\mathrm{Pulsed}} \simeq 42\,\mathrm{kW} \times 1.15 \times 10^{-3} = 48\,\mathrm{W/cm^3}$$

Thus the power budget reduction afforded by the repetitively pulsed discharge in comparison with the DC discharge is a factor of 150.

The optimal power budget that can be achieved with a pulse of given duration τ_1 in air at a given gas temperature depends on the minimum and maximum electron number densities in each pulse ($n_{e,\mathrm{min}}$ and $n_{e,\mathrm{max}}$), the concentrations of heavy species, the electric field during (or equivalently the electron temperature imposed by) the pulse, the interval between pulses τ_2, and the desired average electron number density in the repetitive discharge. From analysis of the full 38-reaction mechanism for the case of ionization with a pulse $\tau_1 = 10$ ns, we find that the dominant chemical reactions during the ionization phase are the electron impact ionization of O_2 and N_2. Shortly after the end of the ionization phase, the dominant ion becomes NO^+ as a result of fast charge transfer and charge exchange reactions. Thus for the recombination phase, we consider that the dominant reaction is the dissociative recombination of NO^+. Based on these observations, the electron number density evolution during the ionization and recombination phases can be approximated as

$$\left.\frac{\mathrm{d}n_e}{\mathrm{d}t}\right|_{\mathrm{ionization}} \simeq k_{\mathrm{ion},N_2} n_e n_{N_2} + k_{\mathrm{ion},O_2} n_e n_{O_2} \simeq k_{\mathrm{ion}} n_e N$$

and

$$\left.\frac{\mathrm{d}n_e}{\mathrm{d}t}\right|_{\mathrm{recombination}} \simeq -k_{\mathrm{DR,NO+}} n_e n_{\mathrm{NO+}} \simeq k_{\mathrm{DR}} (n_e)^2$$

where the rate coefficients of electron impact ionization of N_2 and O_2 (which depend on the electron temperature T_e) and the rate coefficient for dissociative recombination of NO^+ are taken from Ref. 2.

The ratio R of the power required to produce a given average electron number density n_e^* with a repetitively pulsed discharge relative to the power required to produce the same electron number density with a DC discharge can be expressed as

$$R = \frac{(\sigma E^2)_{\mathrm{DC}}}{(\sigma E^2)_{\mathrm{Pulse}}} \times \frac{\tau_1 + \tau_2}{\tau_1}$$

Using the electron energy equation and Ohm's law (see Ref. 2), R can be approximated by

$$R \simeq \frac{n_e^*}{\langle n_e \rangle^{\mathrm{ion}}} \frac{[T_{e,\mathrm{DC}}]^{3/2}}{[T_{e,\mathrm{Pulse}}]^{3/2}} \times \frac{\tau_1 + \tau_2}{\tau_1}$$

where $\langle n_e \rangle^{\mathrm{ion}}$ stands for the average electron number density during the ionization phase of the pulse.

By solving the electron number density rate equations, analytical expressions can be obtained for $\langle n_e \rangle^{\mathrm{ion}}$ and τ_2 as a function of τ_1, T_e, and the various rate coefficients. Assuming that the duration τ_2 of the recombination phase is much longer than the ionization phase τ_1 , we obtain

$$R \simeq \frac{k_{\mathrm{ion}}(T_e) N}{k_{\mathrm{DR}} n_e^*} \times \frac{\alpha^2 e^\alpha}{(e^\alpha - 1)^2} \times \left(\frac{T_{e,\mathrm{DC}}}{T_{e,\mathrm{Pulse}}}\right)^{3/2}$$

where $\alpha \equiv k_{\mathrm{ion}} N \tau_1$. Additional expressions can also be obtained for τ_2 and for the minimum and maximum electron number densities of the repetitive pulsed discharges.

Figure 7 shows the power reduction factor, minimum and maximum electron number densities, and interval between pulses as a function of the pulsed electron temperature to maintain an average electron number density of 2.6×10^{12} electrons/cm^3 with a 10 ns repetitively pulsed discharge in 2000 K atmospheric pressure air. It can be seen that there exists an optimum electron temperature of 27,000 K for maximum power budget reduction by a factor of 220.

The corresponding optimal parameters are minimum and maximum electron number densities of 1.3×10^{12} and $6.1 \times 10^{12}\,\mathrm{cm}^{-3}$, respectively, and interval between pulses of 8 microseconds. For an electron temperature of 32,900 K corresponding to the case analyzed in the previous section, we find that the predicted power budget reduction is by a factor of 190, which is consistent with the factor of 150 predicted by the more refined analysis presented earlier. This type of analysis is thus useful to optimize repetitive pulsing strategies. It should be noted that care should be exercised in extrapolating the above power budget reduction expression to the case of pulses shorter than 10 ns because the ionization phase may be affected by additional reactions at shorter pulse durations.

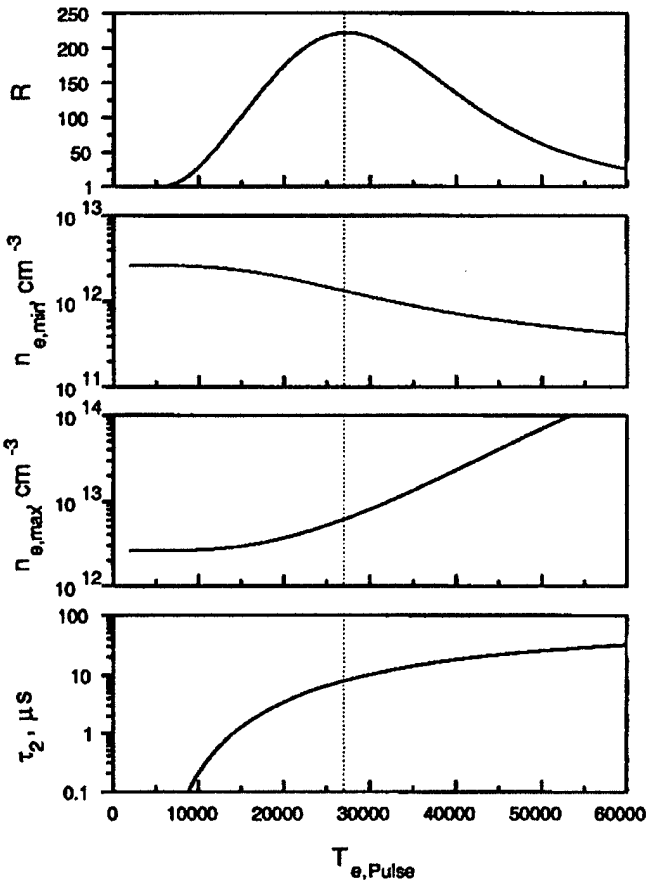

FIGURE 7. Power reduction factor afforded by pulsed vs. DC discharges to maintain an average electron number density of 2.6×10^{12} electrons/cm^3 in 2000 K atmospheric pressure air, as a function of the pulsed electron temperature. Also shown are the minimum and maximum electron number densities, and interval between pulses. All calculations are for a pulse duration of 10 ns.

Numerical Simulations

In this section we discuss our numerical simulations of the DC discharge experiments. The main extension of previous work[3] involves the modeling of the discharge region.

Conservation Equations

The DC discharge flow field is described by the Navier-Stokes equations that have been extended to include the effects of nonequilibrium thermochemistry. We solve separate mass conservation equations for each of the 11 chemical species present, as well as conservation equations for the radial, axial and swirl direction momenta. The energy of the flow is modeled by solving a total energy conservation equation, a vibration-electronic energy conservation equation, and an electron energy conservation equation.

Here we focus on the electron energy conservation equation because the variation of the electron temperature is the most important effect in these flows. We have

$$\frac{\partial E_e}{\partial t} + \nabla \cdot ((E_e + p_e)(\mathbf{u} + \mathbf{v}_e) = -\nabla \cdot \mathbf{q}_e - n_e e \tilde{\mathbf{E}} \cdot \mathbf{u} - Q_{h-e} - Q_{v-e} + w_e e_e,$$

where $\mathbf{q_e} = -k_e \nabla \cdot T_e$, is the flux of electron energy. The conductivity of electron temperature, k_e is taken from Mitchner and Kruger.[4] Q_{h-e}, the heavy particle-electron energy transfer rate, is

$$Q_{h-e} = n_e \sum_h 3k(T_e - T)\left(\frac{m_e}{m_h}\right)\delta_{eh}\nu_{eh}.$$

The vibrational-electron energy transfer rate, Q_{v-e} is from Ref. 5. The electric field, $\tilde{\mathbf{E}}$, may be expressed in terms of the electron pressure, p_e, and current density, j, and the electrical conductivity, σ, as

$$-n_e e \tilde{\mathbf{E}} \cdot \mathbf{u} = \nabla p_e \cdot \mathbf{u} + \frac{j^2}{\sigma}$$

In the above equations, w_e is the chemical source term for the electrons, δ_{eh}, is the nonelastic energy factor and ν_{eh}, is the average frequency of collisions between electrons and heavy particles. For the experimental conditions, the ions have negligible concentrations, and the the collision frequency is well approximated by

$$\nu_{eh} = \frac{p}{kT} g_e Q_{en},$$

where $g_e = \sqrt{8kT_e/\pi m_e}$ is the electron thermal speed and Q_{en} is the average cross-section taken to be $10^{-15}\,\mathrm{cm}^2$.

Discharge Model

To model the discharge region shown in Fig. 3, we generalize the channel model suggested by Steenbeck.[1]

At an infinitesimal time after the discharge is ignited, the current is vanishingly small everywhere except within the discharge region between the electrodes. The current at each axial, x, location is then

$$i = 2\pi \int_r \sigma E r \, dr \approx 2\pi E \int_r \sigma r \, dr,$$

where E is assumed to be only a function of x.

The current is controlled experimentally, and thus is a prescribed parameter. By imposing this current conservation at every location along the axis of the discharge, the field $E(x)$ can be determined from the above equation. Now, we can apply the field to the electron energy equation in the form of the Joule heating source term. The discharge then spreads and attains a steady shape as a result of diffusive processes.

As mentioned earlier, the pin electrodes are placed cross-wise to the plasma flow. Since the stainless steel tubes carrying the electrodes do not significantly disturb the flow, the flow around the electrodes is not modeled. However, the effect of the cathode is considered by injecting a flux of electrons from a region that corresponds to the location of the cathode. This flux is calculated from the total current in the discharge and the effective area of the cathode.

Numerical Method

Under the conditions of the DC discharge experiments, the energy relaxation processes are very fast relative to the fluid motion time scales and the chemical kinetic processes. To handle this large disparity in characteristic time scales, we would usually use an implicit time integration method.[6] However, for this problem a complete linearization of the problem is itself very expensive. (We solve 17 conservation equations, and the cost of evaluating the Jacobians and inverting the system scales with the square of the number of equations.) Therefore we linearize only those terms that are relatively fast, which results in a simple and inexpensive semi-implicit method that very substantially reduces the cost of the calculations.

The relatively fast terms are the internal energy relaxation and the Joule heating terms in the source terms for the three energy equations. Therefore, we split the source vector, W, into these terms, W_{fast}, and all of the other terms, W_{slow}. The conservation equations are then written as

$$\frac{\partial U}{\partial t} + \frac{\partial F}{\partial x} + \frac{1}{r}\frac{\partial r G}{\partial r} = W_{\text{fast}} + W_{\text{slow}},$$

where U is the vector of conserved variables, F is the axial direction flux vector and G is the radial direction flux vector. We then linearize W_{fast} in time

$$W_{\text{fast}}^{n+1} = W_{\text{fast}}^{n} + C_{\text{fast}}^{n} \delta U^{n} + O(\Delta t^2)$$

where C_{fast} is the Jacobian of W_{fast} with respect to U, and $\delta U^n = U^{n+1} - U^n$. Because of the form of W_{fast}, C_{fast} is a simple matrix that can be inverted analytically. Then the solution is integrated in time using

$$\delta U^{n+1} = \left(I - \Delta t\, C_{\text{fast}}^{n}\right)^{-1} \Big(\Delta t \left(W_{\text{fast}}^{n} + W_{\text{slow}}^{n}\right) - \Delta t\Big(\frac{\partial F^n}{\partial x} + \frac{1}{r}\frac{\partial r G^n}{\partial r}\Big)\Big)$$

This approach increases the stable time step by a factor of 50 compared to an explicit Euler method. This results in a very large reduction in the computer time required to obtain a steady-state solution.

A two-block grid is used to facilitate the implementation of the boundary conditions. The first grid block represents the nozzle section, and the second grid block represents the discharge region as well as a portion of the open air which acts as a large constant-pressure exhaust reservoir at one atmosphere.

The inflow boundary conditions are set by choosing the inflow static pressure to give the experimental mass flow rate of 4.9 g/s. The inflow is assumed to be in LTE at the measured temperature profile. This results in a consistent representation of the inflow conditions. The boundary conditions along the test-section surface are straight-forward. The velocity is zero at the surface, the temperature is specified, and the normal-direction pressure gradient is zero. We assume that the metallic surface is highly catalytic to ion recombination. Otherwise, the surface is assumed to be non-catalytic to recombination for neutrals.

The computation is initialized as follows: first, the inflow conditions are specified as above. Then the test-section and reservoir are all initialized at atmospheric pressure, and at each axial location the temperature profiles and chemical concentration profiles are set identical to the inflow boundary profiles. Once a converged solution is obtained for the flow in LTE, the discharge is ignited by injecting a flux of electrons at the cathode and applying the Joule heating source term to the energy equations. Then a steady-state solution for the DC discharge is obtained.

Thermochemical and Transport Properties

We use the Stanford two-temperature 11-species, 38-reaction chemical kinetics model for air plasmas.[1] Transport properties are computed via mixing rules[7] from curve-fitted transport properties of individual species in the air plasma.[8] The electrical conductivity is taken from Ref. 2.

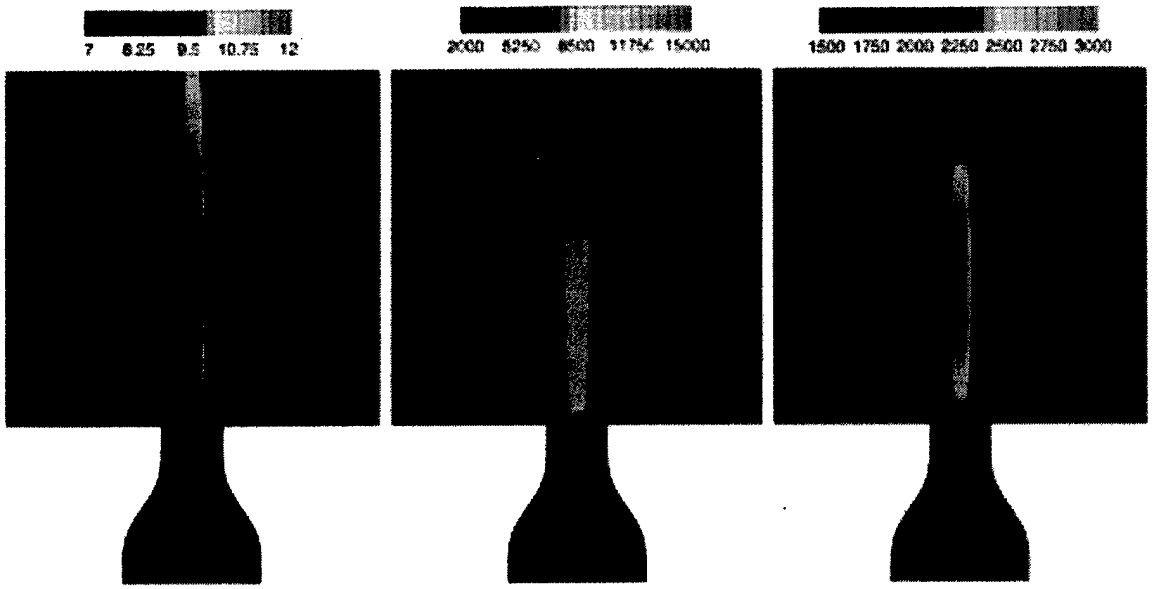

(a) (b) (c)

FIGURE 8. $\log_{10}$ of the electron number density (a); electron Temperature (b); and translational temperature contours in the discharge region.

Computational Results

In this section we present numerical simulations of the DC discharge experiment. Figure 8a shows the $\log_{10}$ of the electron number density contours in the computational domain. The DC discharge region can be observed in this figure. This is the bright region where the electron number density is several orders of magnitude higher than in the region upstream of the cathode where there is no discharge. It can be observed that the electron number density is slightly higher than $10^{12}\,\mathrm{cm}^{-3}$ in most of the discharge region. This is in good agreement with the experimental measurements for the electron number density. The electron number density falls off gradually downstream of the anode region. The shape of the discharge is similar to that observed in the photograph of the discharge in Fig. 3. The photograph also shows that the discharge is constricted at the cathode and diffuses radially outward, away from the cathode. The simulations capture this behavior.

Figure 8b plots the electron temperature contours in the computational domain. It shows that the electron temperature is about 12,000 K in the discharge region. The computed electron temperatures are consistent with the experimental predictions. Figure 8b also shows that the electron temperature drops off sharply just downstream of the anode because the electrons rapidly equilibrate with the heavy particles due to their strong coupling with the heavy species.

Figure 8c shows contours of the translational temperature in the domain. It shows that the temperature in the discharge is about 3000 K in the discharge region. The computed temperatures are generally higher than the experimental measurements. Previous simulations of the Stanford University plasma torch experiments showed a similar over-prediction in the translational temperature. This indicates that the flow model used in the simulations may be missing an energy transport mechanism.

Figure 9 plots the axial variation of the centerline electron number density and the temperatures along with the experimental values. This figure quantitatively shows the variation of the electron concentration and the three temperatures along the centerline of the discharge. From the figure it can be seen that the electron number density remains slightly above $10^{12}\,\mathrm{cm}^{-3}$ in the discharge region. It falls off gradually downstream of the anode. The computed electron temperature is very high in the cathode region and falls to about 12,000 K in most of the discharge region, which is close to the two-temperature kinetic model prediction. As observed in the contour plot for the electron temperature, the electron temperature falls off abruptly in the region downstream of the anode. The translational temperature increases from about 2200 K at the cathode to about 3000 K in the discharge region. This is higher than the measured translational temperature. However, the computed vibrational temperature is slightly lower than the experimentally measured value.

Figure 10 plots the radial profiles of the electron number density at two locations in the discharge. Near the cathode it can be seen that the diameter of the discharge is small and the electron number density is elevated in a region which is nearly equal to that of the cathode area. Near the center of the discharge the electron density is more diffuse and the diameter of the discharge is about to 4 mm, which compares well with the experimentally observed diameter.

Figure 11 plots the computed potential along the centerline of the discharge. The computed potential is nearly linearly increasing with a finite cathode fall of about 300 V. The experiments indicate 290 V.

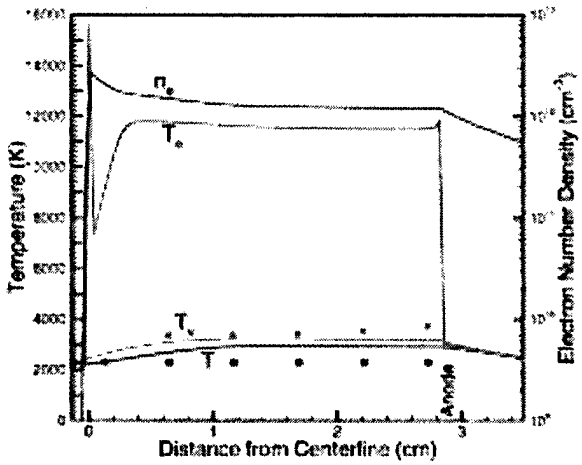

FIGURE 9. Computed electron number density and temperatures along the DC discharge centerline. Symbols denote experimentally measured values.

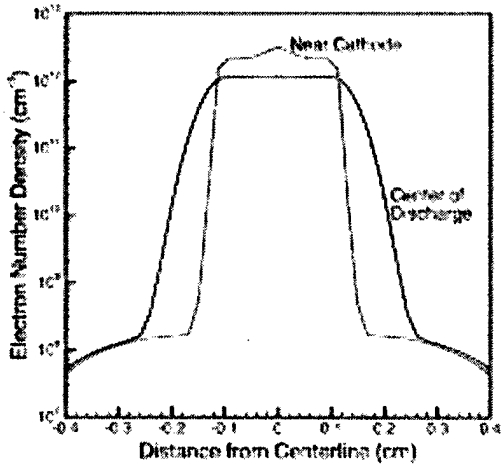

FIGURE 10. Computed radial profiles of electron number density

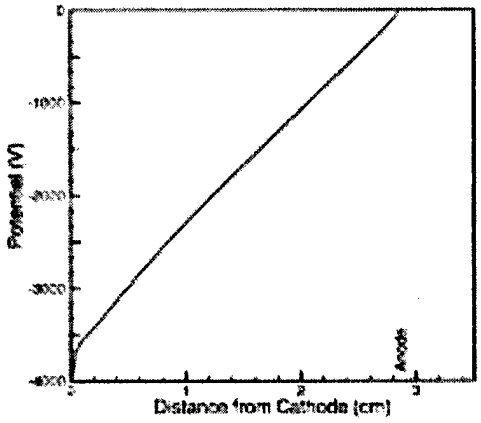

FIGURE 11. Axial variation of the potential along the centerline

Conclusions

The present work demonstrates that stable, diffuse discharges with electron number densities approaching $10^{13}\,\mathrm{cm}^{-3}$ at gas temperatures below 2000 K can be produced in atmospheric pressure air. This result stands in sharp contrast with the widespread belief that these diffuse discharges cannot exist without arcing instabilities or high levels of gas heating. The experiments also show that the power required to sustain an ionization level of $10^{13}\,\mathrm{cm}^{-3}$ with a DC discharge is close to $20\,\mathrm{kW/cm}^3$. Repetitively pulsed electron heating strategies were investigated as a way to reduce the power consumption. The experimental and modeling results presented here demonstrate that the power consumption can be dramatically reduced, by over two orders of magnitude, through the use of 10 ns pulsed electrical discharges with pulse characteristics tailored to match the ionization and recombination reaction times. A computational fluid dynamics code for the simulation of flowing nonequilibrium air plasmas including the presence of a DC discharge was developed and compared to the DC experiments conducted at Stanford University. The code uses a detailed two-temperature chemical kinetic mechanism, along with appropriate internal energy relaxation mechanisms. The discharge region was modeled by generalizing the channel model of Steenbeck, and a new semi-implicit time integration method was developed to reduce the computational cost. The computational results show good agreement with the experimental data, however the heat loss is more rapid in the experiment than predicted by the computations. Work is being carried out to fully understand this discrepancy. The code will be extended to handle the modeling of the pulsed discharges under investigation.

Acknowledgments

This work was funded by the Director of Defense Research & Engineering (DDR&E) within the Air Plasma Ramparts MURI program managed by the Air Force Office of Scientific Research (AFOSR). Computer time was provided by the Minnesota Supercomputing Institute.

References

[1] Raizer, Y.P, *Gas Discharge Physics* Springer, New York, pp. 278-279, 1991.

[2] Laux, C., Pierrot, L., Gessman, R. and Kruger, C.H., "Ionization Mechanisms of Two-temperature Plasmas," *30th AIAA Plasmadynamics and Lasers Conference, AIAA 99-3476,* Norfolk, VA, June. 1999

[3] Nagulapally. M., D. Kolman, G.V. Candler, C.O. Laux, R.J. Gessman, and C.H. Kruger, " Numerical Simulation of Nonequilibrium Nitrogen and Air Plasma Experiments," *29th AIAA Plasmadynamics and Lasers Conference, AIAA 98-2665,* Albuquerque, NM, June 1998.

[4] Mitchner, M. and C.H. Kruger, *Partially Ionized Gases,* Wiley, New York, pp. 92-94, 1973

[5] Lee, J-H.,"Electron-Impact Vibrational Relaxation in High-temperature Nitrogen," *30th Aerospace Sciences Meeting and Exhibit AIAA 92-0807,* Reno, NV, January. 1992

[6] Candler, G.V. and R.W. MacCormack, "The Computation of Hypersonic Ionized Flows in Chemical and Thermal Nonequilibrium," *J. Thermophysics Heat Transfer,* Vol. 5, No. 3, pp. 266-273, July 1991.

[7] Wilke, C.R., "A Viscosity Equation for Gas Mixtures," *J. Chem. Phys.,* Vol. 18, No. 4, p. 517, Apr. 1950.

[8] Gupta, R.N., Yos, J.M., Thompson, R.A., and Lee, K.-P., "A Review of Reaction Rates and Thermodynamic and Transport Properties for an 11-Species Air Model for Chemical and Thermal Nonequilibrium Calculations to 30,000 K," *NASA RP-1232,* Aug. 1990.

Abstracts

Abdel-Aleam H. Mohamed, Frank Leipold, Juergen Kolb, Sususmu Kono, and Karl H. Schoenbach, "Atmospheric Pressure Glow Discharge Micro-Plasma Jet," Conference Record, 2003 IEEE Intern. Conf. Plasma Science, Jeju, Korea, June 2 –5,, 2003, Paper 1PA13, p. 148.

Frank Leipold and Karl H. Schoenbach, "Electron Density and Electron Temperature in Pulsed Atmospheric Pressure Air Plasmas," Conference Record, 2002 IEEE Intern. Conf. Plasma Science, Banff, Alberta, Canada, May 26-30, 2002, Paper 2P03, p. 143.

Frank Leipold, Abdel-Aleam Hufney Mohamed, and Karl H. Schoenbach, "Measurements of Electron Temperature and Gas Temperature in a Pulsed Atmospheric Pressure Air Discharge," GEC, Penn State University, October 2001, Bulletin of the American Physical Soc., Vol. 46, No. 6, Abstract DTP 45, page. 22.

Chunqi Jiang, Robert H. Stark, and Karl H. Schoenbach, "Benzene Dissociation in DC Atmospheric Pressure Air Glow Discharges," GEC, Penn State University, October 2001, Bulletin of the American Physical Soc., Vol. 46, No. 6, Abstract JWP 4, page. 34.

Frank Leipold, Robert Stark, and Karl H. Schoenbach, "Electron Density and Temperature Measurements in Pulsed Atmospheric Pressure Air Plasmas," APP Spring Meeting, Bad Honnef 2001, "Diagnostics of Non-Equilibrium High Pressure Plasmas" Physikzentrum Bad Honnef, Feb. 18-21, 2001, in www.ilp.physik.uni-essen.de/doebele/Spring2001

Robert H. Stark, Hisham Merhi, and Karl H. Schoenbach, "Pulsed Electron Heating in Atmospheric Pressure Glow Discharges," APP Spring Meeting, Bad Honnef 2001, "Diagnostics of Non-Equilibrium High Pressure Plasmas" Physikzentrum Bad Honnef, Feb. 18-21, 2001, in www.ilp.physik.uni-essen.de/doebele/Spring2001

Robert H. Stark, Frank Leipold, Chunqi Jiang, Hisham Merhi, and Karl H. Schoenbach, "Electron Heating in Pulsed Atmospheric Pressure Glow Discharges," Bull APS (GEC), Vol. 45, No. 6, October 2000, CT2 6, p. 17.

Frank Leipold, Robert H. Stark, and Karl H. Schoenbach, "Measurement of Electron Densities in a Pulsed Atmospheric Pressure Air Discharge," Bull APS (GEC), Vol. 45, No. 6, October 2000, ETP 53, p. 30.

Robert H. Stark and Karl H. Schoenbach, "Electron Heating in Atmospheric Pressure Air Discharges," Conf. Record, IEEE Intern. Conf. Plasma Science, New Orleans, 2000, paper 1A05, p. 83.

Rolf Block, Abdel-Aleam H. Mohamed, and Karl H. Schoenbach, "Plasma Cathode Sustained Filamentary Glow Discharges in Atmospheric Air," Conf. Record, IEEE Intern. Conf. Plasma Science, New Orleans, 2000, paper 1P23, p. 110.

Robert H. Stark, Ahmed El-Habachi, and Karl H. Schoenbach, "Parallel Operation of Microhollow Cathode Discharges," Conf. Record, IEEE Intern. Conf. Plasma Science, New Orleans, 2000, paper 1P24, p. 111.

1PA13

Atmospheric Pressure Glow Discharge Micro-Plasma Jet[†]

Abdel-Aleam H. Mohamed, Frank Leipold, Juergen Kolb, Susumu Kono and Karl H. Schoenbach

Physical Electronics Research Institute, Old Dominion University, Norfolk, VA 23529, USA

Atmospheric pressure microhollow cathode discharges (MHCDs) offer the possibility to generate non-thermal plasma by relatively simple means [1]. When operated in rare gases or rare gas-halide mixtures it emits excimer radiation with high efficiency. Operating the discharges in atmospheric pressure air has been shown to allow their use as plasma cathodes for stable large volume atmospheric pressure air plasmas. The plasma results from a direct current discharge between two molybdenum electrodes (0.25 mm thick) that are separated by an alumina insulator of the same thickness. A tapered discharge channel is drilled through all layers, leaving a 0.2 mm wide opening in the cathode and an opening of $\sim$ 0.1 mm in diameter in the anode. By flowing air or nitrogen at atmospheric pressure through this hole, a well-defined plasma jet is generated with typical dimensions of millimeters in axial direction. The power consumption ranges from 2 W to 8 W. The optical and thermal characteristics of this micro plasma jet have been studied. The gas temperature was measured by means of emission spectroscopy using the 0-0 band within the second positive system of nitrogen. Increasing the nitrogen flow rate from 0 to 200 ml/min while applying a constant discharge current of 10 mA resulted in a considerable decrease of gas temperature from 2000 K to 800 K. This novel plasma source offers the opportunities for applications such as fine surface treatment of organic materials [2], plasma surgery [3], and cleaning of semiconductor chips.

[1] Karl H. Schoenbach, Ahmed El-Habachi, Wenhui Shi, and Marco Ciocca, Plasma Sources Science and Technology 6, 468 (1997).
[2] E. Stoffels, A.J. Flikweert, W.W. Stoffels and G.M.W. Kroesen, Plasma Sources Sci. Technol. 11, 383 (2002).
[3] A.I. Necha, G.A. Kostiuk, S.V. Dzhaiani, A.S. Iushkin, and S.A. Kalashnikov, Vestnik Khirurgii Imeni I. I. Grekova 143, no. 10, 7 (1989).

This work is supported by the Air Force Office of Scientific Research (AFOSR).

[†] kschoenb@odu.edu

Atmospheric Pressure Glow Discharge Micro-Plasma Jet

Abdel-Aleam H. Mohamed, Srinivas Suddala, Frank Leipold, Juergen Kolb, Susumu Kono, and Karl H. Schoenbach

Physical Electronics Research Institute, Old Dominion University Norfolk, VA 23529, USA

Abstract

Atmospheric pressure microhollow cathode discharges (MHCDs) offer the possibility to generate a non-thermal plasma by relatively simple means [1]. When operated in rare gases or rare gas-halide mixtures it emits excimer radiation with high efficiency. Operating the discharges in atmospheric pressure air has been shown to allow their use as plasma cathodes for stable large volume atmospheric pressure air plasmas [2]. The plasma results from a direct current discharge between two molybdenum electrodes (0.25 mm thick) that are separated by an alumina insulator of the same thickness. A tapered discharge channel is drilled through all layers, leaving a 0.2 mm wide opening in the cathode and an opening of ~ 0.1 mm in diameter in the anode. By flowing air, nitrogen, or oxygen at atmospheric pressure through this hole, a well-defined plasma jet is generated with typical dimensions of millimeters in axial direction. The power consumption ranges from 1 W to 10 W. The optical and thermal characteristics of this micro plasma jet have been studied. The gas temperature was measured by means of micro-thermocouples. Increasing the gas flow rate from 0 to 200 ml/min while applying a constant discharge current resulted in a considerable decrease of gas temperature to values close to 300 K. This cold plasma jet offers the opportunities for applications such as surface treatment of organic materials [3], plasma surgery [4], and cleaning of semiconductor chips.

[1] Karl H. Schoenbach, Ahmed El-Habachi, Wenhui Shi, and Marco Ciocca, Plasma Sources Science and Technology 6, 468 (1997).

[2] R.H. Stark and K.H. Schoenbach, Appl. Phys. Lett. 74, 3770 (1999).

[3] E. Stoffels, A.J. Flikweert, W.W. Stoffels and G.M.W. Kroesen, Plasma Sources Sci. Technol. 11, 383 (2002).

[4] A.I. Necha, G.A. Kostiuk, S.V. Dzhaiani, A.S. Iushkin, and S.A. Kalashnikov, Vestnik Khirurgii Imeni I. I. Grekova 143, no. 10, 7 (1989).

Experimental Setup

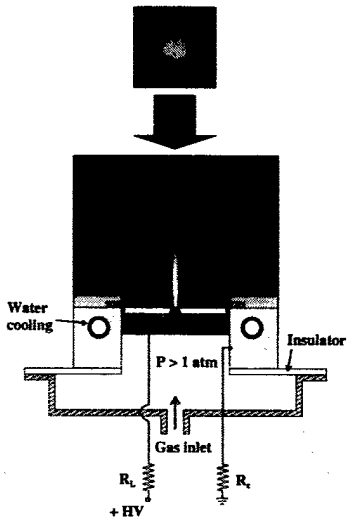

Current-Voltage Characteristics

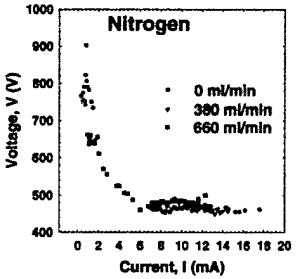

The microhollow cathode discharge has a negative I-V characteristic, which is slightly dependent on the flow rate. This indicates that for parallel operation of micro-plasma jets ballast resistors are required.

Gas Temperature Measurements (Micro - Thermocouple)

Current Dependency

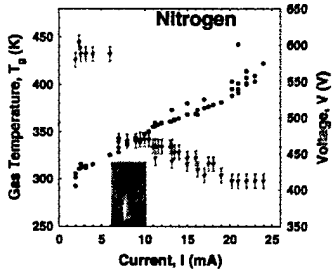

The micro-plasma jet gas temperature is measured at 1.65 mm from the MHC at 300 ml/min flow rate. The micro-plasma jet gas temperature is linearly dependent on the discharge current.

Cold Plasma

A low temperature (room temperature) micro plasma jet is produced in air and nitrogen at low currents and high flow rate (turbulent flow).

Flow Rate Dependency

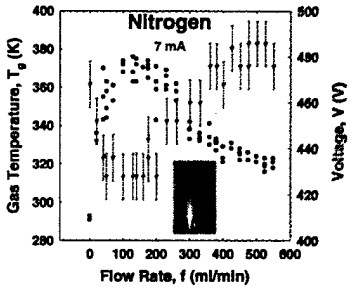

For laminar flow the gas temperature increases with flow rate (up to 140 ml/min). Above 140 ml/min where the flow changes from laminar to turbulent, the temperature decreases with flow rate to almost room temperature.

Axial Temperature Distribution

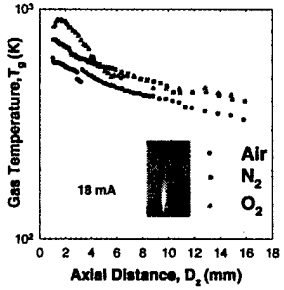

The gas temperature decreases exponentially with distance. In case of oxygen this decay is characterized by two decay constants, a faster decay up to 6 mm followed by a slow decay.

Radial Temperature Distribution

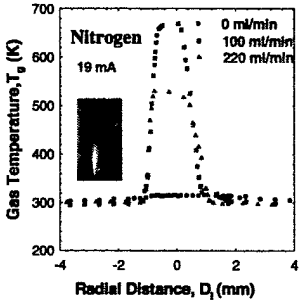

The temperature distribution is measured at 2.12 mm above the MHCD anode.

Transition from Laminar to Turbulent Flow (air, 20 mA)

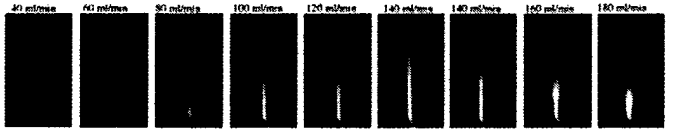

The parameter that describes the transition from laminar to turbulent flow is the Reynolds number (Re=ρvd/μ). Here ρ is gas density, v is the jet velocity, d is the diameter of the anode opening, and μ is the viscosity. The jet flow is laminar for low Reynolds numbers (Re < 1000). The transition from laminar to turbulent flow occurs in the range 1000 < Re < 2000. The flow becomes turbulent for Re > 2000. In our case the transition from laminar to to turbulent flow occurs at a flow rate of 140 ml/min.

Emission Spectroscopy

Experimental Setup

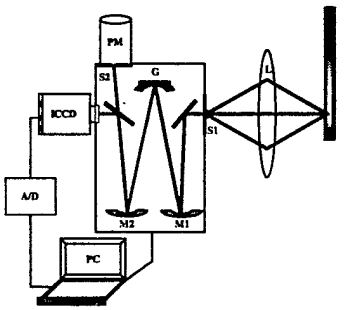

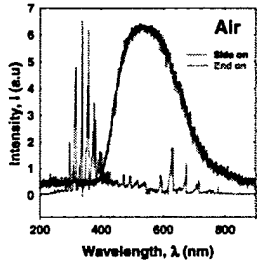

Whereas end-on measurements show the typical emission spectrum of nitrogen, side-on measurements show a continuous spectrum, which peaks at 550 nm and has a width of about 200 nm.

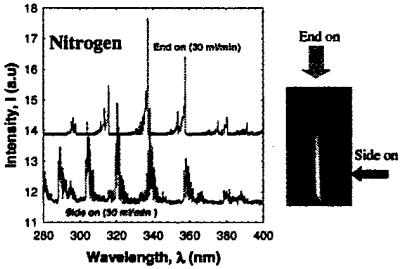

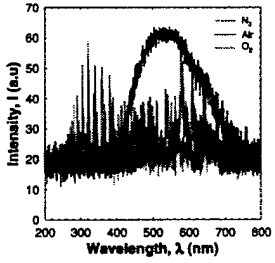

Summary

- Stable micro-plasma jets at atmospheric pressure in nitrogen, oxygen and air have been generated by flowing these gases through a microhollow cathode discharge.
- The temperature in these micro-plasma jets approaches room temperature when operated in a turbulent flow mode. The transition from laminar to turbulent flow was observed at a flow rate of 140 ml/min.
- A continuum in the spectral emission of microjets in atmospheric pressure air was observed side-on.

Acknowledgement

This work was funded by the U.S Air Force Office of Scientific Research (AFOSR)

Conference Record, 2002
IEEE ICOPS, Banff, Alberta,
Canada May 2002

2P03:

Electron Density and Electron Temperature in Pulsed Atmospheric Pressure Air Plasmas

Frank Leipold and Karl H. Schoenbach
Physical Electronics Research Institute
Old Dominion University, Norfolk, VA 23529

The use of atmospheric pressure air plasmas as reflectors for microwave radiation with frequencies up to 30 GHz requires electron densities of approximately 10^{13} cm^{-3}. It has been shown, that direct current microhollow cathode sustained (MCS) discharges meet this requirement [1]. However, the power consumption of such air glow discharges of 5 kW/cm^3 does not permit scaling to large volumes. Pulsing the discharge on a time scale, which is less than the characteristic time for glow-to-arc transition allows us to reduce the power density while keeping the average electron density at the required high value [2]. So far the electron density in these pulsed discharges has been estimated using information on the plasma conductivity; data on the electron energy which is sharply shifted towards higher energies during the pulse have only been obtained through modeling. We have measured the electron density in a pulsed atmospheric air plasma by means of heterodyne interferometry [3]. A measure for the electron energy, the electron temperature, was obtained by means of emission spectroscopy. 20% argon was added to atmospheric air, and the relative intensities of two argon lines, at 810.37 nm and 811.52 nm, were measured. Assuming a Maxwell-Boltzmann distribution of the electron energies allowed us to determine a value for the electron temperature. For a 10 ns pulse of 1.6 kV superimposed to a direct current discharge between electrodes 1.6 mm apart, the electron density increased from 10^{13} cm^{-3} to more than 3 10^{15} cm^{-3}. Over a time of 600 ns it decayed by one order of magnitude. Higher values of the electron density, and correspondingly longer decay times, which are determined by recombination, can be achieved by increasing the pulsed electric field [2]. The electron temperature reached values of 50 eV. This value is in accordance with modeling results. The presence of such high energy in relatively large plasma volumes indicates that pulsed high pressure discharges in air, but also in other gases, have applications not only a plasma ramparts but also a plasma reactors, e.g for chemical decontamination. Other applications, where both high pressure and high electron energy is required is excimer formation in rare gases and rare gas halides. First experiments in xenon have already demonstrated increased excimer emission for pulsed operation [4].

[1] R.H. Stark and K.H. Schoenbach, Appl. Phys. Lett. 74, 3770 (1999).
[2] R.H. Stark and K.H. Schoenbach, J. Appl. Phys. 89, 3568 (2001)
[3] Frank Leipold, Robert H. Stark, Ahmed El-Habachi, and Karl H. Schoenbach, J. Phys. D: Appl. Phys. 33, 2268 (2000).
[4] R.H. Stark, H. Merhi, C. Jiang, and K.H. Schoenbach, Proc. Ninth Intern. Symp. Gaseous Dielectrics, May 2001, Ellicott City, ML, paper 40.

This work was supported by the Air Force Office of Scientific Research.

GEC, Penn State Univ., Oct. 2001, Bull APS, 46, 6, p. 22.

DTP 45 Measurements of Electron Temperature and Gas Temperature in a Pulsed Atmospheric Pressure Air Discharge* FRANK LEIPOLD, *Old Dominion University, Physical Electronics Research Institute, Norfolk, VA 23529* ABDEL-ALEAM HUFNEY MOHAMED, *Old Dominion University, Physical Electronics Research Institute, Norfolk, VA 23529* KARL H. SCHOENBACH, *Old Dominion University, Physical Electronics Research Institute, Norfolk, VA 23529* The application of electrical pulses with duration shorter than the time constant for glow-to-arc transition allows us to shift the electron energy distribution in high pressure glow discharges temporally to high energy values [1]. Application of these nonequilibrium plasmas are plasma ramparts, plasma reactors, and excimer light sources. In order to obtain information on the electron energy distribution , or electron energy, respectively, and the gas temperature with the required temporal resolution of 1 ns, we have explored two diagnostic methods. One is based on the evaluation of the bremsstrahlung. This method allows us to determine the electron temperature [2]. The gas temperature is obtained from the rotational spectrum of the second positive system of nitrogen. The results of measurement on a 10 ns pulsed atmospheric pressure air glow will be presented. References [1] Robert H. Stark and Karl H. Schoenbach, J. Appl. Phys. 89, 3568 (2001) [2] Jaeyoung Park, Ivars Henins, Hans W. Herrmann, and Gary S. Selwyn, Physics of Plasmas 7, 3141 (2000). [3] R. Block, O. Toedter, and K. H. Schoenbach, Bull. APS 43, 1478 (1998)

*This work was funded by the Air Force Office of Scientific Research

GEC, Penn State Univ., Oct. 2001, Bull APS, 46, 6, p. 34.

JWP 4 Benzene Dissociation in DC Atmospheric Pressure Air Glow Discharges CHUNQI JIANG, ROBERT H. STARK, KARL H. SCHOENBACH, *Physical Electronics Research Institute, Old Dominion University* By using a micro-hollow cathode discharge (MHCD) as an electron source to lower or eliminate the cathode fall voltage, a glow discharge could be operated in a dc atmospheric pressure air [1]. The effect of this glow discharge plasma on VOC (Volatile Organic Compound) remediation, particularly, benzene remediation, has been studied. A higher than 90 % destruction rate has been obtained by flowing a 300 ppm benzene/ dry air mixture through the plasma filament. The plasma is confined by a dielectric to a cross-section of 1 mm by 1.5 mm and extends over a depth of 0.8 mm. With a flow rate of 100 sccm, the residence time of the gas in the plasma column is 0.7 ms. A destruction efficiency of more than 0.5 L/kJ has been measured. The energy efficiency is 0.9 g/kWh which is comparable to that achieved by low pressure glow discharges in benzene/ noble gas mixtures [2]. References: [1] R. H. Stark and K. H. Schoenbach, "Direct Current Glow Discharges in Atmospheric Air," Appl. Phys. Lett. 89, 3568 (2001). [2] D. L. McCorkle, W. Ding, C. Ma and L. A. Pinnaduwage, "Dissociation of Benzene and Methylene Chloride Based on Enhanced Dissociative Electron Attachment to Highly Excited Molecules," J. Phys. D: Appl. Phys. 32, 46 (1999). Acknowledgments: This work is supported by the Air Force Office of Scientific Research.

APP Spring Meeting, Bad Honnef 2001, Physikzentrum Bad Honnef Feb 18-21, 2001

Electron Density and Temperature Measurements in Pulsed Atmospheric Pressure Air Plasmas

Frank Leipold, Robert H. Stark, and Karl H. Schoenbach
Physical Electronics Research Institute
Old Dominion University, Norfolk, VA 23529

In order to measure the spatially resolved electron density in high pressure glow discharges with characteristic dimensions of less than one millimeter, CO_2 laser interferometry has been used [1]. At this wavelength (10.6 μm) the index of refraction of atmospheric air plasmas with electron densities on the order of 10^{13} cm^{-3} and less is mainly determined by the neutral particles. In order to obtain information on the density of the electrons, the discharge was operated in a pulsed repetitive mode with pulse duration varying between 100 μs and 50 ms. Since the electrons have a much shorter relaxation time than the heavy particles, the fast change of the refractive index of a pulsed discharge during breakdown was considered to represent the electron part in the index of refraction, slower changes the heavy particle part. Conclusions on the dc values of the index of refraction, and consequently the dc density of electrons and neutral particles were obtained by extrapolating the results obtained with pulsed operation.

The temporal resolution of the interferometric method is on the order of microseconds [2]. In order to obtain information on electron densities (and electron temperatures) with a temporal resolution on the order of nanoseconds, as required for pulsed nonequilibrium plasmas [3], continuum radiation spectroscopy is being used [4]. Due to the low degree of ionization (approximately 10^{-6} cm^{-3}) in the high pressure glow discharges, interaction of electrons with neutrals is the dominant mechanism for bremsstrahlung radiation. The electron temperature is obtained by comparing the measured continuum spectra to computed spectra. The electron density can be obtained through absolute radiation measurement. First successful experiments with argon as working gas have been performed. Experiments with atmospheric pressure air as working gas are under preparation.

[1] Frank Leipold, Robert H. Stark, Ahmed El–Habachi, and Karl H. Schoenbach, J. Phys. D: Appl. Phys. 33, 2268 (2000).

[2] Frank Leipold, Robert H. Stark, and Karl H. Schoenbach, Bull APS (GEC), Vol. 45, No. 6, October 2000, ETP 53, p. 30

[3] Robert H. Stark and Karl H. Schoenbach, "Electron Heating in Pulsed Atmospheric Pressure Glow Discharges," to appear in J. Appl. Phys.

[4] Jaeyoung Park, Ivars Henins, Hans W. Herrmann, and Gary S. Selwyn, Physics of Plasmas 7, 3141 (2000).

Acknowledgement
This work was supported by the Air Force Office of Scientific Research in Cooperation with the DDR&E Air Plasma Ramparts MURI Program, and by the National Science Foundation.

APP Spring Meeting, Bad Honnef 2001, Physikzentrum Bad Honnef Feb 18-21, 2001

Pulsed Electron Heating in Atmospheric Pressure Glow Discharges

Robert H. Stark, Hisham Merhi, and Karl H. Schoenbach
Physical Electronics Research Institute, Old Dominion University,
Norfolk, Virginia 23529

Atmospheric pressure plasmas have gained much interest because of their possible uses as plasma reactors, as light sources, for thin film deposition or surface modification, and as plasma ramparts. For plasma ramparts the electron density needs to be on the order of 10^{13} cm^{-3} at a gas temperature below 2000 K. At equilibrium conditions, where the electron energy distribution (EEDF) is fully determined by the reduced electric field, E/N, the power required to sustain such plasmas is on the order of 5 kW/cm^3 [1]. However, by shifting the EEDF temporarily (on a time scale of less than the time constant for glow-to-arc transition) towards higher energies, and consequently increase the rate coefficient for ionization it is possible to reduce the average sustaining power considerably. This power savings effect has been demonstrated with a single 10 ns pulse applied to a dc glow in atmospheric pressure air [2]. The experimental setup and the pulse form of the 10 ns pulse are shown in Fig. 1. Electrical and optical diagnostics, including high-speed photography was used to study the temporal development of the plasma. An increase in the plasma decay time, which is inversely related to the sustaining power, from several tens of nanoseconds to several microseconds was measured when the pulsed electric field was raised from 10 kV/cm to 40 kV/cm (Fig. 2). Calculations with ELENDIF, a zero-dimensional Boltzmann solver show that use of ns-high voltage pulses can reduce the power budget in atmospheric pressure air discharges by more than two orders in magnitude. Results of this calculation for the temporal range below 20 ns are shown in Fig. 3. Besides allowing power reduction, pulsed electron heating has also the potential to enhance plasma processes, which require elevated electron energies, such as excimer generation for ultra violet lamps. Experiments with double pulse generators, as a first step towards quasi-dc operation of these nonequilibrium plasmas are under way. A pulse generator, with two 10 Ω pulse forming networks, and pulse durations of 10 ns has been constructed and tested up to voltages of 13 kV. The interval between the pulses can be varied continuously between 1 μs and 1 ms. Results of first experiments on the ignition and sustainment phase of pulsed high pressure glow discharges will be reported.

[1] Robert H. Stark and Karl H. Schoenbach, Appl. Phys. Lett. 74, 3770 (1999).
[2] Robert H. Stark and Karl H. Schoenbach "Electron Heating in Pulsed Atmospheric Pressure Glow Discharges", to appear in J. Appl. Phys.

Acknowledgement
This work was solely funded by the Air Force Office of Scientific Research (AFOSR) in cooperation with the DDR&E Air Plasma Ramparts MURI program.

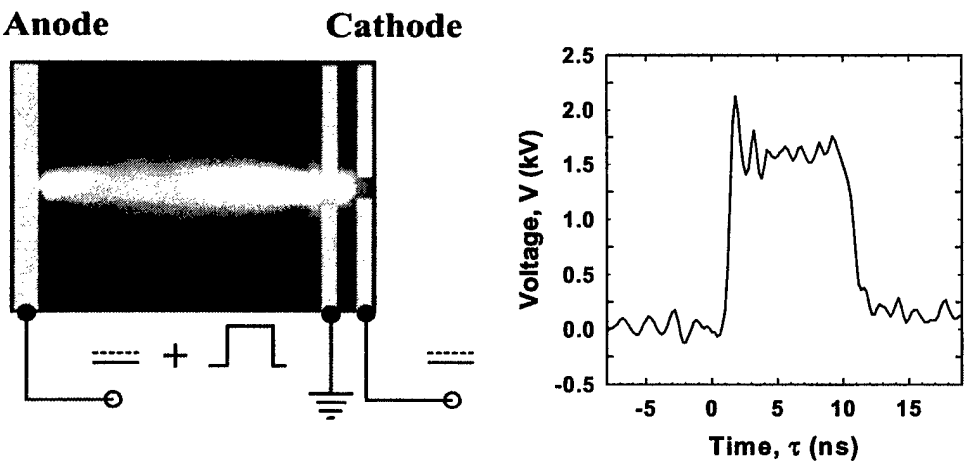

Fig. 1 Experimental setup and temporal development of the 10 ns high voltage pulse (V_{pulse} = 1.6 kV). The microhollow cathode discharge and the MHCD sustained glow are operated in a direct current mode (I = 10 mA). A 10 ns high voltage pulse of variable amplitude is applied at the anode, superimposed to the dc voltage.

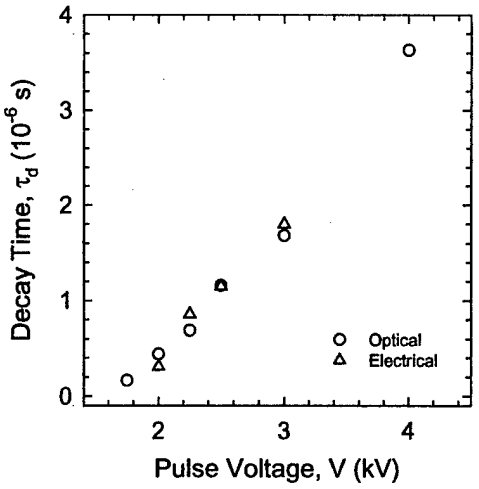

Fig. 2 Decay time versus pulsed electric field, obtained from electrical and optical measurements.

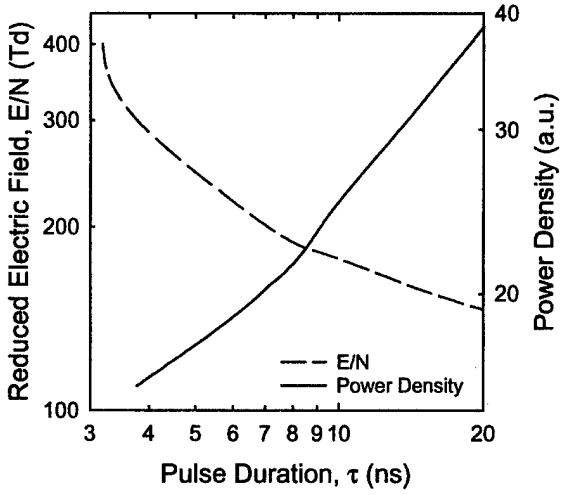

Fig. 3 Pulse duration and electric field amplitude, required to increase the electron density from the dc-value ($n_0 = 10^{13}$ cm^{-3}) to a peak value ($n_p = 5 \cdot 10^{13}$ cm^{-3}), and corresponding electrical power density, $(E/N)^2 \cdot \tau/\tau_d$, where τ is the pulse duration and τ_d is the decay time.

[CT2.006] Electron Heating in Pulsed Atmospheric Pressure Glow Discharges

Robert H. Stark, Frank Leipold, Chunqi Jiang, Hisham Merhi, Karl H. Schoenbach (Old Dominion University, Norfolk, Virginia 23529)

Atmospheric pressure glow discharges in air and noble gases have been operated by using microhollow cathode discharges as plasma cathodes [1]. In these discharges the electron energy distribution is determined by the value of the reduced electric field (E/N). Pulsing the discharges causes the electron energy distribution to shift into an energy range where the ionization rate increases strongly. In order to study this effect, a 10 ns high voltage pulse was applied to a dc glow discharge in atmospheric air. Electrical measurements of the temporal development of current and voltage and optical measurements of the integral emission intensity during the pulse and in the afterglow of the discharge have shown an increase in electron life time from 200 ns at 10 kV/cm to approximately 1.6 \mu at 30 kV/cm. The measured effect can be used to reduce the power consumption of glow discharges and to induce and enhance certain plasma processes.

[1] Robert H. Stark and Karl H. Schoenbach, Appl. Phys. Lett., 74, 3770 (1999)

This work was funded by the Air Force Office of Scientific Research (AFOSR).

[ETP.053] Measurement of Electron Densities in a Pulsed Atmospheric Pressure Air Discharge

Frank Leipold, Robert H. Stark, Karl H. Schoenbach (Old Dominion University, Physical Electronics Research Institute, Norfolk, VA 23529)

Microhollow cathode discharges have been shown to serve as plasma cathodes for atmospheric pressure air discharges [1]. The high pressure discharges are operated dc at currents from 10 mA up to 30 mA and at average electric fields of 1.25 kV/cm. The electron density in the dc discharge was measured by an interferometrique technique [2]. For a dc filamentary air discharge with a current of 10 mA, the radial electron density distribution was found to be parabolic with a total width of 660 \mu m and an electron density of n_e = 10^13 cm^-3 in the center of the discharge. The diagnostic technique has now also been applied to pulsed discharges. It was found that the method provides electron densities measurements for discharges with durations as low as 5 \mu s. The spatial distribution of the index of refraction in the pulsed discharge was obtained by shifting the discharge volume through the laser beam and by using an inversion method to obtain the radial index profile. For the electron density with a assumed parabolic profile, the maximum value was measured as 1.17*10^14 cm^-3. (10 mA atmospheric pressure air discharge. The temperature profile was found to be gaussian with a half width of 1.3 mm.

Acknowledgement

This work was funded by the Air Force Office of Scientific Research in Cooperation with the DDRamp;E Air Plasma Ramparts MURI Program.

References

[1] Robert H. Stark and Karl H. Schoenbach, Appl. Phys. Lett. 74, 3770 (1999) [2] Frank Leipold, Robert H. Stark, and Karl H. Schoenbach, to appear in J. Phys. D., Appl. Phys.

1A05

Electron Heating in Atmospheric Pressure Air Discharges

Robert H. Stark and Karl H. Schoenbach
Physical Electronics Research Institute, Old Dominion University,
Norfolk, Virginia 23529

Atmospheric pressure air plasmas have gained interest because of possible use as plasma reactors, light sources, for thin film deposition, surface modification, and as plasma ramparts. For plasma ramparts, which are air plasmas serving as protective shields against incident microwave radiation, the required free electron density must be on the order of 10^{13} cm^{-3} at gas temperatures of less than 2000 K. At equilibrium conditions, where the electron energy distribution is determined only by the value of the reduced electric field (E/N), the power density required to sustain an atmospheric pressure air plasma of 10^{13} cm^{-3} electron density is approximately 5 kW/cm^3, a value which makes the generation and sustainment of large plasma volumes extremely expensive. However, since the rate coefficient for electron gain and loss processes, which define the power consumption, are dependent on the electron energy distribution function (EEDF), manipulation of the EED might allow us to reduce the power. Particularly shifting the EEDF towards higher electron energies (electron heating), without heating the gas, will cause an increase in ionization rate and decrease in attachment and recombination rate. Experiments with nanosecond high voltage pulses applied to a dc atmospheric pressure air plasma have been performed to study this effect. A 10 ns high voltage pulse with a rise time of 1 ns, was superimposed to a dc microhollow cathode discharge sustained air glow with a current of 10 mA. The applied pulse generated electric fields of 10-30 kV/cm in the plasma. Electrical measurements of the temporal development of current and voltage and optical measurements of the integral emission intensity during the pulse and in the afterglow of the discharge have shown an increase in electron life time from 200 ns at 10 kV/cm to approximately 1.6 μs at 30 kV/cm. Beyond reduction in power consumption, indicated by the experimental results, pulsed electron heating might also be used to influence the plasma chemistry in high pressure plasma reactors.

[1] Robert H. Stark and Karl H. Schoenbach, "Direct Current High Pressure Glow Discharges," J. Appl. Phys., **85**, 2075 (1999)

[2] Robert H. Stark and Karl H. Schoenbach, "Direct Current Glow Discharges in Atmospheric Air," Appl. Phys. Lett., **74**, 3770 (1999)

Acknowledgements

This work was solely funded by the Air Force Office of Scientific Research (AFOSR) in cooperation with the DDR&E Air Plasma Ramparts MURI program.

1P23

Plasma Cathode Sustained Filamentary Glow Discharges in Atmospheric Air

Rolf Block, Abdel-Aleam H. Mohamed, and Karl H. Schoenbach
Physical Electronics Research Institute, Old Dominion University,
Applied Research Center, Newport News, VA

Glow-to-arc transitions in filamentary glow discharges in atmospheric air can be largely avoided by use of a plasma cathode, as has been demonstrated in short filamentary discharges in air [1]. In these experiments a dc-driven microhollow cathode discharge (MHCD) was used as a plasma cathode to sustain a stable, direct current discharge between the plasma cathode and a third positively biased electrode. We have, using the same concept, extended the gap distance (distance between plasma cathode and third electrode) from previously 2 mm to the range from 6 mm to 20 mm and have studied the electrical, optical and plasma properties of such long filamentary glow discharges in atmospheric air. The MHCD is ignited between closely spaced molybdenum electrodes, separated by a 130 μm thick alumina layer, with a 130 μm hole through the sample. The filamentary discharge was ignited at small gap distances, in order to keep the ignition voltage at a low level, and then the gap was extended to the desired distance. In a certain range of current the filamentary glow discharge (FGD) current was found to be identical to the microhollow cathode discharge current. In this range control of the FGD by the MHCD is possible. From previous measurements of short gap filamentary discharge the gas temperature was found to be approximately 2,000 K [2], the electron density was estimated as close to 10^{13} cm^{-3} [1]. We will report on the results of measurements of these plasma parameters in long filamentary air discharges, and the electrical parameters, which determine the current range of MHCD control of the FGD. Parallel operation of these controlled filamentary glow discharges by using individual or distributed ballast might allow the generation of large volume, high pressure glows in air.

[1] Robert H. Stark and Karl H. Schoenbach, "Direct Current Glow Discharges in Atmospheric Air," Appl. Phys. Lett. 74, 3770 (1999).
[2] Robert H. Stark, Uwe Ernst, Mohamed El-Bandrawy, Christophe Laux, and Karl H. Schoenbach, "Direct Current Glow Discharges in Atmospheric Air," Proc. 30th AIAA Plasmadynamics and Lasers Conf., Norfolk, VA, July 1999, paper AIAA-99-3666.

This work was solely funded by the Air Force Office of Scientific Research (AFOSR) in cooperation with the DDR&E Air Plasma Ramparts MURI program.